ARMY RESEARCH LABORATORY

SELECTED UPPER-AIR WIND SPEED DISTRIBUTIONS

Elton P. Avara

ARL-TR-38

December 1992

NOTICES

Disclaimers

The findings in this report are not to be construed as an official Department of the Army position, unless so designated by other authorized documents.

The citation of trade names and names of manufacturers in this report is not to be construed as official Government indorsement or approval of commercial products or services referenced herein.

Disposition

When this document is [illegible]d, destroy it by any method that will prevent disclosure of its contents or reconstruction of the document.

REPORT DOCUMENTATION PAGE

Form Approved
OMB No. 0704-0188

1. AGENCY USE ONLY (Leave blank)	2. REPORT DATE	3. REPORT TYPE AND DATES COVERED
	December 1992	Final

4. TITLE AND SUBTITLE
SELECTED UPPER-AIR WIND SPEED DISTRIBUTION

5. FUNDING NUMBERS
62784/AH71 (6.2)

6. AUTHOR(S)
Elton P. Avara

7. PERFORMING ORGANIZATION NAME(S) AND ADDRESS(ES)
U.S. Army Research Laboratory
Battlefield Environment Directorate
White Sands Missile Range, NM 88002-5501

8. PERFORMING ORGANIZATION REPORT NUMBER
ARL-TR-38

9. SPONSORING/MONITORING AGENCY NAME(S) AND ADDRESS(ES)
U.S. Army Research Laboratory
2800 Powder Mill Road
Adelphi, MD 20783-1145

10. SPONSORING/MONITORING AGENCY REPORT NUMBER

11. SUPPLEMENTARY NOTES

12a. DISTRIBUTION/AVAILABILITY STATEMENT
Approved for public release; distribution unlimited.

12b. DISTRIBUTION CODE

13. ABSTRACT (Maximum 200 words)

Some weapon systems are sensitive to winds in the lower part of the atmosphere. Wind speed distributions and random wind speeds derived from the distributions are often required to help determine the operational capabilities of these systems. A literature survey revealed that investigators usually used either a log-normal or a Weibull distribution as the model for the distribution of wind speeds independent of direction. In addition to these two distributions, a gamma distribution is also evaluated in this report. Wind speeds observed in three different geographical regions at 10 altitudes up to 5 km 3 diurnal time periods, and 5 seasonal time periods were evaluated. This report contains the results of the wind speed analysis for some of the combinations of altitude, diurnal time periods, and seasonal time periods for each of the three geographical regions--European Lowlands, European Highlands, and Mideast Desert. The observed wind speed distributions were adequately represented by the analytical distributions.

14. SUBJECT TERMS	15. NUMBER OF PAGES
Weibull, gamma, log-normal, upper air, wind speed	117
	16. PRICE CODE

17. SECURITY CLASSIFICATION OF REPORT	18. SECURITY CLASSIFICATION OF THIS PAGE	19. SECURITY CLASSIFICATION OF ABSTRACT	20. LIMITATION OF ABSTRACT
Unclassified	Unclassified	Unclassified	SAR

TABLE OF CONTENTS

LIST OF TABLES 4

LIST OF FIGURES 5

1. INTRODUCTION 11

2. CLIMATOLOGY DATA BASE AVAILABLE 11

3. ANALYTICAL DISTRIBUTIONS 13

3.1 Method of Moments 14

3.2 Maximum Likelihood 15

3.3 Nonlinear Least Squares Fit 16

4. WIND SPEED DISTRIBUTIONS 19

5. ANALYSIS RESULTS 34

5.1 European Lowlands 34

5.2 European Highlands 34

5.3 Mideast Desert 34

6. CONCLUSIONS 35

REFERENCES 117

DISTRIBUTION LIST 119

LIST OF TABLES

1. Stations Located in the European Lowlands, Highlands, and Mideast Desert Geographical Regions 12

2. Probabilities of Calm Wind Speeds for all Wind Speed Distribution Cases 20

3. The Number of Noncalm Wind Speed Observations for all Wind Speed Distribution Cases 22

4. The Mean Absolute Deviation Between the Observed and Analytical Cumulative Distribution 24

5. The Root-Mean-Square Deviation Between the Observed and Analytical Cumulative Distributions 26

6. The Names of the Best Analytical Distributions to Represent the Observed Wind Speed Distributions 28

7. The Shape Parameter Corresponding to the Best Analytical Distribution for all Wind Speed Distribution Cases 30

8. The Scale Parameter Corresponding to the Best Analytical Distribution for all Wind Speed Distribution Cases 32

LIST OF FIGURES

1. Regression fitted Weibull distribution for European Lowlands winter wind speeds for height level 0.5 km 36

2. Regression fitted gamma distribution for European Lowlands wind speeds for height level 0.5 km 37

3. Regression fitted Weibull distribution for European Lowlands winter wind speeds for height level 1.0 km 38

4. Regression fitted gamma distribution for European Lowlands wind speeds for height level 1.0 km 39

5. Regression fitted Weibull distribution for European Lowlands winter wind speeds for height level 1.5 km 40

6. Regression fitted gamma distribution for European Lowlands wind speeds for height level 1.5 km 41

7. Regression fitted Weibull distribution for European Lowlands winter wind speeds for height level 2.0 km 42

8. Regression fitted gamma distribution for European Lowlands wind speeds for height level 2.0 km 43

9. Regression fitted Weibull distribution for European Lowlands winter wind speeds for height level 2.5 km 44

10. Regression fitted gamma distribution for European Lowlands wind speeds for height level 2.5 km 45

11. Regression fitted Weibull distribution for European Lowlands winter wind speeds for height level 3.0 km 46

12. Regression fitted gamma distribution for European Lowlands wind speeds for height level 3.0 km 47

13. Regression fitted Weibull distribution for European Lowlands winter wind speeds for height level 3.5 km 48

14. Regression fitted gamma distribution for European Lowlands wind speeds for height level 3.5 km 49

15. Regression fitted Weibull distribution for European Lowlands winter wind speeds for height level 4.0 km 50

16. Regression fitted Weibull distribution for European Lowlands wind speeds for height level 4.0 km 51

17. Regression fitted Weibull distribution for European Lowlands winter wind speeds for height level 4.5 km 52

18. Regression fitted Weibull distribution for European Lowlands wind speeds for height level 4.5 km 53

19. Regression fitted Weibull distribution for European Lowlands winter wind speeds for height level 5.0 km 54

20. Regression fitted Weibull distribution for European Lowlands wind speeds for height level 5.0 km 55

21. Regression fitted gamma distribution for European Highlands winter wind speeds for height level 0.5 km 56

22. Regression fitted Weibull distribution for European Highlands wind speeds for height level 0.5 km 57

23. Regression fitted Weibull distribution for European Highlands winter wind speeds for height level 1.0 km 58

24. Regression fitted gamma distribution for European Highlands wind speeds for height level 1.0 km 59

25. Regression fitted Weibull distribution for European Highlands winter wind speeds for height level 1.5 km 60

26. Regression fitted gamma distribution for European Highlands wind speeds for height level 1.5 km 61

27. Regression fitted Weibull distribution for European Highlands winter wind speeds for height level 2.0 km 62

28. Regression fitted gamma distribution for European Highlands wind speeds for height level 2.0 km 63

29. Regression fitted Weibull distribution for European Highlands winter wind speeds for height level 2.5 km 64

30. Regression fitted gamma distribution for European Highlands wind speeds for height level 2.5 km 65

31. Regression fitted Weibull distribution for European Highlands winter wind speeds for height level 3.0 km 66

32. Regression fitted Weibull distribution for European Highlands wind speeds for height level 3.0 km 67

33. Regression fitted Weibull distribution for European Highlands winter wind speeds for height level 3.5 km 68

34. Regression fitted Weibull distribution for European Highlands wind speeds for height level 3.5 km 69

35. Regression fitted Weibull distribution for European Highlands winter wind speeds for height level 4.0 km 70

36. Regression fitted Weibull distribution for European Highlands wind speeds for height level 4.0 km 71

37. Regression fitted Weibull distribution for European Highlands winter wind speeds for height level 4.5 km 72

38. Regression fitted Weibull distribution for European Highlands wind speeds for height level 4.5 km 73

39. Regression fitted Weibull distribution for European Highlands winter wind speeds for height level 5.0 km 74

40. Regression fitted Weibull distribution for European Highlands wind speeds for height level 5.0 km 75

41. Regression fitted gamma distribution for Mideast Desert nighttime summer wind speeds for height level 0.5 km 76

42. Regression fitted Weibull distribution for Mideast Desert daytime summer wind speeds for height level 0.5 km 77

43. Regression fitted gamma distribution for Mideast Desert nighttime wind speeds for height level 0.5 km 78

44. Regression fitted Weibull distribution for Mideast Desert daytime wind speeds for height level 0.5 km 79

45. Regression fitted gamma distribution for Mideast Desert nighttime summer wind speeds for height level 1.0 km 80

46. Regression fitted Weibull distribution for Mideast Desert daytime summer wind speeds for height level 1.0 km 81

47. Regression fitted gamma distribution for Mideast Desert nighttime wind speeds for height level 1.0 km 82

48. Regression fitted gamma distribution for Mideast Desert daytime wind speeds for height level 1.0 km 83

49. Regression fitted gamma distribution for Mideast Desert nighttime summer wind speeds for height level 1.5 km 84

50. Regression fitted gamma distribution for Mideast Desert daytime summer wind speeds for height level 1.5 km 85

51. Regression fitted Weibull distribution for Mideast Desert nighttime wind speeds for height level 1.5 km 86

52. Regression fitted gamma distribution for Mideast Desert daytime wind speeds for height level 1.5 km 87

53. Regression fitted gamma distribution for Mideast Desert nighttime summer wind speeds for height level 2.0 km 88

54. Regression fitted gamma distribution for Mideast Desert daytime summer wind speeds for height level 2.0 km 89

55. Regression fitted gamma distribution for Mideast Desert nighttime wind speeds for height level 2.0 km 90

56. Regression fitted gamma distribution for Mideast Desert daytime wind speeds for height level 2.0 km 91

57. Regression fitted gamma distribution for Mideast Desert nighttime summer wind speeds for height level 2.5 km 92

58. Regression fitted gamma distribution for Mideast Desert daytime summer wind speeds for height level 2.5 km 93

59. Regression fitted gamma distribution for Mideast Desert nighttime wind speeds for height level 2.5 km 94

60. Regression fitted gamma distribution for Mideast Desert daytime wind speeds for height level 2.5 km 95

61. Regression fitted log-normal distribution for Mideast Desert nighttime summer wind speeds for height level 3.0 km 96

62. Regression fitted gamma distribution for Mideast Desert daytime summer wind speeds for height level 3.0 km 97

63. Regression fitted gamma distribution for Mideast Desert nighttime wind speeds for height level 3.0 km 98

64. Regression fitted gamma distribution for Mideast Desert daytime wind speeds for height level 3.0 km 99

65. Regression fitted gamma distribution for Mideast Desert nighttime summer wind speeds for height level 3.5 km 100

66. Regression fitted gamma distribution for Mideast Desert daytime summer wind speeds for height level 3.5 km 101

67. Regression fitted gamma distribution for Mideast Desert nighttime wind speeds for height level 3.5 km 102

68. Regression fitted gamma distribution for Mideast Desert daytime wind speeds for height level 3.5 km 103

69. Regression fitted gamma distribution for Mideast Desert nighttime summer wind speeds for height level 4.0 km 104

70. Regression fitted gamma distribution for Mideast Desert daytime summer wind speeds for height level 4.0 km 105

71. Regression fitted gamma distribution for Mideast Desert nighttime wind speeds for height level 4.0 km 106

72. Regression fitted gamma distribution for Mideast Desert daytime wind speeds for height level 4.0 km 107

73. Regression fitted gamma distribution for Mideast Desert nighttime summer wind speeds for height level 4.5 km 108

74. Regression fitted gamma distribution for Mideast Desert daytime summer wind speeds for height level 4.5 km 109

75. Regression fitted gamma distribution for Mideast Desert nighttime wind speeds for height level 4.5 km 110

76. Regression fitted gamma distribution for Mideast Desert daytime wind speeds for height level 4.5 km 111

77. Regression fitted gamma distribution for Mideast Desert nighttime summer wind speeds for height level 5.0 km 112

78. Regression fitted gamma distribution for Mideast Desert daytime summer wind speeds for height level 5.0 km 113

79. Regression fitted gamma distribution for Mideast Desert nighttime wind speeds for height level 5.0 km 114

80. Regression fitted gamma distribution for Mideast Desert daytime wind speeds for height level 5.0 km 115

1. INTRODUCTION

The Program Manager (PM) for BAT (PM-BAT) and his associated contractors (CAS, Incorporated, and Dynetics, Incorporated) have a requirement to find analytical distributions to adequately represent the observed wind speed distributions obtained in the lower 5 km of the atmosphere, at different time periods, and at different geographical regions of the world. These distributions are required to test the operational capabilities of the BAT system. The U.S. Army Research Laboratory, Battlefield Environment Directorate (ARL-BED), was requested to perform the task.

Dramatic changes in the atmosphere occur each day on the average as the sun rises and sets. Because diurnal variations are most prominent in the atmosphere's lower layer, changes in boundary layer winds have been documented as well as for other atmospheric variables (Holton, 1967). Frequency of occurrence of low altitude wind speeds has important applications in air pollution analysis or for nuclear-biological-chemical (NBC) predictions for military applications. The distributions of surface wind speeds for selected time periods, geographical regions, and meteorological conditions have been reported in Avara and Miers (1992). This report will present the wind speed analysis for altitudes above the surface up to 5 km.

The upper-air winds are obtained by tracking a pibal or radiosonde balloon as it ascends into the atmosphere. The relative horizontal movement of the balloon as it traverses successive layers of the atmosphere can be determined from the positions of the balloon over the ground at successive observing times as it is tracked. The displacement of the balloon as it ascends through a layer is assumed to be entirely due to the wind. Furthermore, the horizontal velocity of the balloon is assumed to be the horizontal velocity of the wind. Wind speed measurement errors typically occur through balloon tracking errors and errors induced by assuming the balloon is 100 percent responsive to the wind field. This report does not address upper-air wind speed measurement errors. The observed wind speeds were assumed free from error.

The efforts of several previous investigators in using the Weibull, gamma, or log-normal distributions to model wind speeds are reported in Avara and Miers (1992) and will not be repeated in this report. All three distributions were considered in the upper-air wind speed analysis.

2. CLIMATOLOGY DATA BASE AVAILABLE

The ARL-BED maintains a climatology data base containing historical upper-air weather observations from numerous locations in North America, Northern and Central Europe, the Mideast, Southwest Asia, and Korea. These data were obtained over a period of years from the U.S. Air Force Environmental Technical Applications Center (USAFETAC) at Scott Air Force Base, Illinois. The period of record for the data from each station is generally 11 years or less and may be anywhere from 1966-76 to 1976-86, depending upon the year the data were obtained from the USAFETAC.

The regions of interest were the European Lowlands, European Highlands, and the Mideast Desert geographical areas (Miers et al., 1985a, Miers et al., 1985b). The upper-air stations located in each of these regions are listed in table 1. The period of record for the data from these stations is 1973-83.

TABLE 1. STATIONS LOCATED IN THE EUROPEAN LOWLANDS, HIGHLANDS, AND MIDEAST DESERT GEOGRAPHICAL REGIONS

Station Number	Station Name	Latitude (Deg:Min)	Longitude (Deg:Min)	Elevation (Meters)
	EUROPEAN LOWLANDS			
100350	Schleswig, FRG	+54:32	-009:33	+0048
100460	Kiel/Holtenau, FRG	+54:23	-010:09	+0031
102380	Bergen/Hohne, FRG	+52:49	-009:56	+0068
103040	Meppen, FRG	+52:43	-007:19	+0019
103380	Hannover, FRG	+52:28	-009:42	+0055
103840	Berlin/Templehof, FRG	+52:28	-013:24	+0050
104100	Essen, FRG	+51:24	-006:58	+0161
	EUROPEAN HIGHLANDS			
095480	Meiningen, DD	+50:34	-010:23	+0450
106180	IDAR/Oberstein, FRG	+49:42	-007:20	+0376
106870	Graftenwohr, FRG	+49:42	-011:57	+0414
107710	Garmersdorf, FRG	+49:26	-011:54	+0419
	MIDEAST DESERT			
400800	Damascus New Intl, SY	+33:25	-036:31	+0610
402650	Mafraq, TJ	+32:22	-036:16	+0686
406500	Baghdad Int (ORBW), IQ	+33:14	-044:14	+0034
407540	Tehran/Mehrabad, IR	+35:41	-051:19	+1204

For the two European regions, the winter and annual wind speed distributions were obtained by grouping the observations from all hours of the day together. Winter for these regions is defined to be November, December, January, and February. For the Mideast Desert region, the summer and annual wind speed distributions were obtained by grouping the observations taken at night into one group and the observations taken during the daytime into another group. Summer for the Mideast Desert region is defined to be June, July, and August.

The upper-air observations tend to be taken at 0000 and 1200 GMT with possibly a few observations taken at other times of day on a nonroutine basis. Therefore, performing an analysis of upper-air data over more than two periods of the day is not practical for any geographical region or season.

The historical upper-air wind speed observations were linearly interpolated to give wind speeds every 500 m from 500 m altitude up to 5000 m. All altitudes referred to in this report are relative to mean sea level (MSL). The wind speeds at these 10 altitude levels were used in the analysis.

3. ANALYTICAL DISTRIBUTIONS

Three analytical distributions were selected for potential use in representing the observed wind speed distributions. They were chosen based upon the work of previous researchers referred to in Avara and Miers (1992). These three candidate distributions were the gamma, log-normal, and Weibull. Each of these distributions performed reasonably well at representing the observed wind speed distributions.

The gamma probability distribution is defined by

$$f(x;\alpha,\beta) = \frac{(\frac{x}{\beta})^{(\alpha-1)}\exp[-(\frac{x}{\beta})]}{\beta\Gamma(\alpha)}, \tag{1}$$

where $\Gamma(\alpha)$ is the gamma function with argument α, $x > 0$, $\alpha > 0$, and $\beta > 0$.

The log-normal probability distribution is defined by

$$f(x;\mu,\sigma) = \frac{\exp[-\frac{1}{2}(\frac{\ln(x)-\mu}{\sigma})^2]}{x\sigma\sqrt{2\pi}}, \tag{2}$$

where μ is the expected value and σ is the standard deviation of $\ln(x)$ and $x > 0$.

The Weibull probability distribution is defined by

$$f(x;\alpha,\beta) = (\frac{\alpha}{\beta})(\frac{x}{\beta})^{\alpha-1}\exp[-(\frac{x}{\beta})^{\alpha}], \tag{3}$$

where $x > 0$, $\alpha > 0$, and $\beta > 0$.

In this report μ and β are referred to as scale parameters because changing their values either tends to move the center or skew the distribution toward higher or lower values. σ and α are referred to as shape parameters because changing their values tends to change the shape of the distribution to either a more peaked or a flatter form.

Three procedures for computing values for α and β or μ and σ were considered for fitting the analytical distributions to the observed wind speed distributions (histograms). These procedures are the method of moments, maximum likelihood, and nonlinear least squares fit to the observed cumulative probability distribution. For each observed wind speed distribution the best of the three analytical distributions and the associated parameter values were determined. Once the name of the best analytical distribution and the distribution parameter values are known, the estimation of the tail probability of the wind speed is possible.

The "goodness-of-fit" of the analytical distributions was compared by computing both the mean absolute difference and the root-mean-square (rms) difference between the observed and each of the three analytical cumulative distributions After thoroughly comparing the analytical distributions by using both criteria, the author decided to use the minimum rms difference to make the final selection.

When this criterion is used, the method of moments generally yields parameter estimates that do not perform as well as the other two procedures. The maximum likelihood procedure tends to yield better estimates of the parameters than the method of moments. The nonlinear least squares fit gives the best parameter estimates, as expected by the selection criterion.

3.1 Method of Moments

The expected value of x for the gamma distribution is given by

$$E[x] = \alpha\beta, \tag{4}$$

and the variance of x is given by

$$VAR[x] = \alpha\beta^2. \tag{5}$$

These two equations can be used to compute values of α and β for the gamma distribution using observed data to estimate E[x] by the mean value of the observed data and VAR[x] by the sample variance of the observed data, giving

$$\beta = \frac{VAR[x]}{E[x]} \tag{6}$$

and

$$\alpha = \frac{E[x]}{\beta}. \tag{7}$$

This procedure for obtaining values for the distribution parameters is called the method of moments.

Using the method of moments to compute values for μ and σ in the log-normal distribution gives

$$\mu = E[\ln(x)] \tag{8}$$

and

$$\sigma = \sqrt{VAR[\ln(x)]}, \tag{9}$$

where E[ln(x)] and VAR[ln(x)] are estimated from the data by using the mean value and sample variance of the natural logarithm of the wind speed data.

The advantage of using E[ln(x)] and VAR[ln(x)] rather than E[x] and VAR[x] to estimate μ and σ can be seen when one considers the relationship between the distribution parameters and E[x] and VAR[x] given by

$$E[x] = \exp[\mu + \frac{1}{2}\sigma^2] \tag{10}$$

and

$$VAR[x] = \exp(2\mu + \sigma^2)[\exp(\sigma^2) - 1]. \tag{11}$$

The expected value of x for the Weibull distribution is given by

$$E[x] = \frac{\beta}{\alpha}\Gamma(\frac{1}{\alpha}), \tag{12}$$

and the variance of x is given by

$$VAR[x] = \frac{\beta^2}{\alpha}[2\Gamma(\frac{2}{\alpha}) - \frac{1}{\alpha}[\Gamma(\frac{1}{\alpha})]^2]. \tag{13}$$

It is rather difficult to use the method of moments to compute values of α and β for the Weibull distribution using estimates of E[x] and VAR[x] obtained from observed data. When the computational time required to iteratively solve this system of equations and the general inferior quality of the parameter estimates were considered, the author did not use this procedure to compute the Weibull distribution parameters.

3.2 Maximum Likelihood

The maximum likelihood procedure involves finding the parameter values that maximize the likelihood function of the distribution. For the gamma distribution these parameter values are obtained by iteratively solving the following system of equations:

$$\ln(\beta) + \Psi(\alpha) = E[\ln(x)], \tag{14}$$

$$\alpha\beta = E[x], \tag{15}$$

where $\Psi(\alpha)$ is the digamma function defined by the equation

$$\Psi(\alpha) = \frac{d[\ln(\Gamma(\alpha))]}{d\alpha}, \tag{16}$$

with $\Gamma(\alpha)$ being the gamma function with argument α (Abramowitz and Stegun, 1965).

The maximum likelihood estimates of the log-normal distribution parameters are the same as those given in equations (8) and (9) by the method of moments.

The maximum likelihood estimates of the Weibull distribution parameters are obtained by iteratively solving the following system of equations:

$$\frac{E[x^{\alpha}\ln(x)]}{E[x^{\alpha}]} - \frac{1}{\alpha} = E[\ln(x)], \tag{17}$$

$$\beta = E[x^{\alpha}]^{\frac{1}{\alpha}}. \tag{18}$$

3.3 Nonlinear Least Squares Fit

The least squares fit was performed on observed cumulative distribution values $\{P_i, i = 1, 2, \ldots, N\}$ corresponding to discrete values of the wind speed, X, denoted by $\{X_i, i = 1, 2, \ldots, N\}$ where N is the number of wind speed intervals. Each wind speed interval had a width of 0.5 m/s. N was determined by choosing the first interval of the observed wind speed frequency of occurrence histogram such that all intervals greater than the Nth contained no occurrences of wind speed.

The three analytical distributions are clearly nonlinear with respect to the distribution parameters α, β, μ, and σ. To determine the least squares estimates of these parameter values, a procedure was used to linearize the distributions (at least in the neighborhood of any specific values of the parameters).

Consider the integral of the probability distribution given by

$$F(X;\alpha,\beta) = \int_0^X f(x;\alpha,\beta)\,dx. \tag{19}$$

By letting

$$\alpha = \alpha_0 + \delta\alpha \tag{20}$$

and

$$\beta = \beta_0 + \delta\beta \tag{21}$$

equation (19) becomes

$$F(X;\alpha_0 + \delta\alpha, \beta_0 + \delta\beta) = \int_0^X f(x;\alpha_0 + \delta\alpha, \beta_0 + \delta\beta)\,dx. \tag{22}$$

To a first-order approximation using small values for $\delta\alpha$ and $\delta\beta$

$$F(X;\alpha,\beta) = F(X;\alpha_0,\beta_0) + \frac{\partial F(X;\alpha_0,\beta_0)}{\partial\alpha}\delta\alpha + \frac{\partial F(X;\alpha_0,\beta_0)}{\partial\beta}\delta\beta, \tag{23}$$

where

$$\frac{\partial F(X;\alpha_0,\beta_0)}{\partial\alpha} = \int_0^X \frac{\partial f(x;\alpha,\beta)}{\partial\alpha}\bigg|_{\alpha=\alpha_0} dx \tag{24}$$

and

$$\frac{\partial F(X;\alpha_0,\beta_0)}{\partial\beta} = \int_0^X \frac{\partial f(x;\alpha,\beta)}{\partial\beta}\bigg|_{\beta=\beta_0} dx. \tag{25}$$

Equation (23) is linear in $\delta\alpha$ and $\delta\beta$.

Let Q represent the sum of the squares of the differences between the analytical, $F(X_i;\ \alpha,\ \beta)$, and observed cumulative P_i, distributions given by

$$Q = \sum_{i=1}^{N} [F(X_i;\alpha,\beta) - P_i]^2. \tag{26}$$

Replacing $F(X_i;\ \alpha,\ \beta)$ by the expression in equation (23) gives

$$Q = \sum_{i=1}^{N} [F(X_i;\alpha_0,\beta_0) + \frac{\partial F(X_i;\alpha_0,\beta_0)}{\partial \alpha}\delta\alpha + \frac{\partial F(X_i;\alpha_0,\beta_0)}{\partial \beta}\delta\beta - P_i]^2. \tag{27}$$

Taking the partial derivatives of Q with respect to $\delta\alpha$ and $\delta\beta$, and setting each derivative equal to zero to find a minimum of Q gives

$$\sum_{i=1}^{N} [\frac{\partial F_0(X_i)}{\partial \alpha}]^2\delta\alpha + \sum_{i=1}^{N} [\frac{\partial F_0(X_i)}{\partial \alpha}\frac{\partial F_0(X_i)}{\partial \beta}]\delta\beta = \sum_{i=1}^{N} [P_i - F_0(X_i)]\frac{\partial F_0(X_i)}{\partial \alpha} \tag{28}$$

and

$$\sum_{i=1}^{N} [\frac{\partial F_0(X_i)}{\partial \alpha}\frac{\partial F_0(X_i)}{\partial \beta}]\delta\alpha + \sum_{i=1}^{N} [\frac{\partial F_0(X_i)}{\partial \beta}]^2\delta\beta = \sum_{i=1}^{N} [P_i - F_0(X_i)]\frac{\partial F_0(X_i)}{\partial \beta}, \tag{29}$$

where the terms involving $F_0(X_i)$ and its partial derivatives denote the function $F(x;\ \alpha,\ \beta)$ and its partial derivatives evaluated at X_i, α_0, and β_0. These two equations are linear in $\delta\alpha$ and $\delta\beta$.

The nonlinear least squares fit procedure begins by getting initial values for α_0 and β_0; solving equations (28) and (29) for $\delta\alpha$ and $\delta\beta$ using the definitions in equations (19), (24), and (25); and getting updated values of α and β according to the iterative equations

$$\alpha_k = \alpha_{k-1} + \delta\alpha \tag{30}$$

and

$$\beta_k = \beta_{k-1} + \delta\beta \tag{31}$$

for k = 1, 2, ... until $\delta\alpha$ and $\delta\beta$ become very small and convergence is obtained. The initial values of the parameters may be selected by any method. Reasonable initial values are obtained by using the method of moments to get α_0 and β_0.

4. WIND SPEED DISTRIBUTIONS

All three of the analytical distributions considered in this analysis have zero probability of occurrence at x = 0. The observed wind speed at any altitude, however, may be calm or zero. To account for this phenomenon, the wind speed cumulative distribution is defined by the equation

$$W(X;p_0,\alpha,\beta) = p_0\delta(0) + (1 - p_0)F(X;\alpha,\beta), \tag{32}$$

where X is the wind speed, $\delta(0)$ is the Dirac delta function, p_0 is the probability of calm wind speeds, and $F(X; \alpha, \beta)$ is the appropriate analytical cumulative distribution function.

The probabilities of calm wind speeds for each region, time period, and height level combination are listed in table 2. Similarly, the numbers of noncalm wind speed observations are listed in table 3.

The observed probability distribution was obtained by forming histograms of frequency of occurrence of observed wind speed with all histogram interval widths being 0.5 m/s. The histogram frequencies of occurrence were converted to probabilities and assigned to the wind speeds at the midpoints of the intervals. The corresponding analytical probability distribution was obtained by evaluating the analytical cumulative probability distribution at the wind speeds corresponding to the beginning and end of each histogram interval and using the difference between the two values assigned to the wind speed at the midpoint of the interval.

The mean absolute deviation between the observed and analytical cumulative distributions for each region, time period, and height level combination is listed in table 4. Similarly, the rms deviation between the cumulative distributions is listed in table 5. Generally, both the mean absolute deviations and the rms deviations are small, indicating the analytical distributions adequately represent the observed wind speed distributions. The names of the corresponding best distribution, the shape parameters, and the scale parameters are listed in tables 6, 7, and 8, respectively.

TABLE 2. PROBABILITIES OF CALM WIND SPEEDS FOR ALL WIND SPEED DISTRIBUTION CASES

Region	Season	Time Period	Height Level (km)	Probability (%)
European lowlands	Winter	All hours	0.5	.09317
			1.0	.04192
			1.5	.02474
			2.0	.01651
			2.5	.02064
			3.0	.04132
			3.5	.02481
			4.0	.01655
			4.5	.01672
			5.0	.00836
European lowlands	Annual	All hours	0.5	.12822
			1.0	.05535
			1.5	.04233
			2.0	.03143
			2.5	.03145
			3.0	.05062
			3.5	.02465
			4.0	.02192
			4.5	.01665
			5.0	.01110
European highlands	Winter	All hours	0.5	.50052
			1.0	.05432
			1.5	.02647
			2.0	.00000
			2.5	.00000
			3.0	.00000
			3.5	.00000
			4.0	.00000
			4.5	.00000
			5.0	.00000
European highlands	Annual	All hours	0.5	.62929
			1.0	.13030
			1.5	.06565
			2.0	.02195
			2.5	.02642
			3.0	.03093
			3.5	.00444
			4.0	.00445
			4.5	.00000
			5.0	.00450

Mideast desert	Summer	Night	0.5	1.59272
			1.0	.74587
			1.5	.33656
			2.0	.12573
			2.5	.12658
			3.0	.08460
			3.5	.00000
			4.0	.00000
			4.5	.04456
			5.0	.04486
Mideast desert	Summer	Day	0.5	.93555
			1.0	.35858
			1.5	.06165
			2.0	.06094
			2.5	.09146
			3.0	.15263
			3.5	.06139
			4.0	.03095
			4.5	.00000
			5.0	.00000
Mideast desert	Annual	Night	0.5	3.26118
			1.0	1.15770
			1.5	.56747
			2.0	.08887
			2.5	.05568
			3.0	.04468
			3.5	.00000
			4.0	.00000
			4.5	.01177
			5.0	.01188
Mideast desert	Annual	Day	0.5	2.90059
			1.0	.95894
			1.5	.49075
			2.0	.12841
			2.5	.07709
			3.0	.08570
			3.5	.01725
			4.0	.01735
			4.5	.00000
			5.0	.00000

TABLE 3. THE NUMBER OF NONCALM WIND SPEED OBSERVATIONS FOR ALL WIND SPEED DISTRIBUTION CASES

Region	Season	Time Period	Height Level (km)	Noncalm Count
European lowlands	Winter	All hours	0.5	23592
			1.0	23845
			1.5	24251
			2.0	24230
			2.5	24215
			3.0	24194
			3.5	24182
			4.0	24170
			4.5	23918
			5.0	23913
European lowlands	Annual	All hours	0.5	71661
			1.0	72230
			1.5	73202
			2.0	73157
			2.5	73106
			3.0	73056
			3.5	73017
			4.0	72983
			4.5	72066
			5.0	72055
European highlands	Winter	All hours	0.5	6759
			1.0	7360
			1.5	7555
			2.0	7547
			2.5	7530
			3.0	7508
			3.5	7503
			4.0	7478
			4.5	7438
			5.0	7395
European highlands	Annual	All hours	0.5	20686
			1.0	22227
			1.5	22832
			2.0	22773
			2.5	22701
			3.0	22623
			3.5	22540
			4.0	22471
			4.5	22343
			5.0	22220

Mideast desert	Summer	Night	0.5	865
			1.0	1863
			1.5	2369
			2.0	2383
			2.5	2367
			3.0	2362
			3.5	2304
			4.0	2268
			4.5	2243
			5.0	2228
Mideast desert	Summer	Day	0.5	953
			1.0	2223
			1.5	3242
			2.0	3280
			2.5	3277
			3.0	3271
			3.5	3256
			4.0	3230
			4.5	3208
			5.0	3192
Mideast desert	Annual	Night	0.5	3352
			1.0	7001
			1.5	8761
			2.0	8994
			2.5	8975
			3.0	8949
			3.5	8734
			4.0	8614
			4.5	8496
			5.0	8416
Mideast desert	Annual	Day	0.5	3448
			1.0	8056
			1.5	11355
			2.0	11666
			2.5	11666
			3.0	11658
			3.5	11590
			4.0	11524
			4.5	11454
			5.0	11397

TABLE 4. THE MEAN ABSOLUTE DEVIATION BETWEEN THE OBSERVED AND ANALYTICAL CUMULATIVE DISTRIBUTIONS

Region	Season	Time Period	Height Level (km)	Mean Absolute Deviation (%)
European lowlands	Winter	All hours	0.5	.14902
			1.0	.28980
			1.5	.32437
			2.0	.26155
			2.5	.26858
			3.0	.24476
			3.5	.23916
			4.0	.16868
			4.5	.11883
			5.0	.09139
European lowlands	Annual	All hours	0.5	.20985
			1.0	.29884
			1.5	.29448
			2.0	.24106
			2.5	.26972
			3.0	.29805
			3.5	.30699
			4.0	.27436
			4.5	.25471
			5.0	.23513
European highlands	Winter	All hours	0.5	.38035
			1.0	.30137
			1.5	.30301
			2.0	.40481
			2.5	.28888
			3.0	.19688
			3.5	.18850
			4.0	.25313
			4.5	.24869
			5.0	.20566
European highlands	Annual	All hours	0.5	.42646
			1.0	.26195
			1.5	.21188
			2.0	.12471
			2.5	.22099
			3.0	.15987
			3.5	.16872
			4.0	.20203
			4.5	.21563
			5.0	.16645

Mideast desert	Summer	Night	0.5	1.07418
			1.0	.38178
			1.5	.65171
			2.0	.29377
			2.5	.39364
			3.0	.57006
			3.5	.44411
			4.0	.35257
			4.5	.28585
			5.0	.29915
Mideast desert	Summer	Day	0.5	.30531
			1.0	.51226
			1.5	.45835
			2.0	.30314
			2.5	.34658
			3.0	.22126
			3.5	.49947
			4.0	.35426
			4.5	.31233
			5.0	.30977
Mideast desert	Annual	Night	0.5	.31784
			1.0	.23407
			1.5	.56314
			2.0	.25396
			2.5	.14807
			3.0	.36652
			3.5	.12457
			4.0	.20725
			4.5	.12137
			5.0	.14451
Mideast desert	Annual	Day	0.5	.43033
			1.0	.25526
			1.5	.26052
			2.0	.24431
			2.5	.12826
			3.0	.23874
			3.5	.09874
			4.0	.25631
			4.5	.32095
			5.0	.25691

TABLE 5. THE ROOT-MEAN-SQUARE DEVIATION BETWEEN THE OBSERVED AND ANALYTICAL CUMULATIVE DISTRIBUTIONS

Region	Season	Time Period	Height Level (km)	Root Mean Square Deviation (%)
European lowlands	Winter	All Hours	0.5	.29728
			1.0	.44189
			1.5	.50877
			2.0	.42723
			2.5	.43830
			3.0	.37937
			3.5	.35263
			4.0	.26514
			4.5	.21340
			5.0	.18355
European lowlands	Annual	All Hours	0.5	.30101
			1.0	.46328
			1.5	.44992
			2.0	.36094
			2.5	.34462
			3.0	.38526
			3.5	.40791
			4.0	.42809
			4.5	.40682
			5.0	.40449
European highlands	Winter	All Hours	0.5	.61938
			1.0	.42085
			1.5	.46469
			2.0	.58212
			2.5	.45906
			3.0	.30152
			3.5	.29192
			4.0	.35293
			4.5	.34589
			5.0	.29311
European highlands	Annual	All Hours	0.5	.79256
			1.0	.32503
			1.5	.31076
			2.0	.22408
			2.5	.37384
			3.0	.34483
			3.5	.36562
			4.0	.39665
			4.5	.41282
			5.0	.33166

Mideast desert	Summer	Night	0.5	1.24607
			1.0	.55307
			1.5	.80162
			2.0	.42284
			2.5	.53262
			3.0	.73705
			3.5	.64822
			4.0	.48737
			4.5	.43040
			5.0	.48113
Mideast desert	Summer	Day	0.5	.42728
			1.0	.83192
			1.5	.67613
			2.0	.48374
			2.5	.50753
			3.0	.30667
			3.5	.69918
			4.0	.51209
			4.5	.43699
			5.0	.48574
Mideast desert	Annual	Night	0.5	.47518
			1.0	.44673
			1.5	.85175
			2.0	.36001
			2.5	.21746
			3.0	.58937
			3.5	.26273
			4.0	.35700
			4.5	.27835
			5 0	.34835
Mideast desert	Annual	Day	0.5	.60093
			1.0	.46991
			1.5	.48737
			2.0	.44501
			2.5	.21835
			3.0	.38982
			3.5	.15114
			4.0	.39980
			4.5	.48940
			5.0	.39138

TABLE 6. THE NAMES OF THE BEST ANALYTICAL DISTRIBUTIONS TO REPRESENT THE OBSERVED WIND SPEED DISTRIBUTIONS

Region	Season	Time Period	Height Level (km)	Distribution
European lowlands	Winter	All hours	0.5	Weibull
			1.0	Weibull
			1.5	Weibull
			2.0	Weibull
			2.5	Weibull
			3.0	Weibull
			3.5	Weibull
			4.0	Weibull
			4.5	Weibull
			5.0	Weibull
European lowlands	Annual	All hours	0.5	Gamma
			1.0	Gamma
			1.5	Gamma
			2.0	Gamma
			2.5	Gamma
			3.0	Gamma
			3.5	Gamma
			4.0	Weibull
			4.5	Weibull
			5.0	Weibull
European highlands	Winter	All hours	0.5	Gamma
			1.0	Weibull
			1.5	Weibull
			2.0	Weibull
			2.5	Weibull
			3.0	Weibull
			3.5	Weibull
			4.0	Weibull
			4.5	Weibull
			5.0	Weibull
European highlands	Annual	All hours	0.5	Weibull
			1.0	Gamma
			1.5	Gamma
			2.0	Gamma
			2.5	Gamma
			3.0	Weibull
			3.5	Weibull
			4.0	Weibull
			4.5	Weibull
			5.0	Weibull

Mideast desert	Summer	Night	0.5	Gamma
			1.0	Gamma
			1.5	Gamma
			2.0	Gamma
			2.5	Gamma
			3.0	Log-Normal
			3.5	Gamma
			4.0	Gamma
			4.5	Gamma
			5.0	Gamma
Mideast desert	Summer	Day	0.5	Weibull
			1.0	Weibull
			1.5	Gamma
			2.0	Gamma
			2.5	Gamma
			3.0	Gamma
			3.5	Gamma
			4.0	Gamma
			4.5	Gamma
			5.0	Gamma
Mideast desert	Annual	Night	0.5	Gamma
			1.0	Gamma
			1.5	Weibull
			2.0	Gamma
			2.5	Gamma
			3.0	Gamma
			3.5	Gamma
			4.0	Gamma
			4.5	Gamma
			5.0	Gamma
Mideast desert	Annual	Day	0.5	Weibull
			1.0	Gamma
			1.5	Gamma
			2.0	Gamma
			2.5	Gamma
			3.0	Gamma
			3.5	Gamma
			4.0	Gamma
			4.5	Gamma
			5.0	Gamma

TABLE 7. THE SHAPE PARAMETER CORRESPONDING TO THE BEST ANALYTICAL DISTRIBUTION FOR ALL WIND SPEED DISTRIBUTION CASES

Region	Season	Time Period	Height Level (km)	Shape Parameters
European lowlands	Winter	All hours	0.5	1.94001
			1.0	1.87258
			1.5	1.87244
			2.0	1.90308
			2.5	1.93556
			3.0	1.92341
			3.5	1.95354
			4.0	1.93692
			4.5	1.93676
			5.0	1.92517
European lowlands	Annual	All hours	0.5	2.99105
			1.0	2.93947
			1.5	2.94049
			2.0	3.05194
			2.5	3.03083
			3.0	2.88379
			3.5	3.00621
			4.0	1.83622
			4.5	1.82808
			5.0	1.81675
European highlands	Winter	All hours	0.5	2.04370
			1.0	1.74782
			1.5	1.72693
			2.0	1.74782
			2.5	1.78564
			3.0	1.79718
			3.5	1.83906
			4.0	1.85042
			4.5	1.86825
			5.0	1.86339
European highlands	Annual	All hours	0.5	1.58353
			1.0	2.59101
			1.5	2.49970
			2.0	2.58219
			2.5	2.72753
			3.0	1.73934
			3.5	1.76690
			4.0	1.77797
			4.5	1.78218
			5.0	1.77553

Mideast desert	Summer	Night	0.5	3.54770
			1.0	2.97721
			1.5	3.06661
			2.0	3.76824
			2.5	3.98637
			3.0	0.54431
			3.5	3.44719
			4.0	4.01631
			4.5	3.98119
			5.0	3.98657
Mideast desert	Summer	Day	0.5	2.74135
			1.0	1.95323
			1.5	3.42313
			2.0	3.93455
			2.5	3.92779
			3.0	3.34170
			3.5	3.89361
			4.0	4.04577
			4.5	4.13176
			5.0	3.98775
Mideast desert	Annual	Night	0.5	3.00832
			1.0	2.48724
			1.5	1.80496
			2.0	3.28748
			2.5	3.51753
			3.0	3.14780
			3.5	3.45259
			4.0	3.65231
			4.5	3.81167
			5.0	3.75729
Mideast desert	Annual	Day	0.5	2.21271
			1.0	2.95545
			1.5	2.81773
			2.0	3.40679
			2.5	3.49887
			3.0	3.12657
			3.5	3.47248
			4.0	3.68069
			4.5	3.73394
			5.0	3.61816

TABLE 8. THE SCALE PARAMETER CORRESPONDING TO THE BEST ANALYTICAL DISTRIBUTION FOR ALL WIND SPEED DISTRIBUTION CASES

Region	Season	Time Period	Height Level (km)	Scale Parameters
European lowlands	Winter	All hours	0.5	10.52280
			1.0	13.23674
			1.5	13.76583
			2.0	14.18878
			2.5	14.81256
			3.0	15.54027
			3.5	16.56613
			4.0	17.62310
			4.5	18.76522
			5.0	19.90936
European lowlands	Annual	All hours	0.5	2.63915
			1.0	3.25972
			1.5	3.42868
			2.0	3.56763
			2.5	3.74912
			3.0	3.95533
			3.5	4.21879
			4.0	14.91398
			4.5	15.87218
			5.0	16.84511
European Highlands	Winter	All Hours	0.5	2.29426
			1.0	10.29712
			1.5	12.23363
			2.0	13.03796
			2.5	13.72103
			3.0	14.52975
			3.5	15.59311
			4.0	16.76794
			4.5	17.92975
			5.0	19.10730
European highlands	Annual	All hours	0.5	4.55167
			1.0	3.07453
			1.5	3.63359
			2.0	3.92955
			2.5	4.18699
			3.0	12.35809
			3.5	13.28000
			4.0	14.31750
			4.5	15.33360
			5.0	16.34973

Mideast desert	Summer	Night	0.5	2.33842
			1.0	2.19361
			1.5	2.24858
			2.0	1.72230
			2.5	1.78385
			3.0	1.89340
			3.5	2.33097
			4.0	2.16897
			4.5	2.34215
			5.0	2.52840
Mideast desert	Summer	Day	0.5	9.18078
			1.0	7.42801
			1.5	1.82355
			2.0	1.62747
			2.5	1.70796
			3.0	2.07340
			3.5	2.01106
			4.0	2.17162
			4.5	2.35531
			5.0	2.51934
Mideast desert	Annual	Night	0.5	2.26933
			1 0	2.30821
			1.5	7.11873
			2.0	2.03827
			2.5	2.29445
			3.0	3.01649
			3.5	2.87908
			4.0	3.21601
			4.5	3.08457
			5.0	3.37354
Mideast desert	Annual	Day	0.5	7.53769
			1.0	2.01991
			1.5	2.11044
			2.0	1.99963
			2.5	2.21907
			3.0	2.91417
			3.5	2.82217
			4.0	3.16577
			4.5	3.49970
			5.0	3.82600

5. ANALYSIS RESULTS

5.1 European Lowlands

The observed noncalm wind speed and analytical distributions along with the observed and analytical cumulative distributions for the European Lowlands are depicted in figures 1 through 20. The figures correspond to winter and annual time periods for the 10 height levels. The upper part of each figure depicts the observed and analytical distributions while the lower part of the figure depicts the observed and analytical cumulative distributions. In each figure the differences between the observed and analytical values are also plotted. The observed distributions are indicated by a dashed line, the analytical distributions by a solid line, and the difference between them by a dotted line.

The figures depict only the noncalm part of the wind speed distributions. The number of noncalm wind observations used to fit the analytical distributions to the observed wind speed distributions is displayed in each figure. In addition, the best analytical probability distribution and the corresponding scale and shape parameters are listed in each figure.

Of the 20 different height level and season combinations there were 13 cases where the Weibull distribution was the best and 7 where the gamma was the best (reference table 6). The Weibull distribution was the best for all winter wind speed distributions and for annual wind speed distributions for height levels above 3.5 km. The gamma distribution was the best for annual wind speed distributions for height levels up to 3.5 km. Overall, the analytical distributions perform well at describing the observed wind speed distributions for the European lowlands.

5.2 European Highlands

Figures 21 through 40 depict the same type of wind speed information for the European highlands. Of the 20 different height level and season combinations there were 15 cases where the Weibull distribution was the best and 5 where the gamma was the best (reference table 6). The Weibull distribution was best for winter wind speed distributions for height levels above 0.5 km and for all annual wind speed distributions except those with height levels greater than 0.5 km and less than 3.0 km. The gamma distribution was the best for the winter wind speed distribution at height level 0.5 km and the annual wind speed distributions for height levels greater than 0.5 km and less than 3.0 km. Overall, the analytical distributions perform well at describing the observed wind speed distributions for the European highlands.

5.3 Mideast Desert

Figures 41 through 80 depict the same type of wind speed information for the Mideast desert region except that the distributions are for summer and annual for nighttime and daytime periods. Of the 40 different height level and time period combinations there were 35 cases where the gamma distribution was the best, four for the Weibull, and one for the log-normal (reference table 6). Generally, the gamma distribution was the best for the wind speed distributions during all

seasons, time periods, and height levels with 5 exceptions. The best distribution for the summer night period for height level 3.0 km was the log-normal. The Weibull distribution was best for the summer day period for height levels 0.5 and 1.0 km, annual night period for height level 1.5 km, and annual day period for height level 0.5 km. For the Mideast the observed wind speed distributions are more "lumpy" than those for the European regions. However, the analytical distributions appear to adequately represent the observed distributions.

6. CONCLUSIONS

The observed wind speed distributions are adequately represented in all but one case by the Weibull or gamma analytical distributions for both the European and Mideast regions. Generally, the Weibull is the best distribution for Europe and the gamma the best distribution for the Mideast. One might use the analytical distributions to generate wind speeds by pseudo random numbers. In all cases, generated wind speeds in excess of 80 m/s should be discarded. Furthermore, occurrences of such large values of wind speed may indicate a problem with the pseudo random number generator.

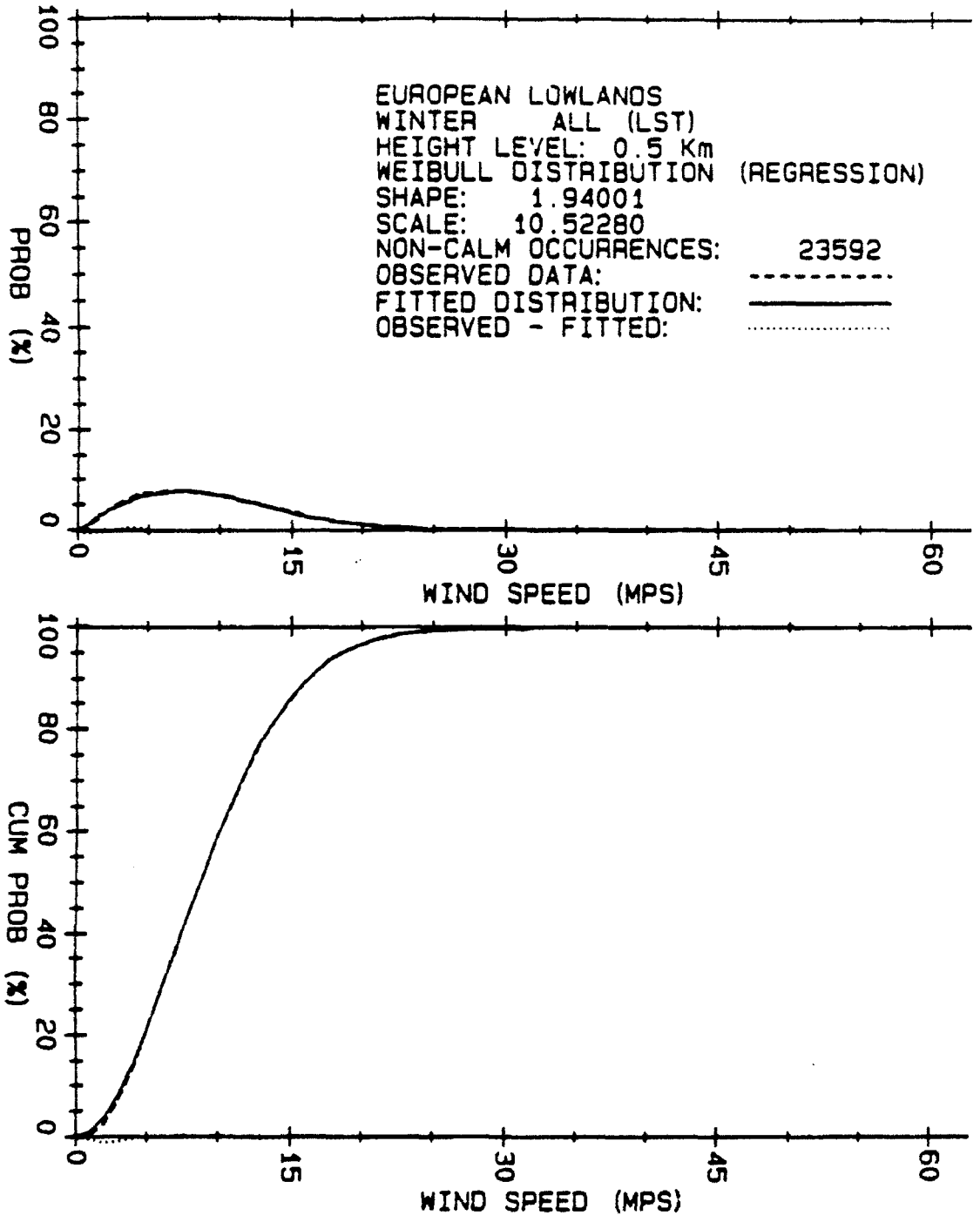

Figure 1. Regression fitted Weibull distribution for European Lowlands winter wind speeds for height level 0.5 km.

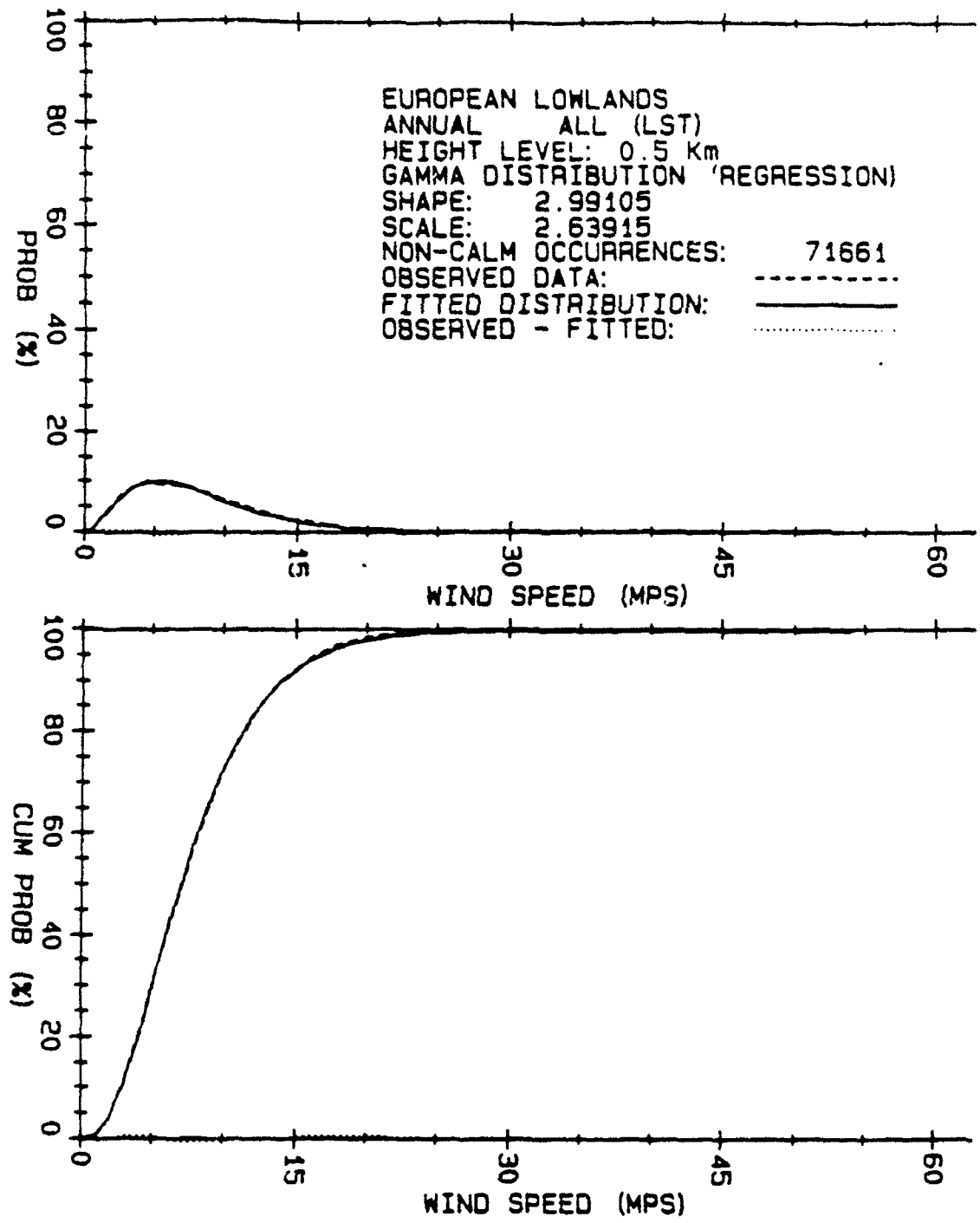

Figure 2. Regression fitted gamma distribution for European Lowlands wind speeds for height level 0.5 km.

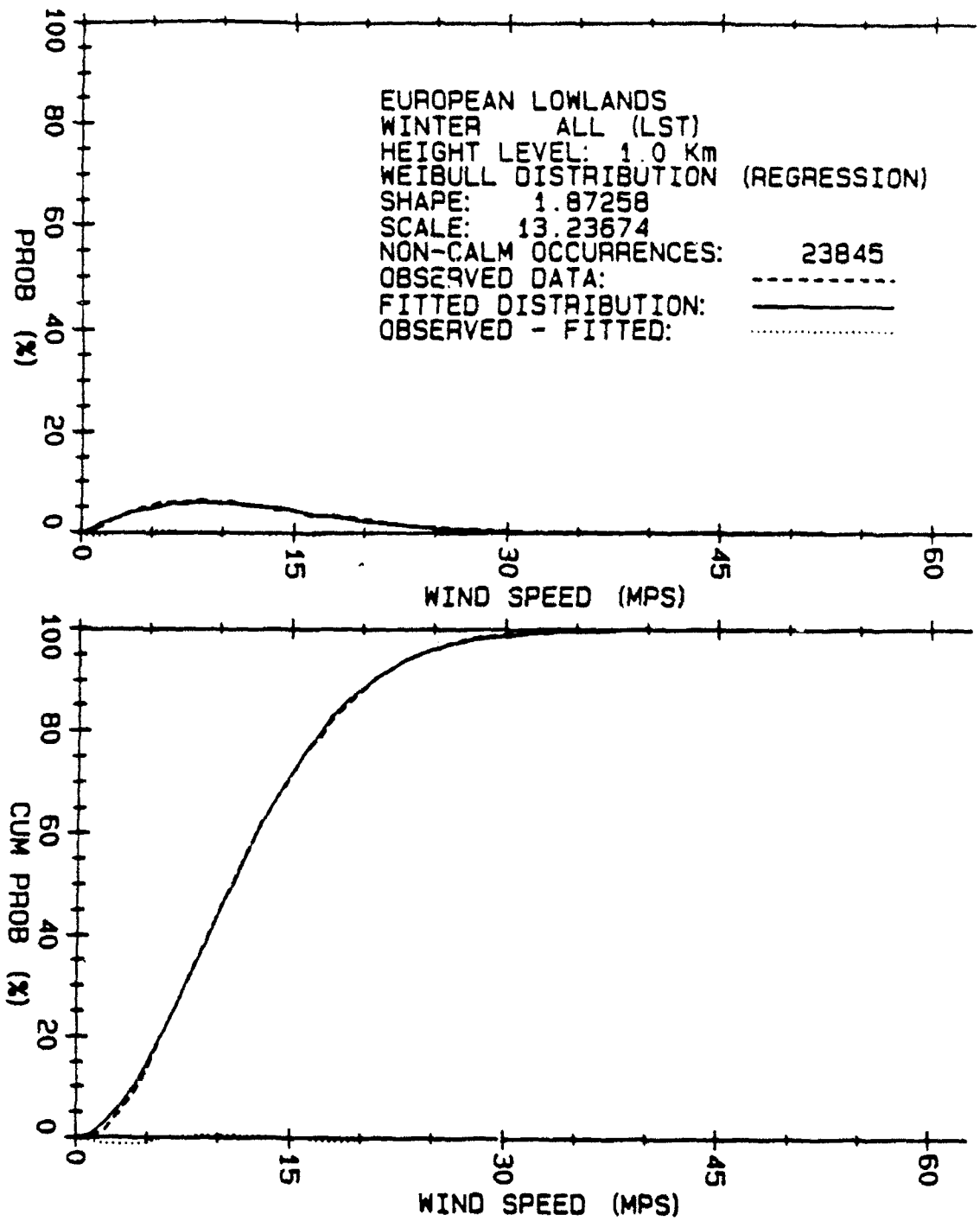

Figure 3. Regression fitted Weibull distribution for European Lowlands winter wind speeds for height level 1.0 km.

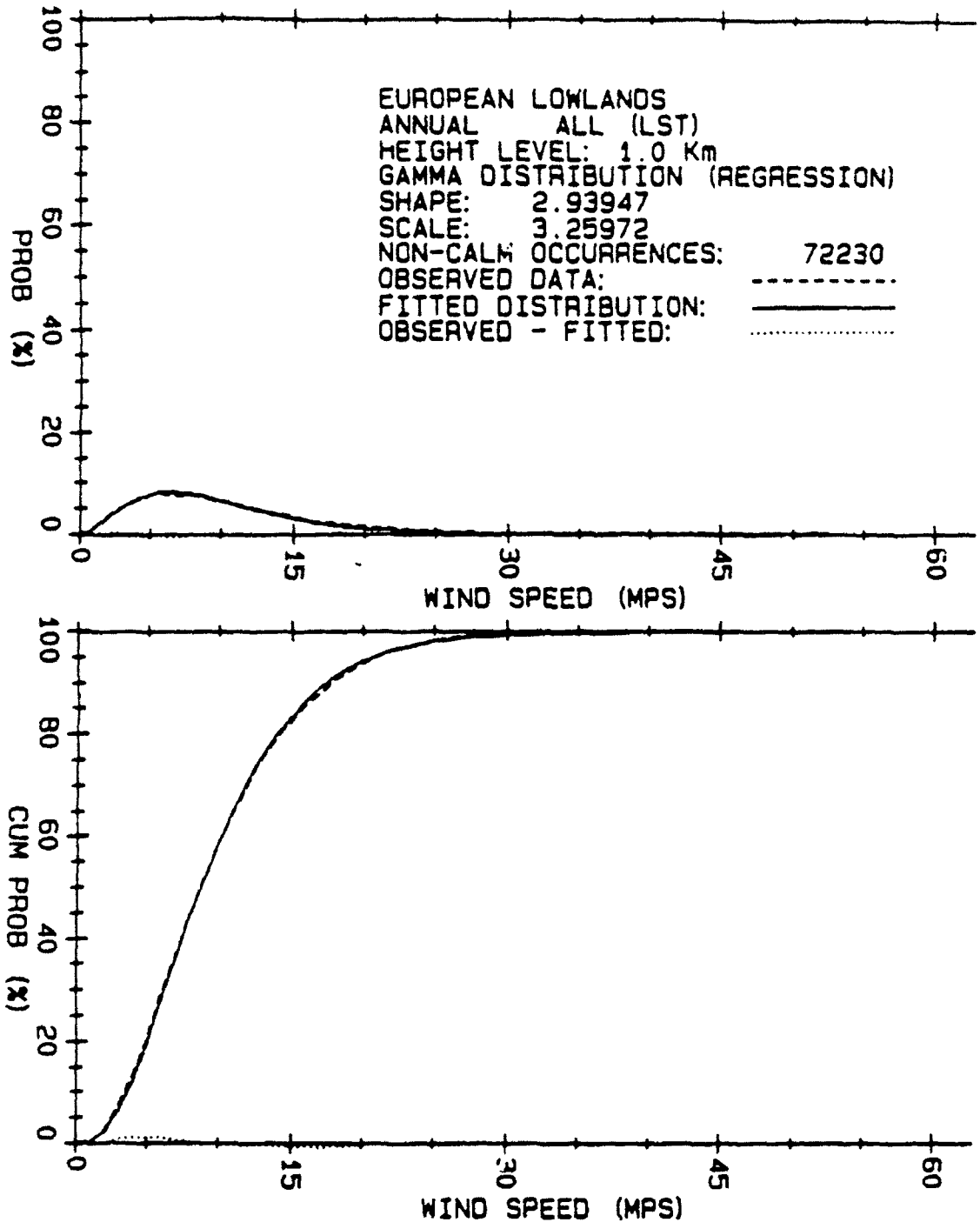

Figure 4. Regression fitted gamma distribution for European Lowlands wind speeds for height level 1.0 km.

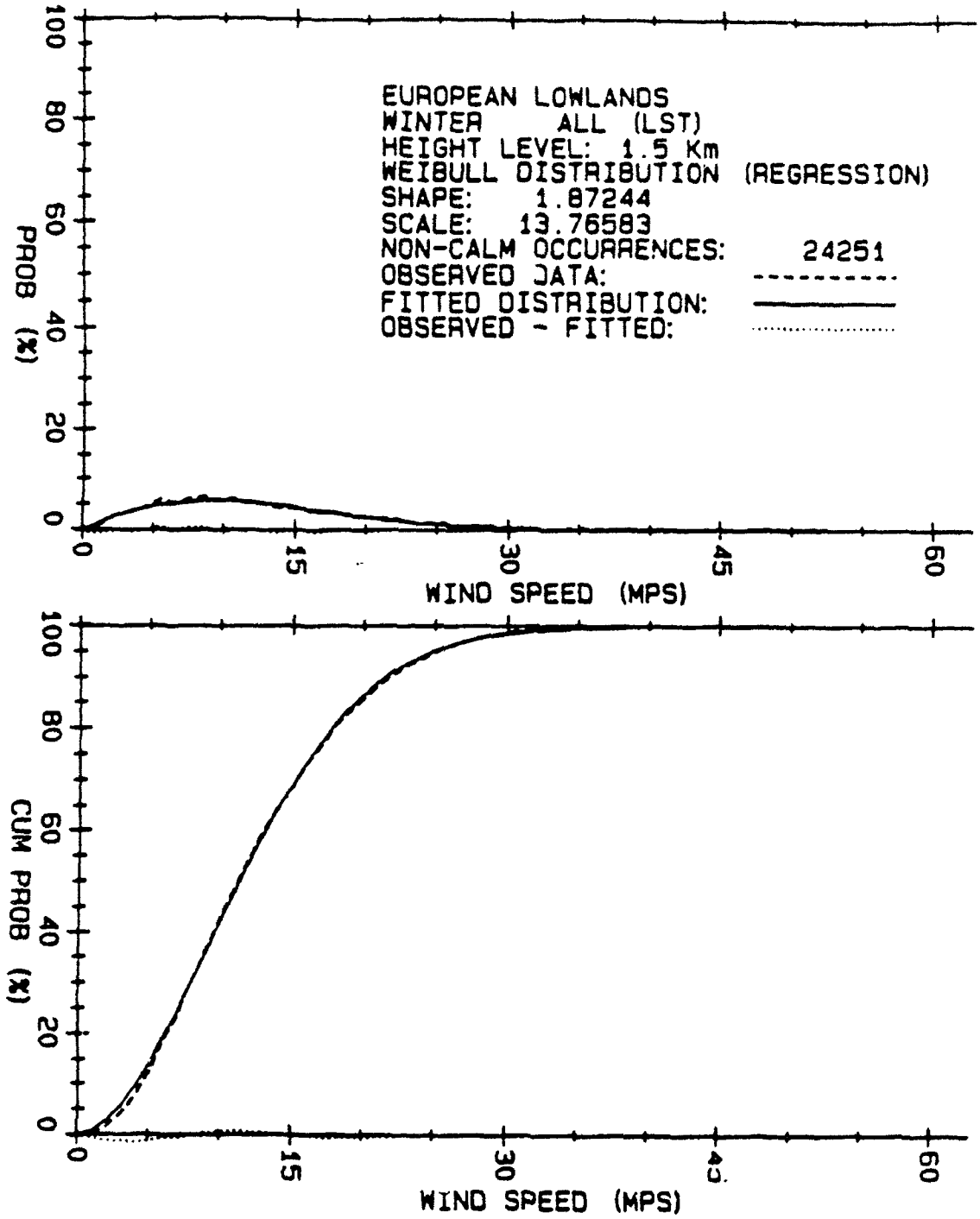

Figure 5. Regression fitted Weibull distribution for European Lowlands winter wind speeds for height level 1.5 km.

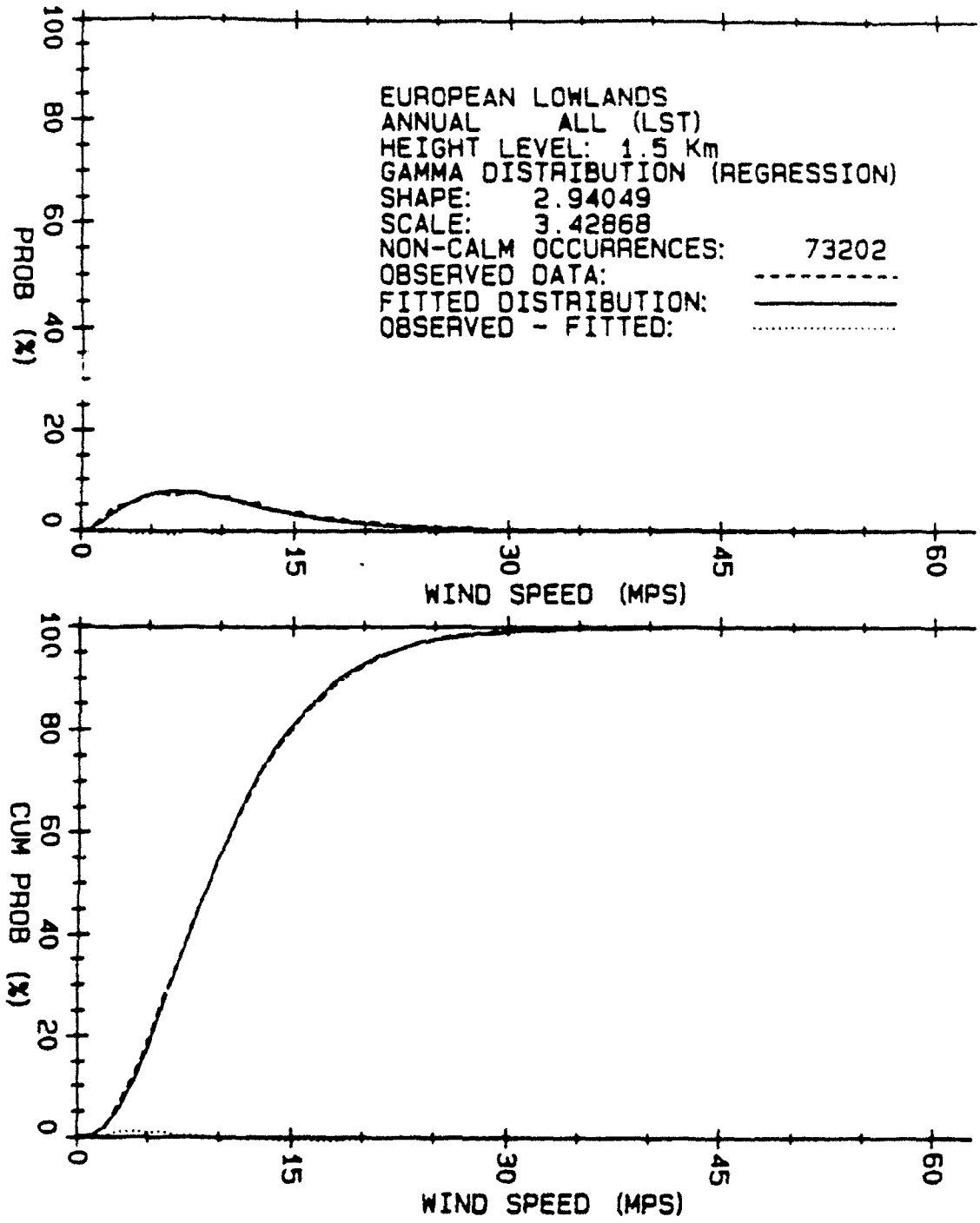

Figure 6. Regression fitted gamma distribution for European Lowlands wind speeds for height level 1.5 km.

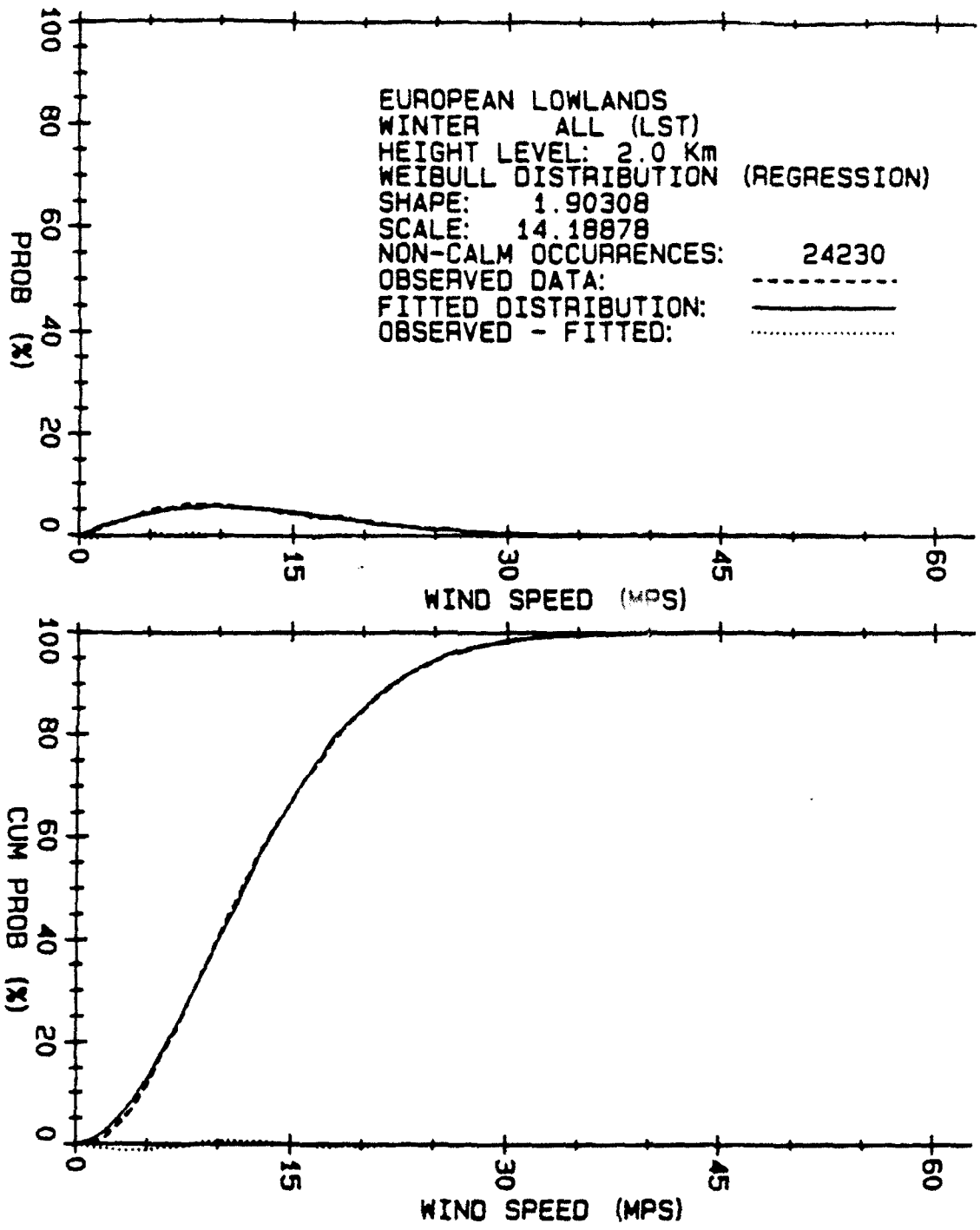

Figure 7. Regression fitted Weibull distribution for European Lowlands winter wind speeds for height level 2.0 km.

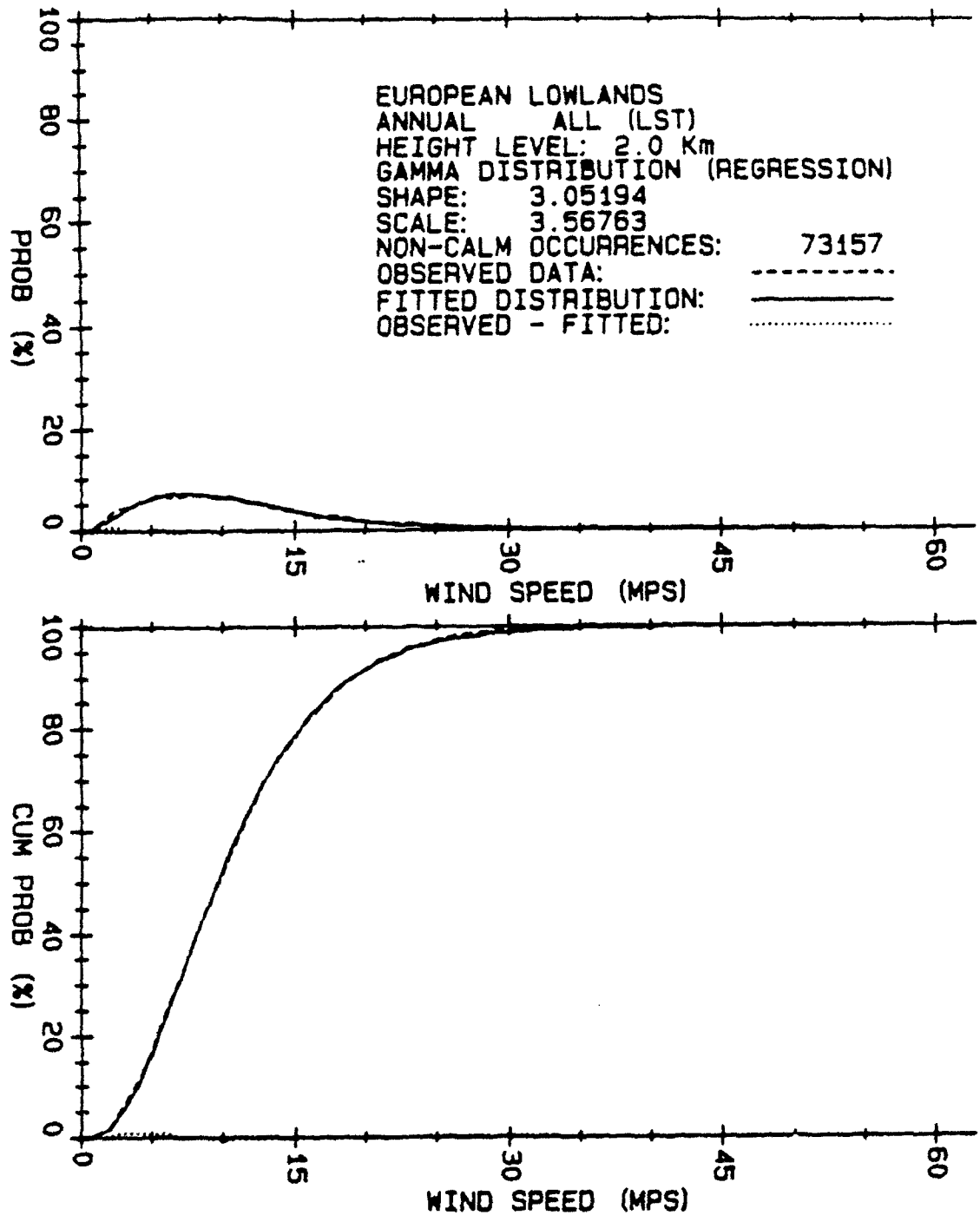

Figure 8. Regression fitted gamma distribution for European Lowlands wind speeds for height level 2.0 km.

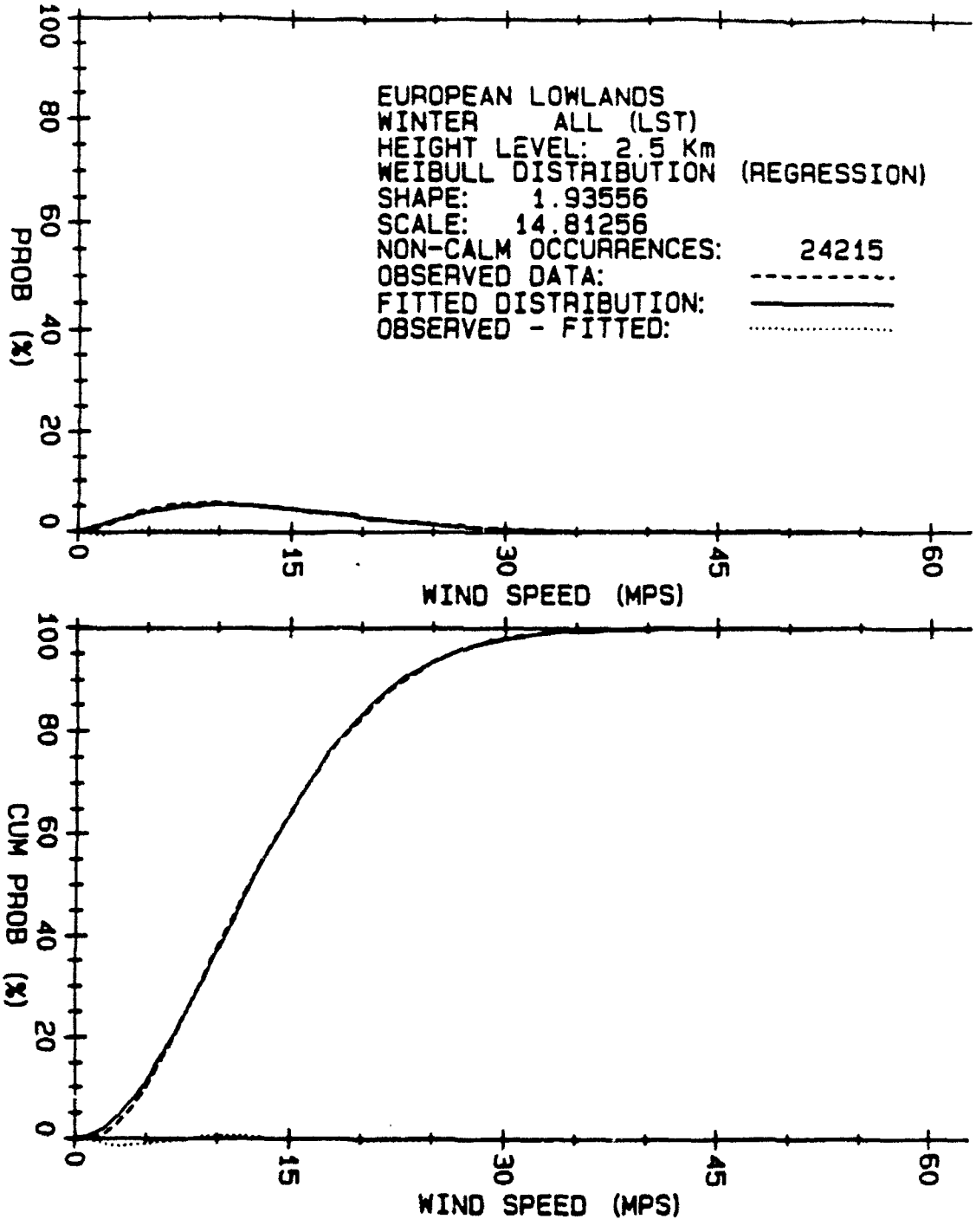

Figure 9. Regression fitted Weibull distribution for European Lowlands winter wind speeds for height level 2.5 km.

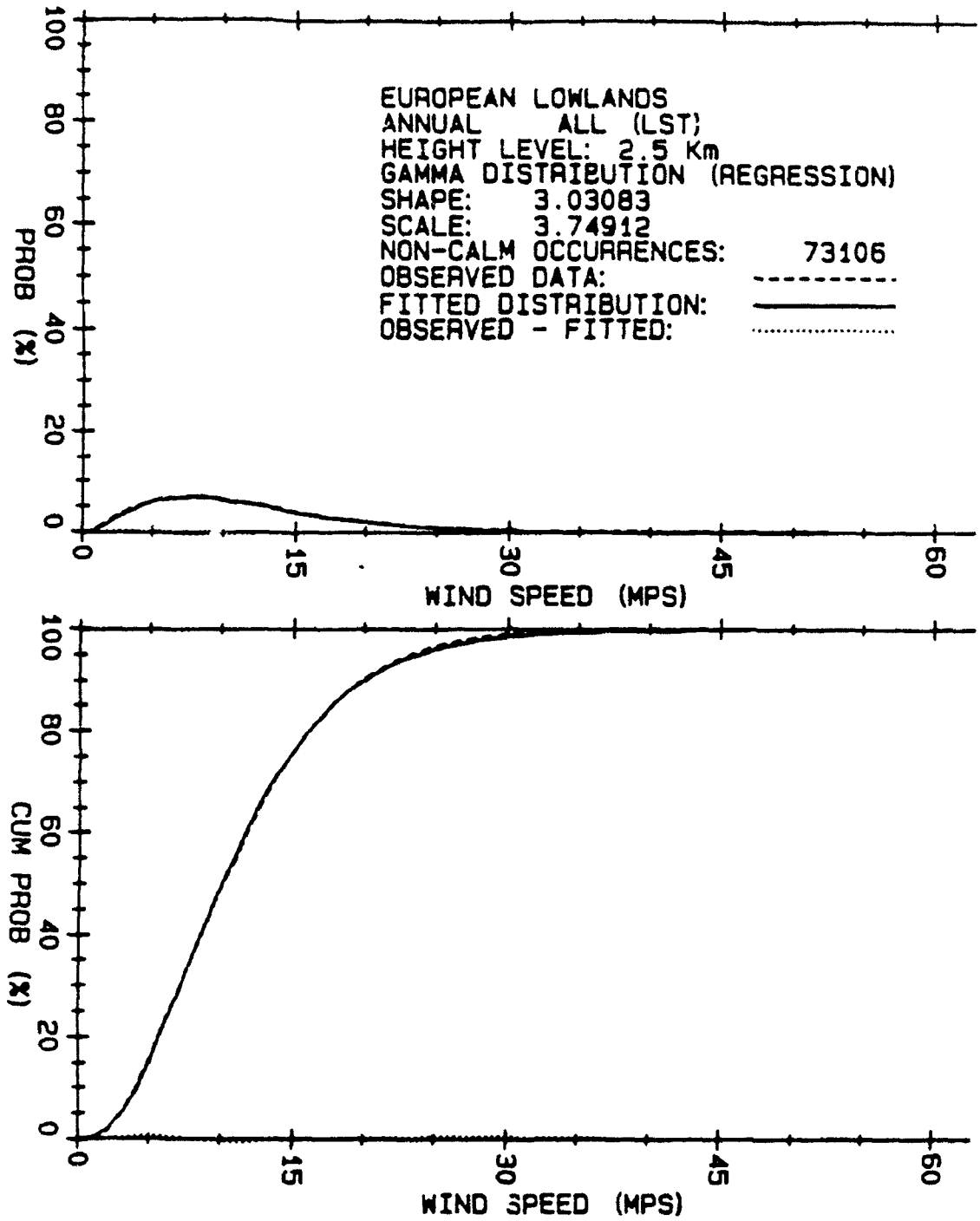

Figure 10. Regression fitted gamma distribution for European Lowlands wind speeds for height level 2.5 km.

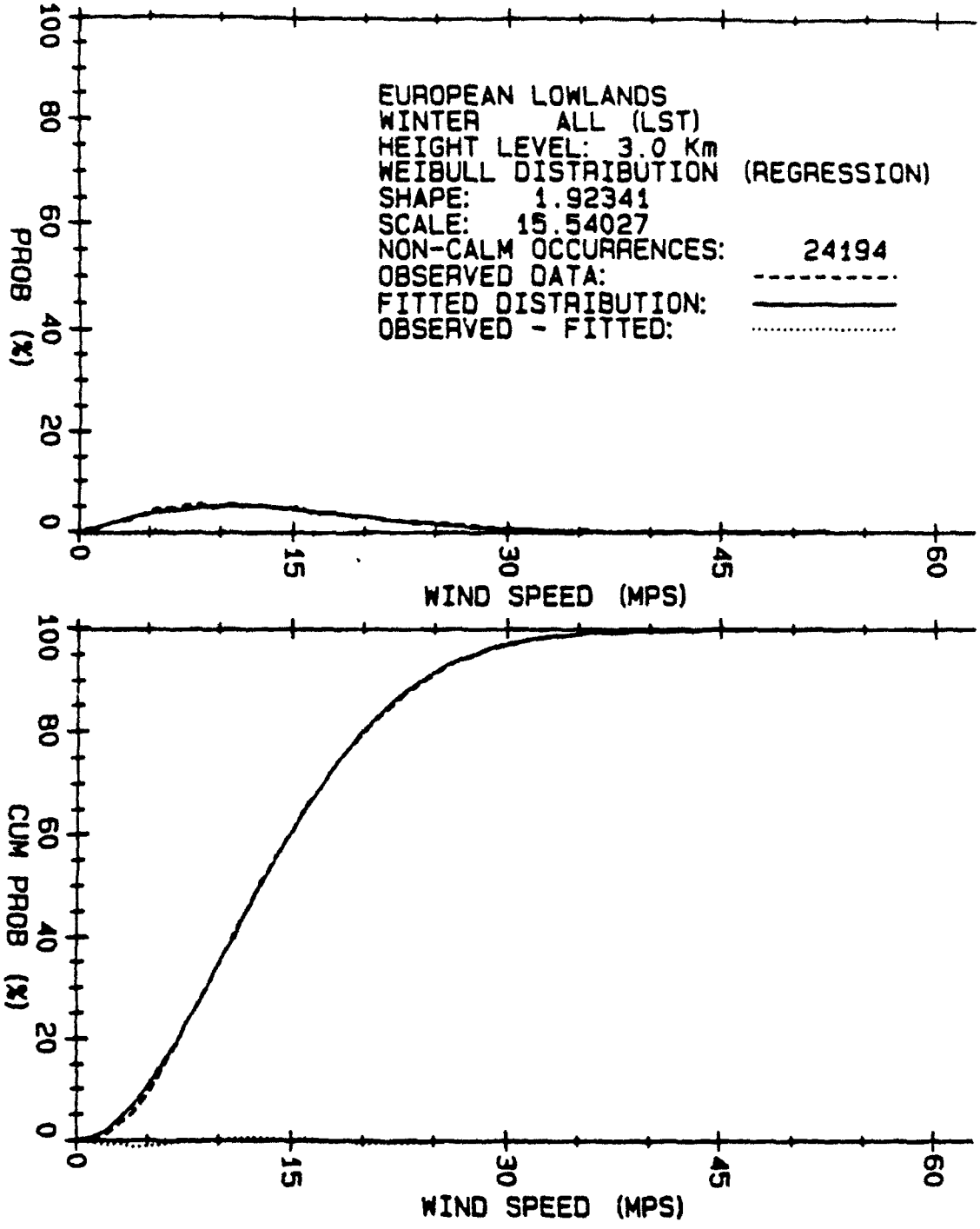

Figure 11. Regression fitted Weibull distribution for European Lowlands winter wind speeds for height level 3.0 km.

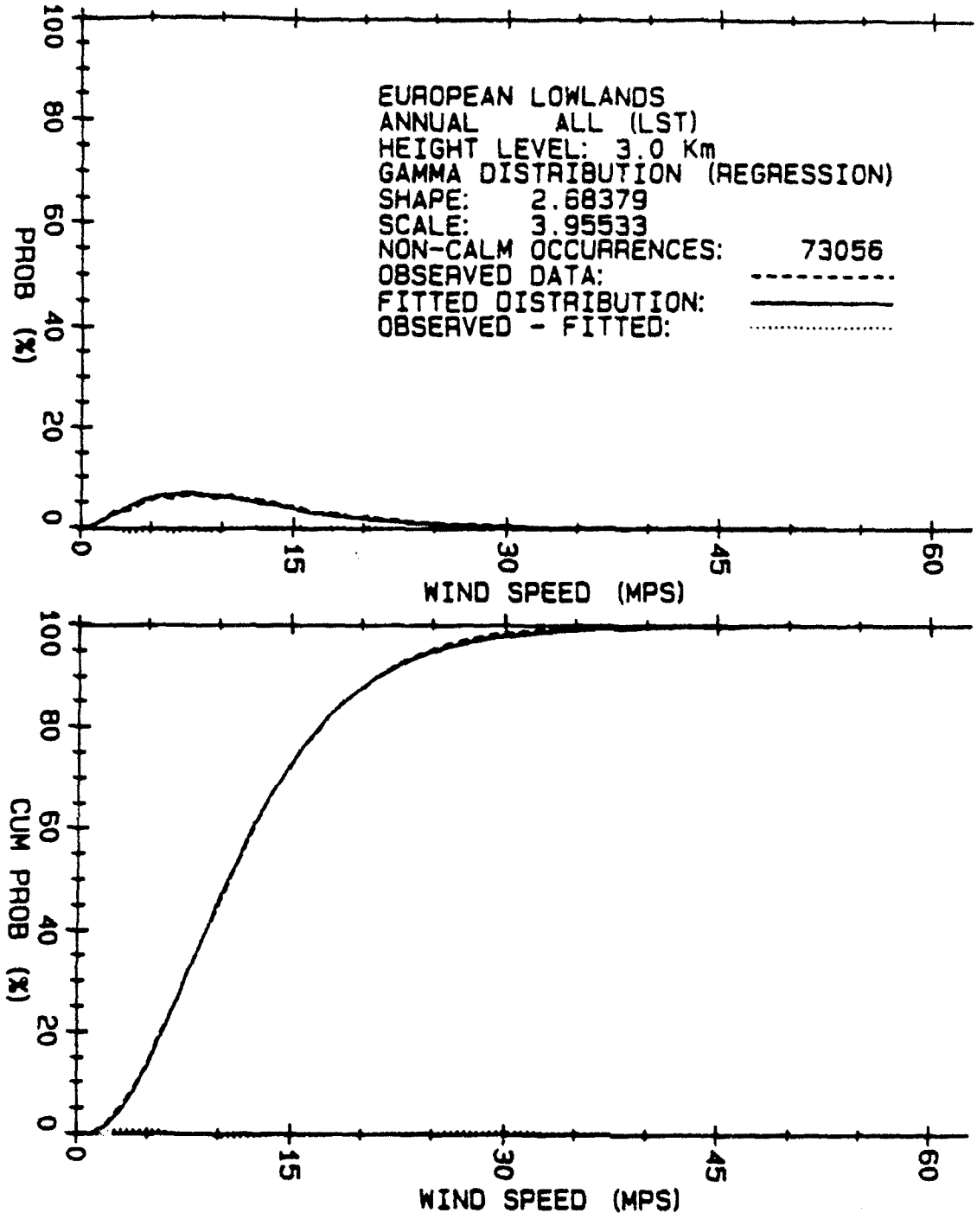

Figure 12. Regression fitted gamma distribution for European Lowlands wind speeds for height level 3.0 km.

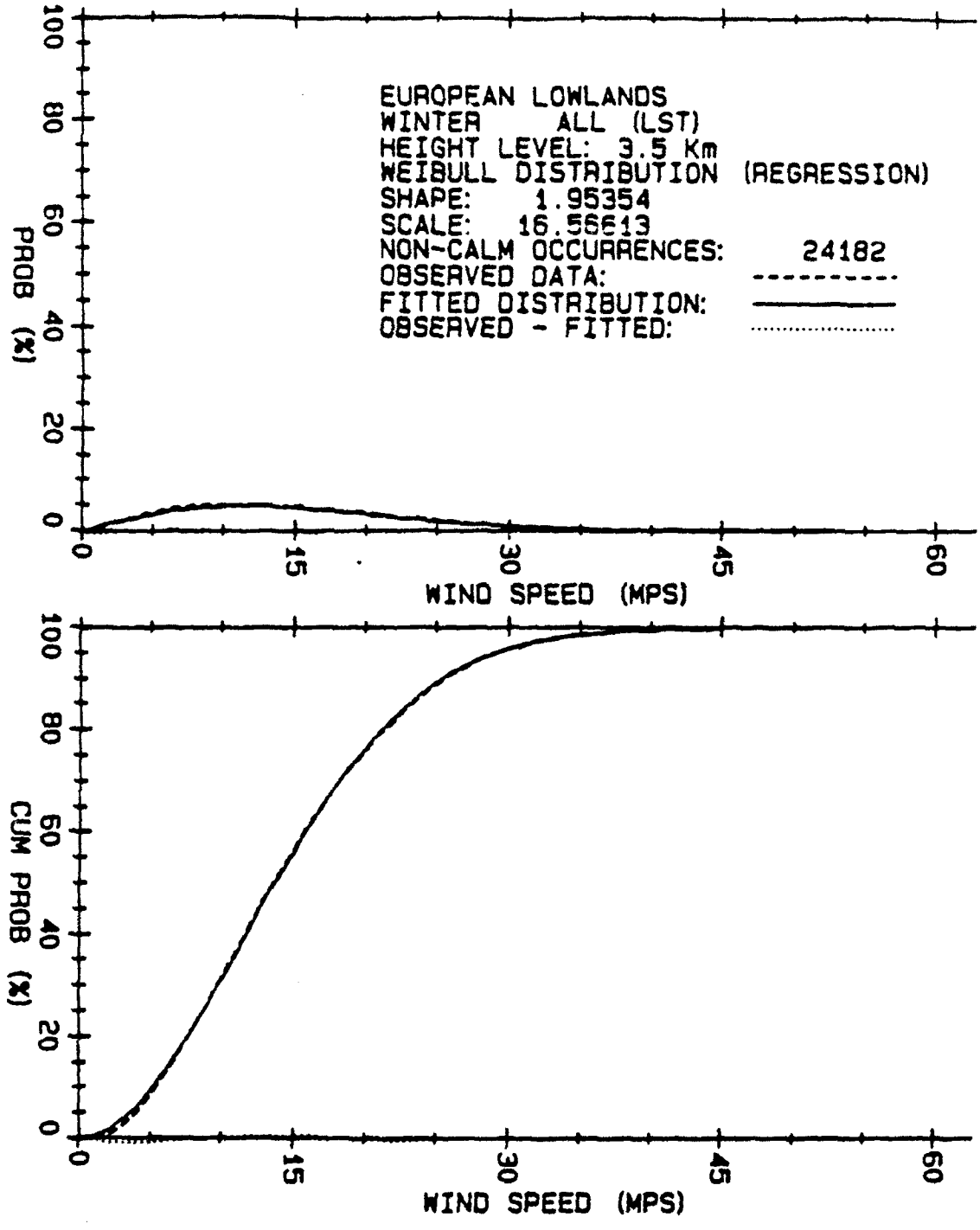

Figure 13. Regression fitted Weibull distribution for European Lowlands winter wind speeds for height level 3.5 km.

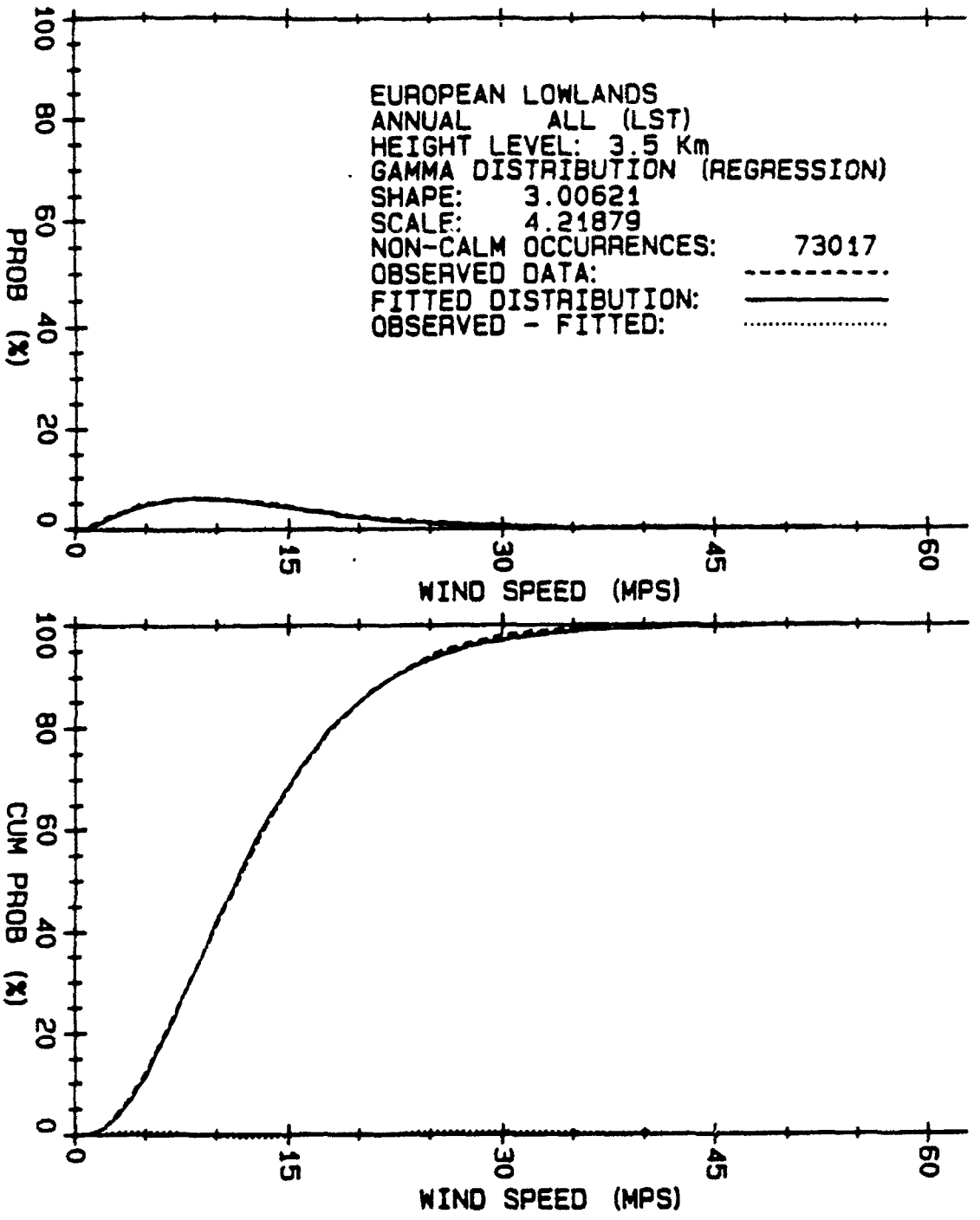

Figure 14. Regression fitted gamma distribution for European Lowlands wind speeds for height level 3.5 km.

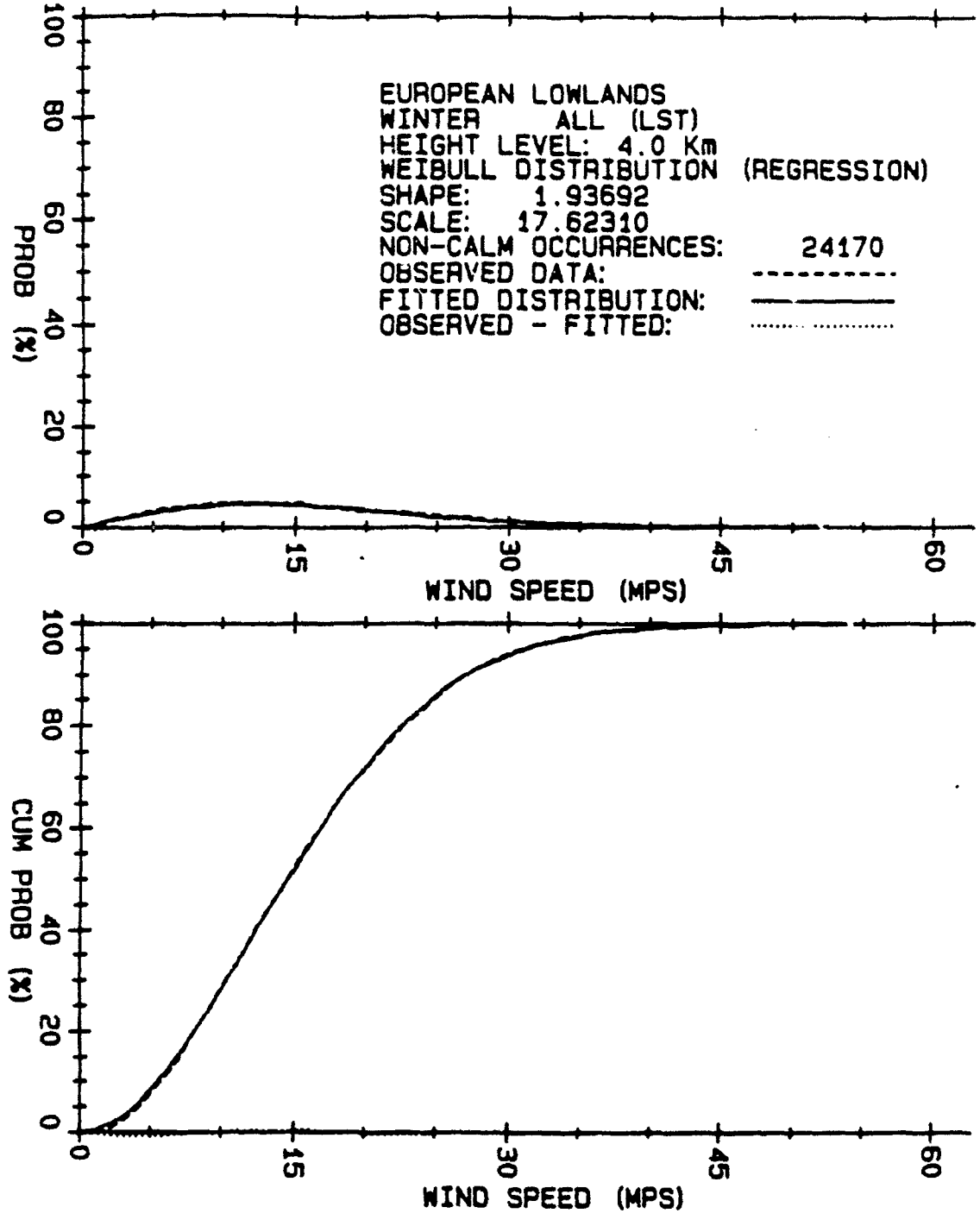

Figure 15. Regression fitted Weibull distribution for European Lowlands winter wind speeds for height level 4.0 km.

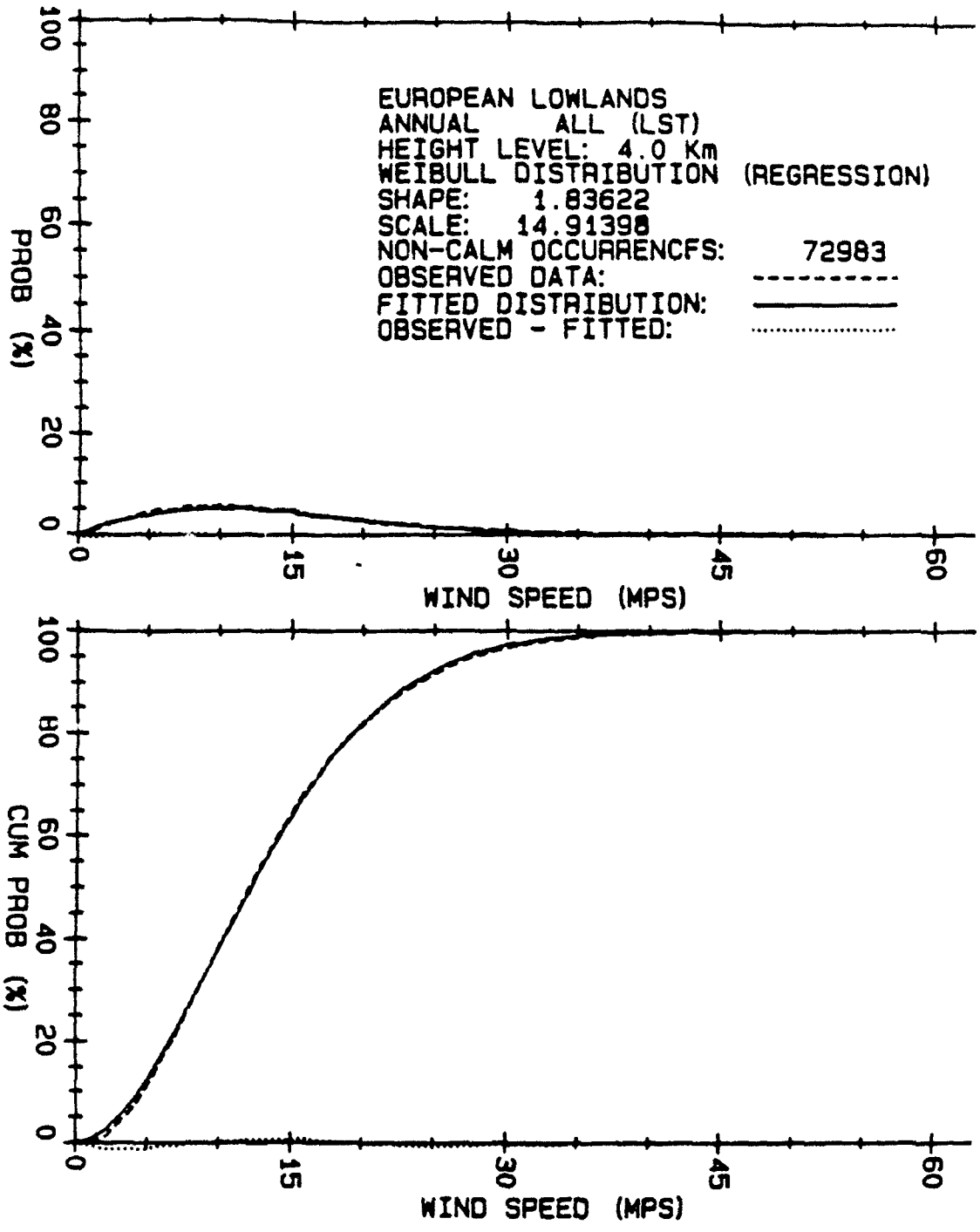

Figure 16. Regression fitted Weibull distribution for European Lowlands wind speeds for height level 4.0 km.

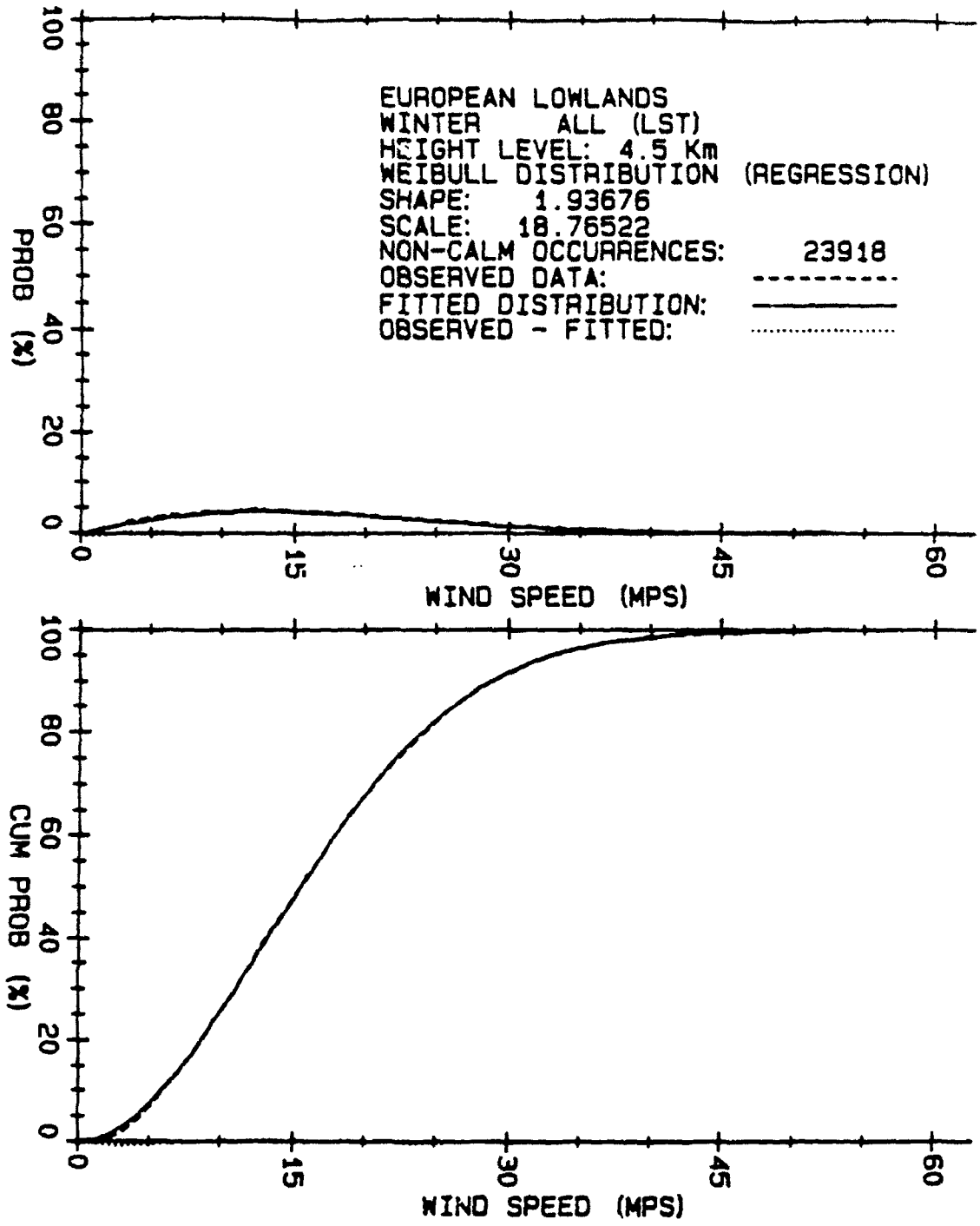

Figure 17. Regression fitted Weibull distribution for European Lowlands winter wind speeds for height level 4.5 km.

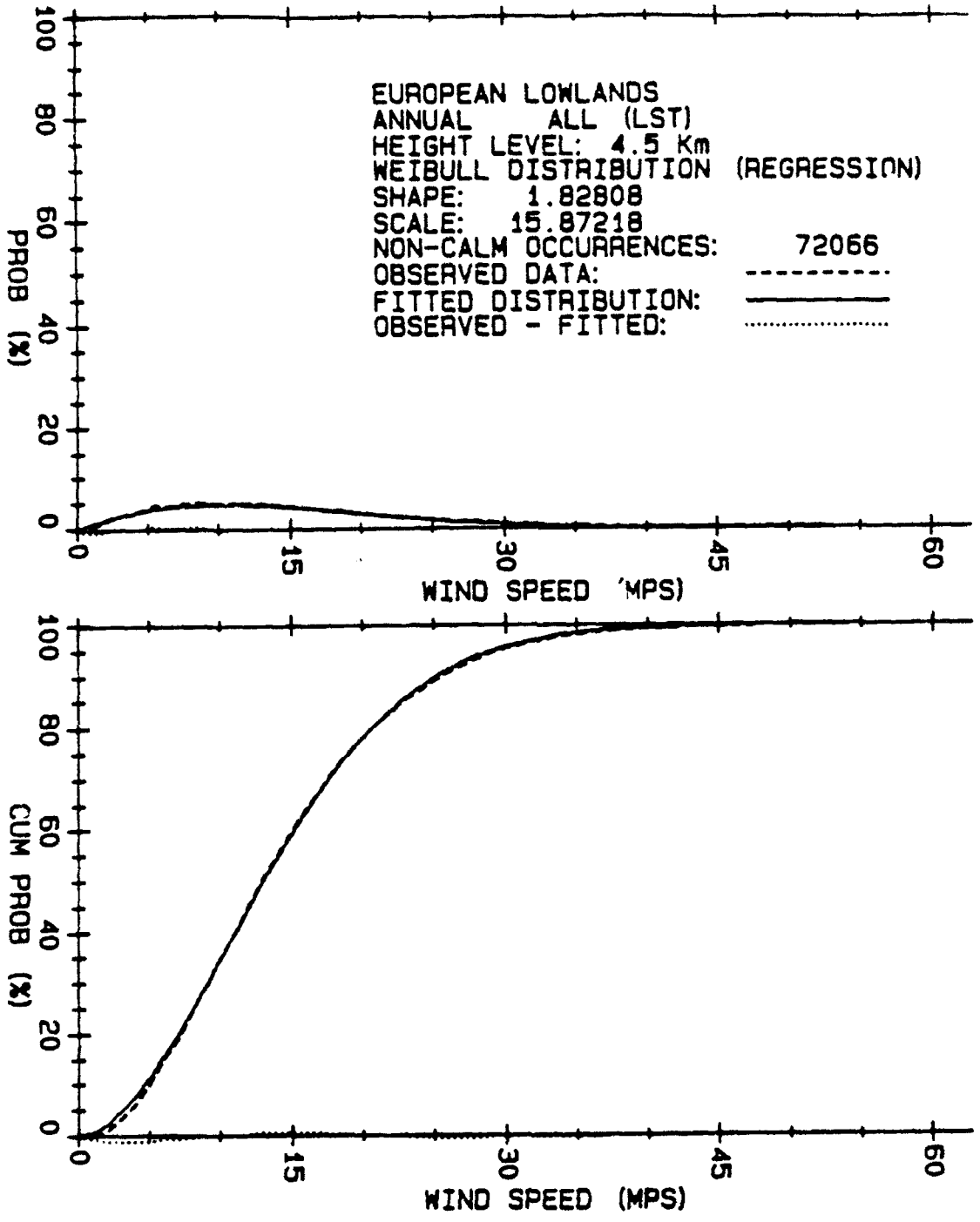

Figure 18. Regression fitted Weibull distribution for European Lowlands wind speeds for height level 4.5 km.

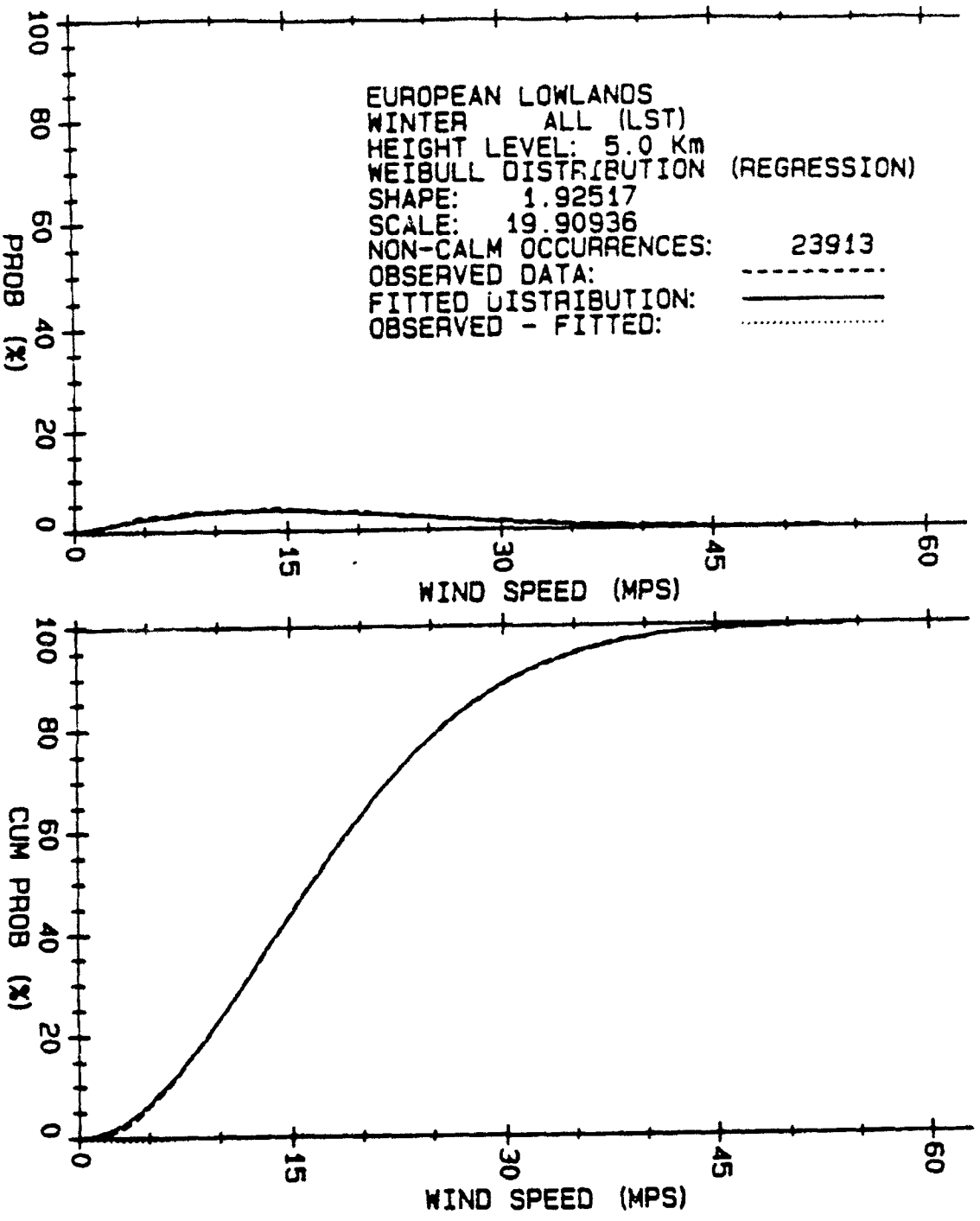

Figure 19. Regression fitted Weibull distribution for European Lowlands winter wind speeds for height level 5.0 km.

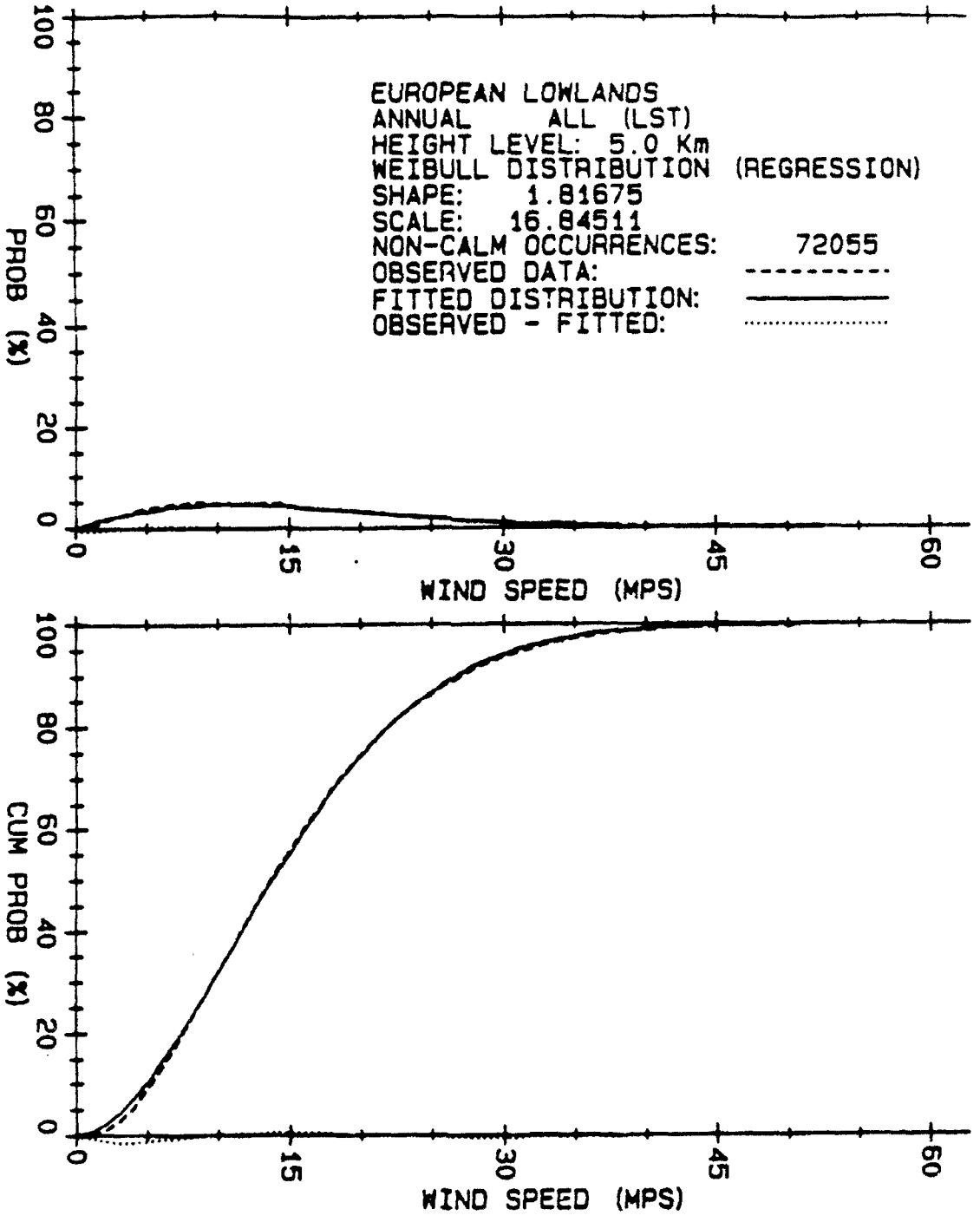

Figure 20. Regression fitted Weibull distribution for European Lowlands wind speeds for height level 5.0 km.

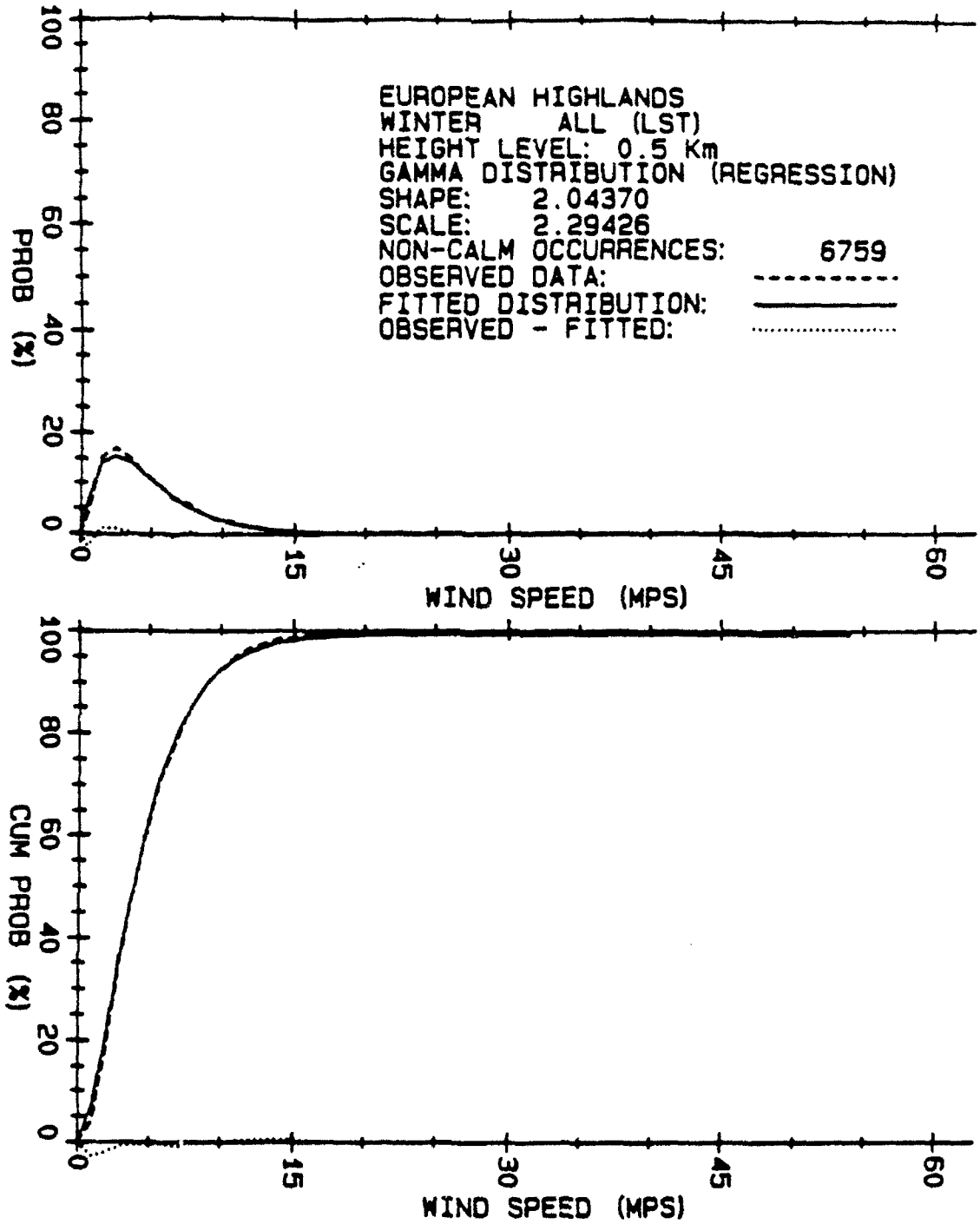

Figure 21. Regression fitted gamma distribution for European Highlands winter wind speeds for height level 0.5 km.

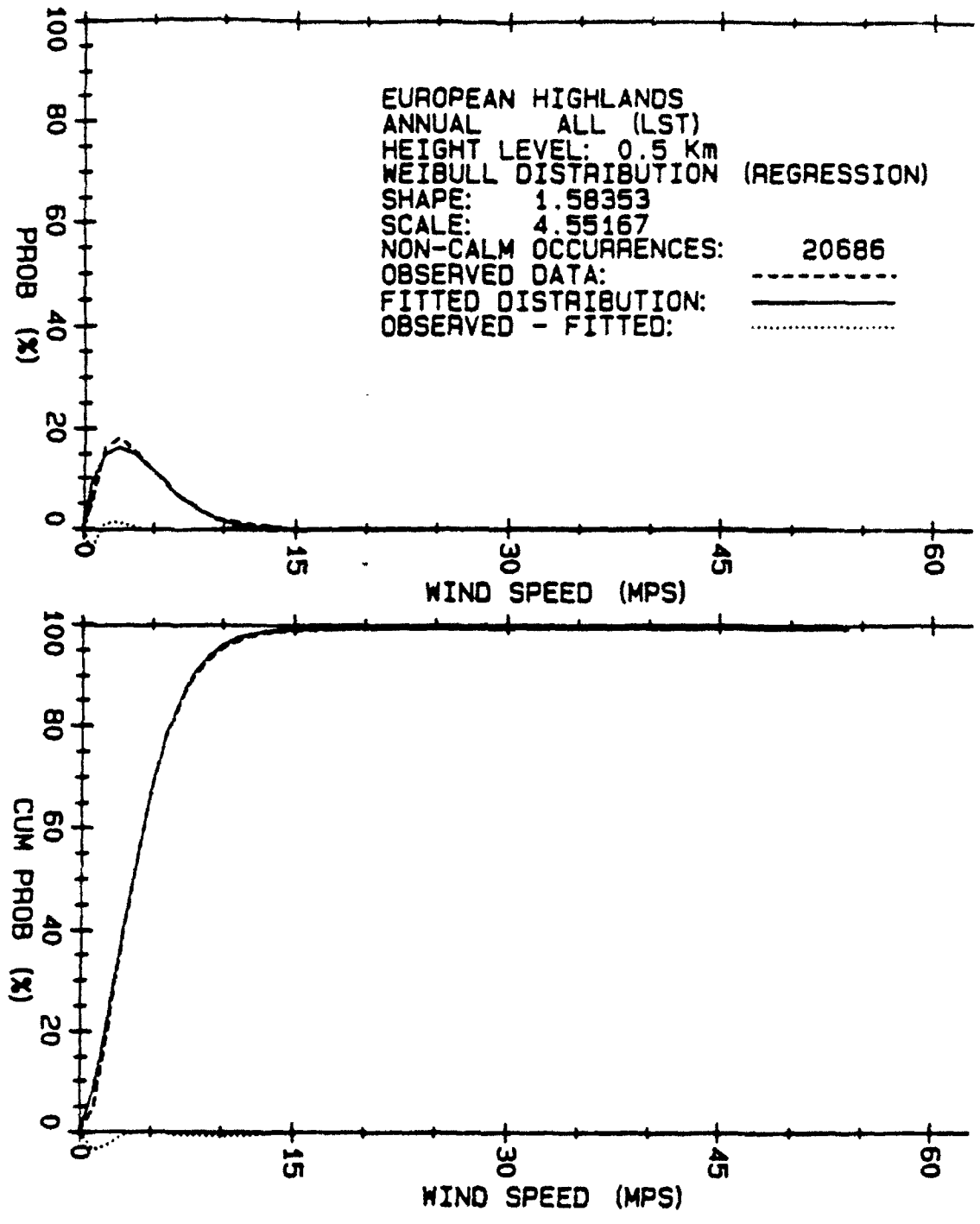

Figure 22. Regression fitted Weibull distribution for European Highlands wind speeds for height level 0.5 km.

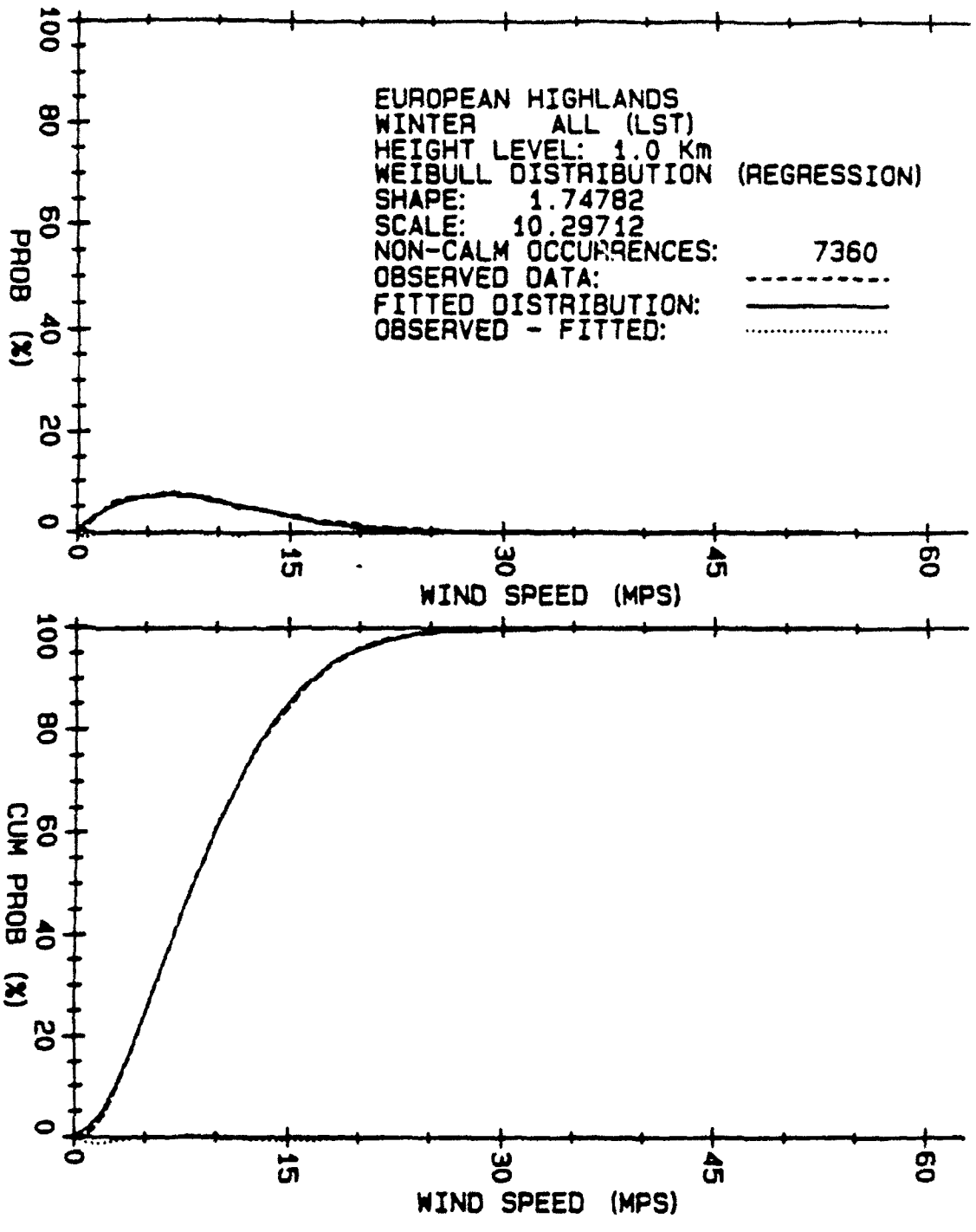

Figure 23. Regression fitted Weibull distribution for European Highlands winter wind speeds for height level 1.0 km.

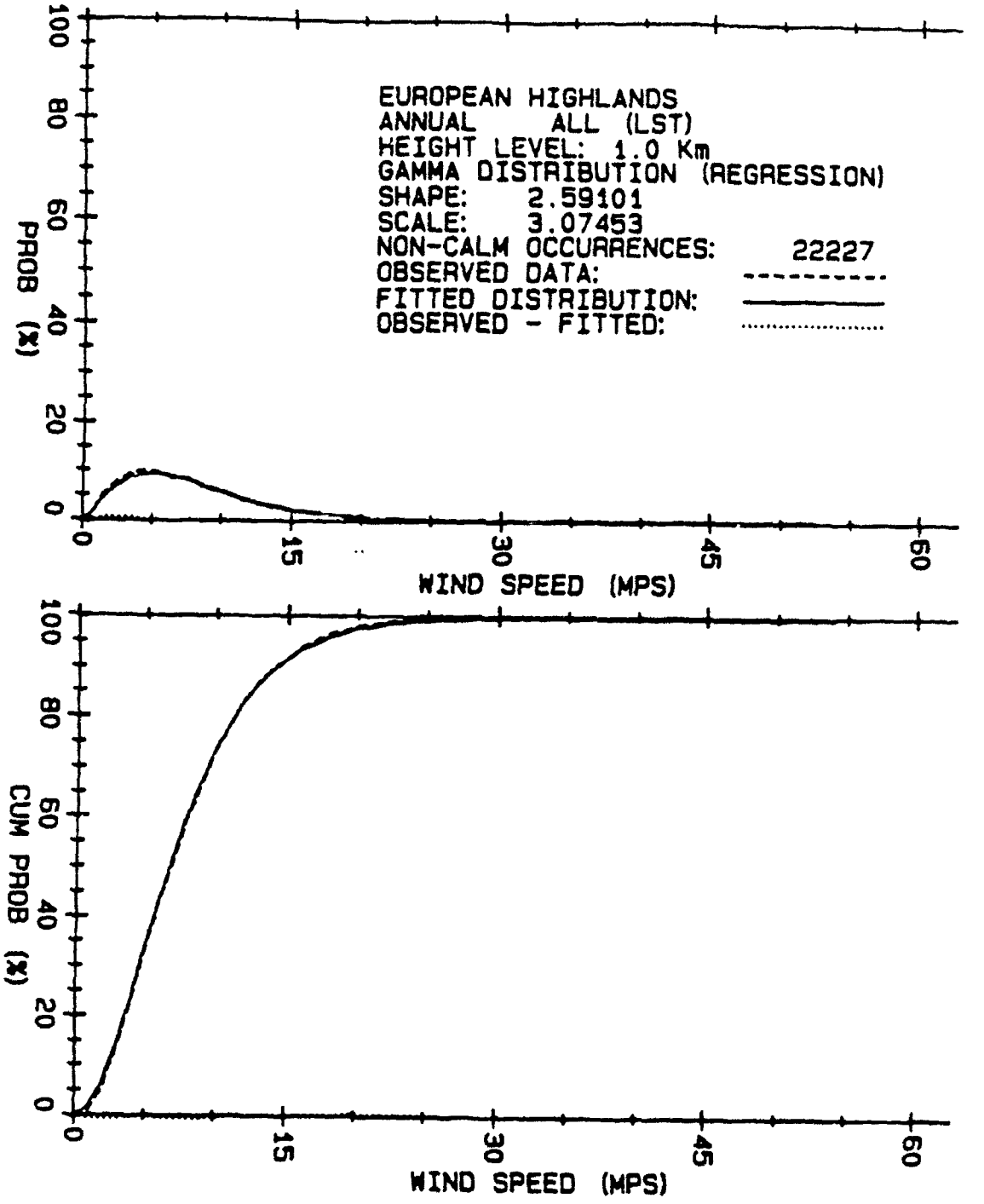

Figure 24. Regression fitted gamma distribution for European Highlands wind speeds for height level 1.0 km.

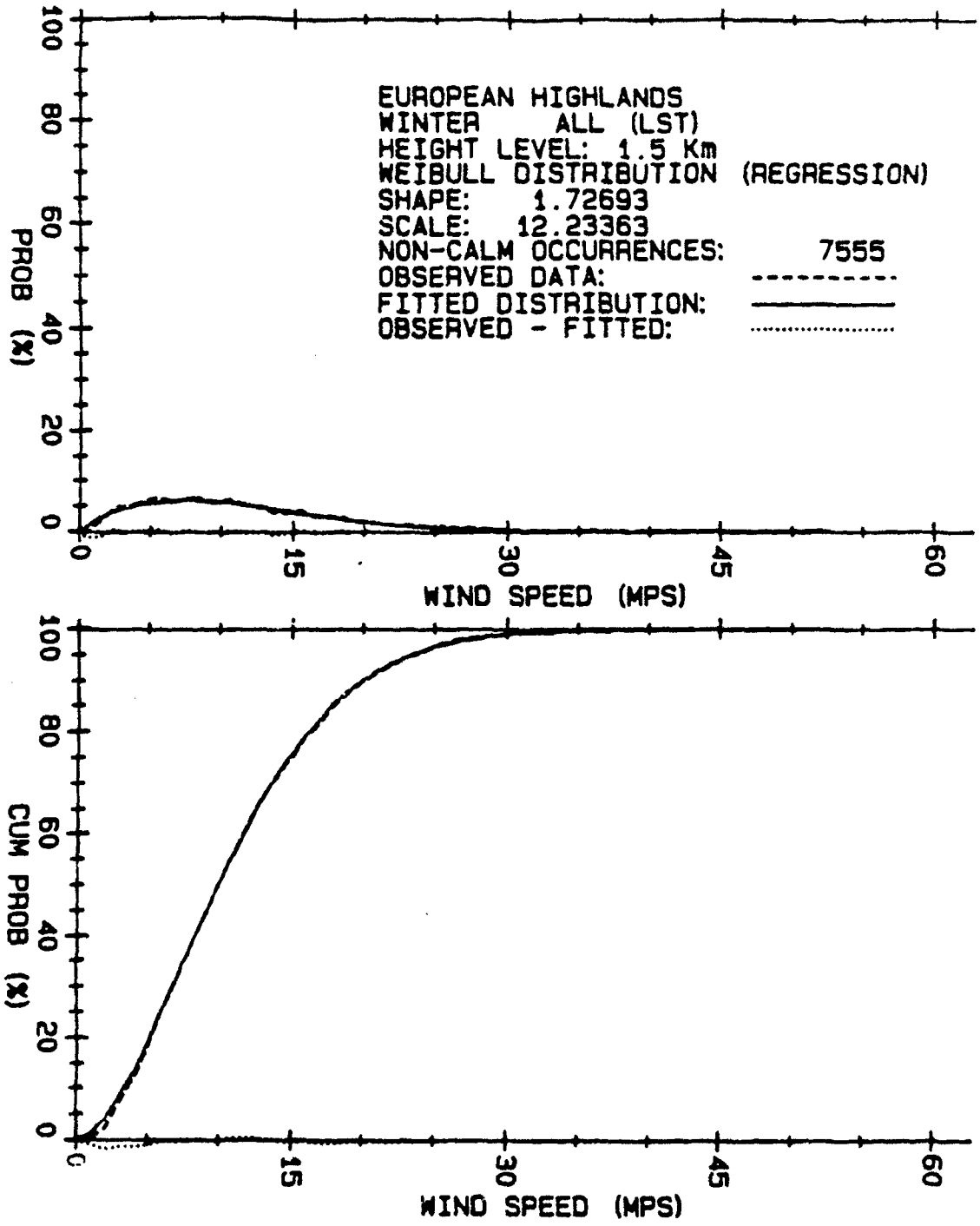

Figure 25. Regression fitted Weibull distribution for European Highlands winter wind speeds for height level 1.5 km.

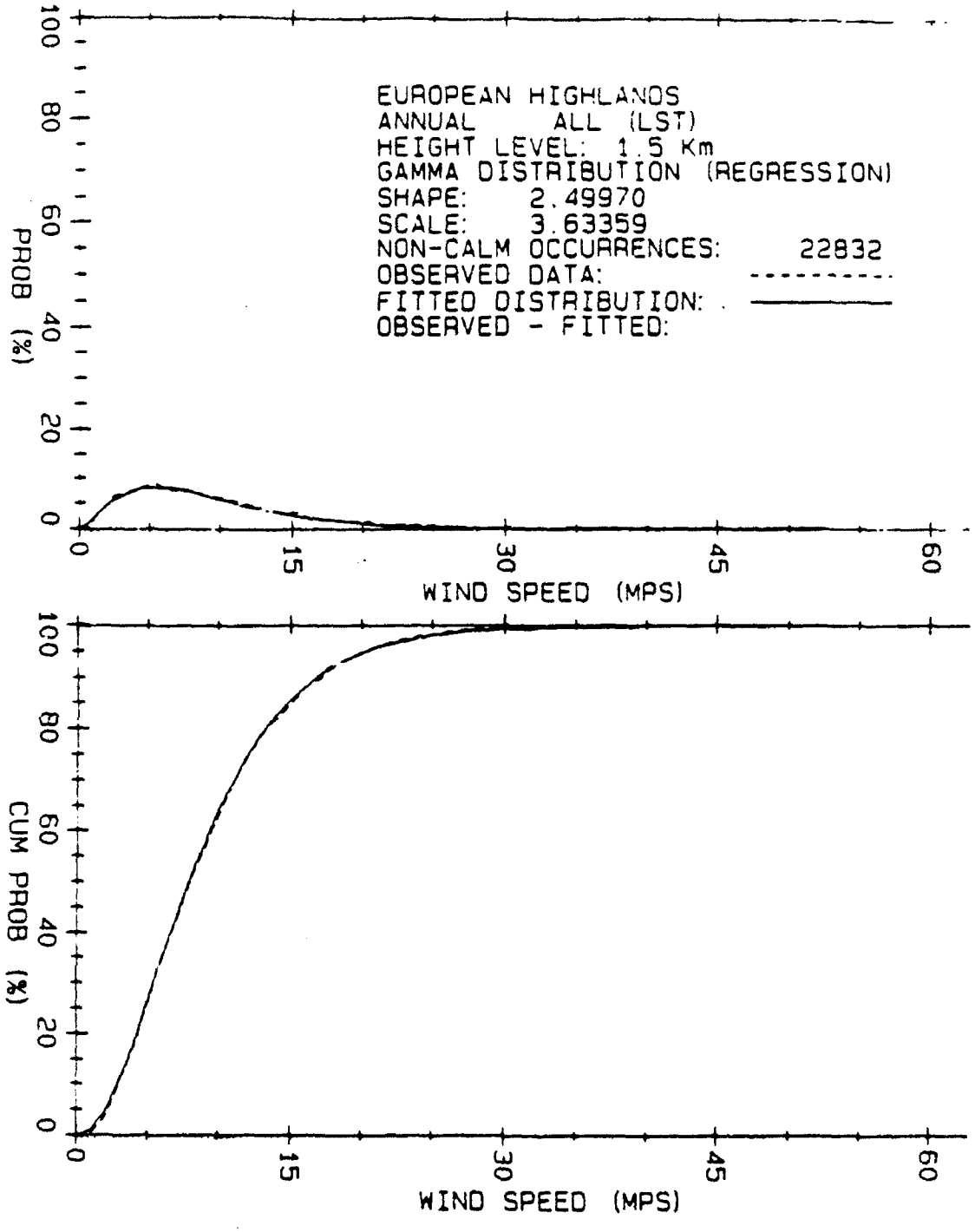

Figure 26. Regression fitted gamma distribution for European Highlands wind speeds for height level 1.5 km.

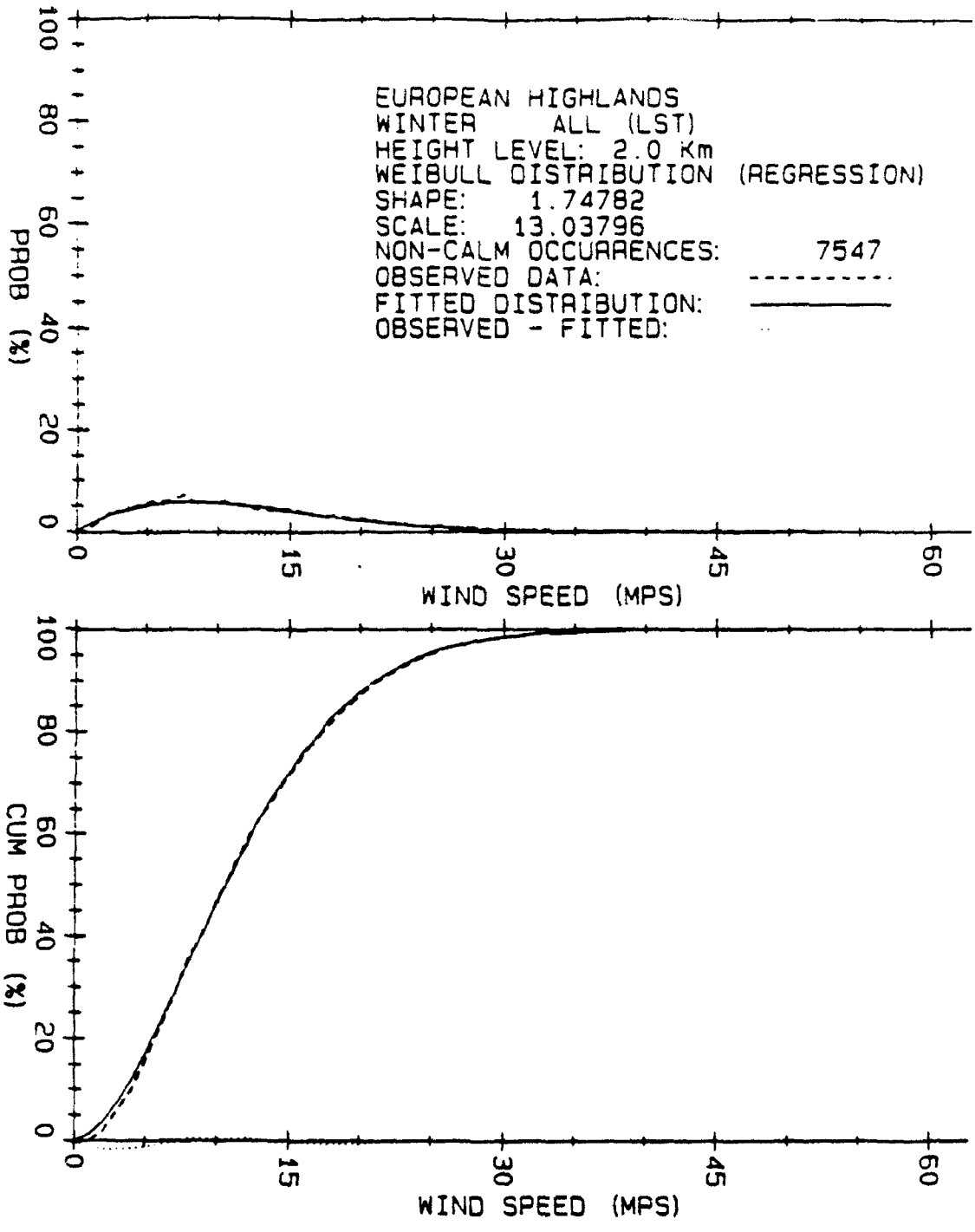

Figure 27. Regression fitted Weibull distribution for European Highlands winter wind speeds for height level 2.0 km.

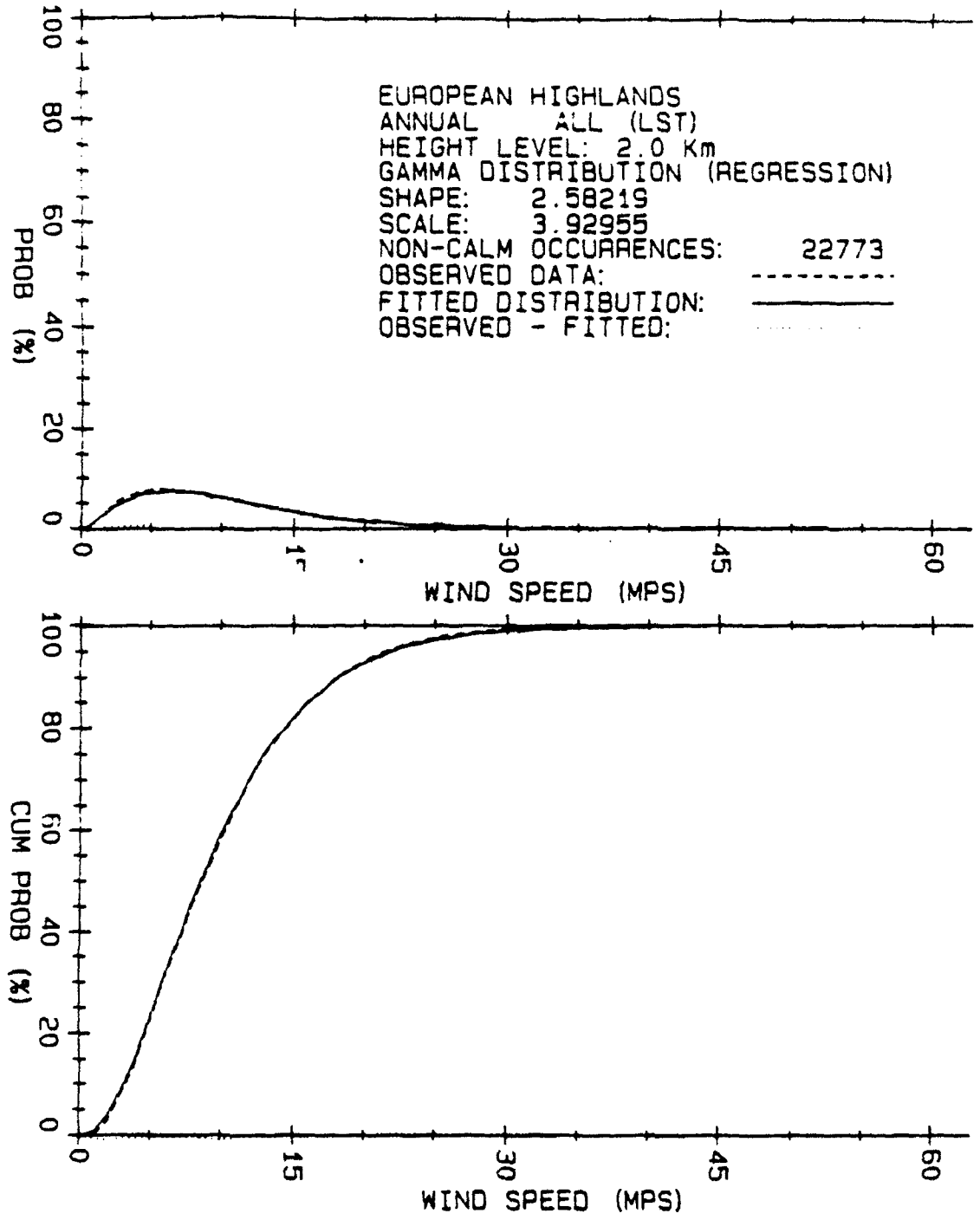

Figure 28. Regression fitted gamma distribution for European Highlands wind speeds for height level 2.0 km.

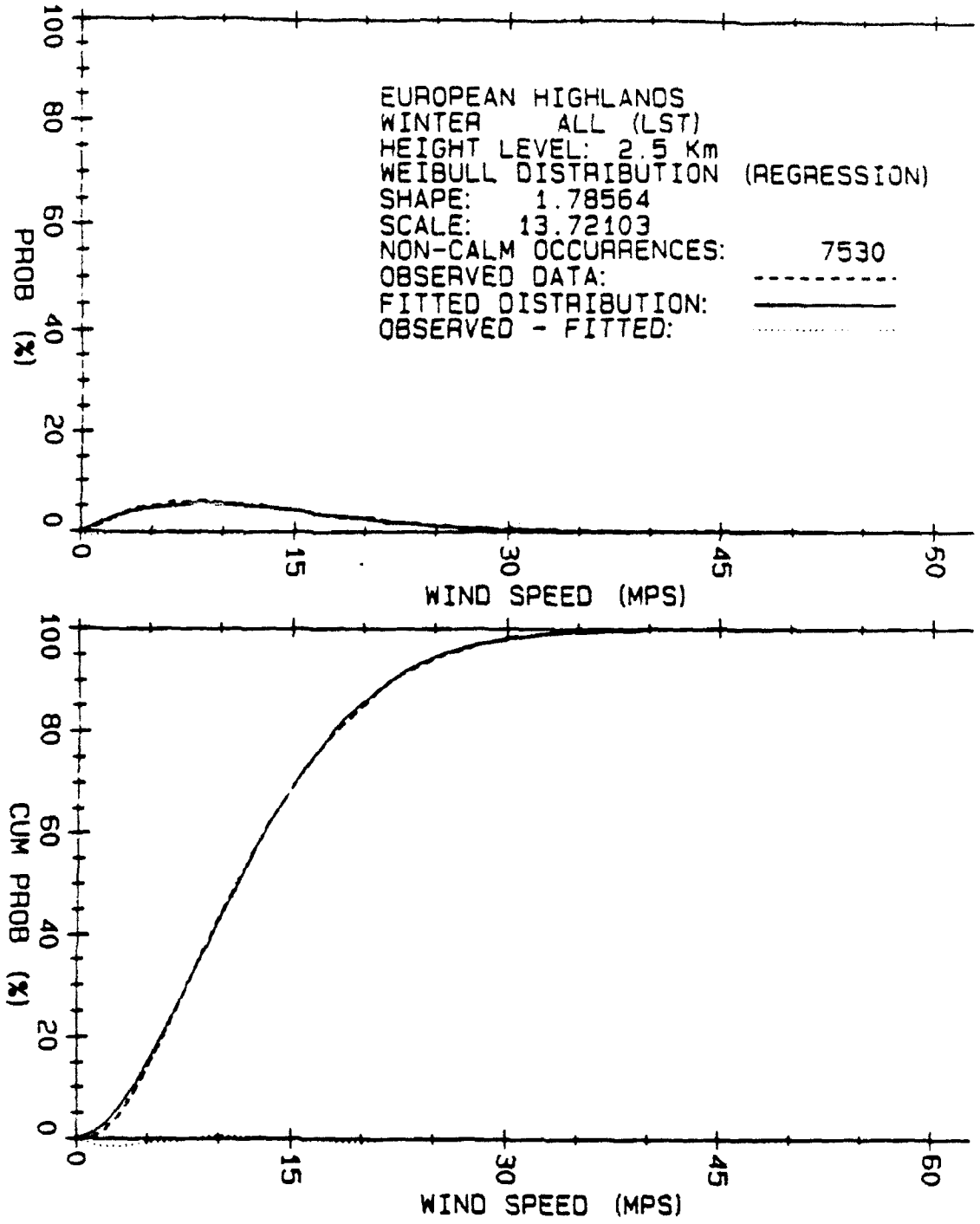

Figure 29. Regression fitted Weibull distribution for European Highlands winter wind speeds for height level 2.5 km.

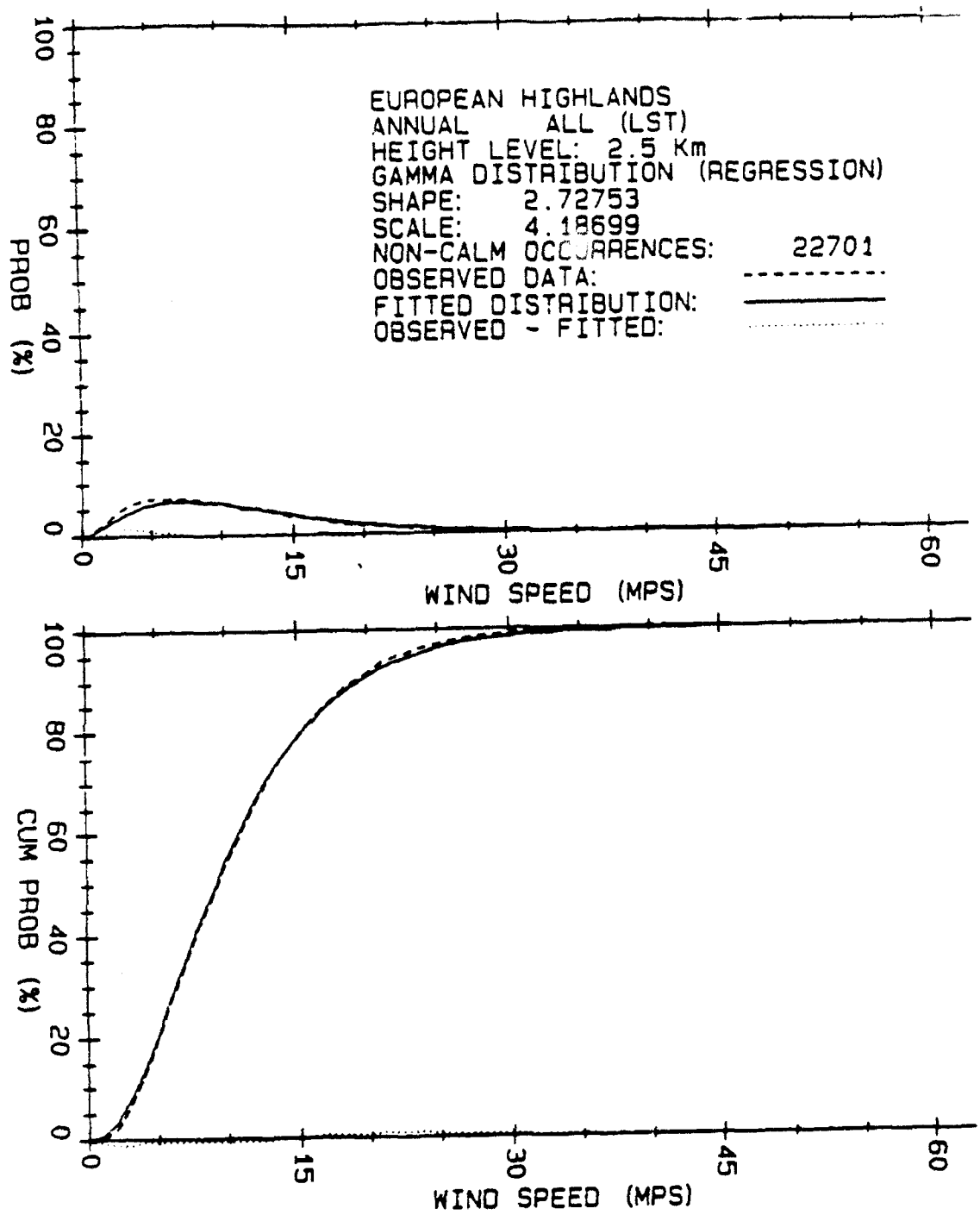

Figure 30. Regression fitted gamma distribution for European Highlands wind speeds for height level 2.5 km.

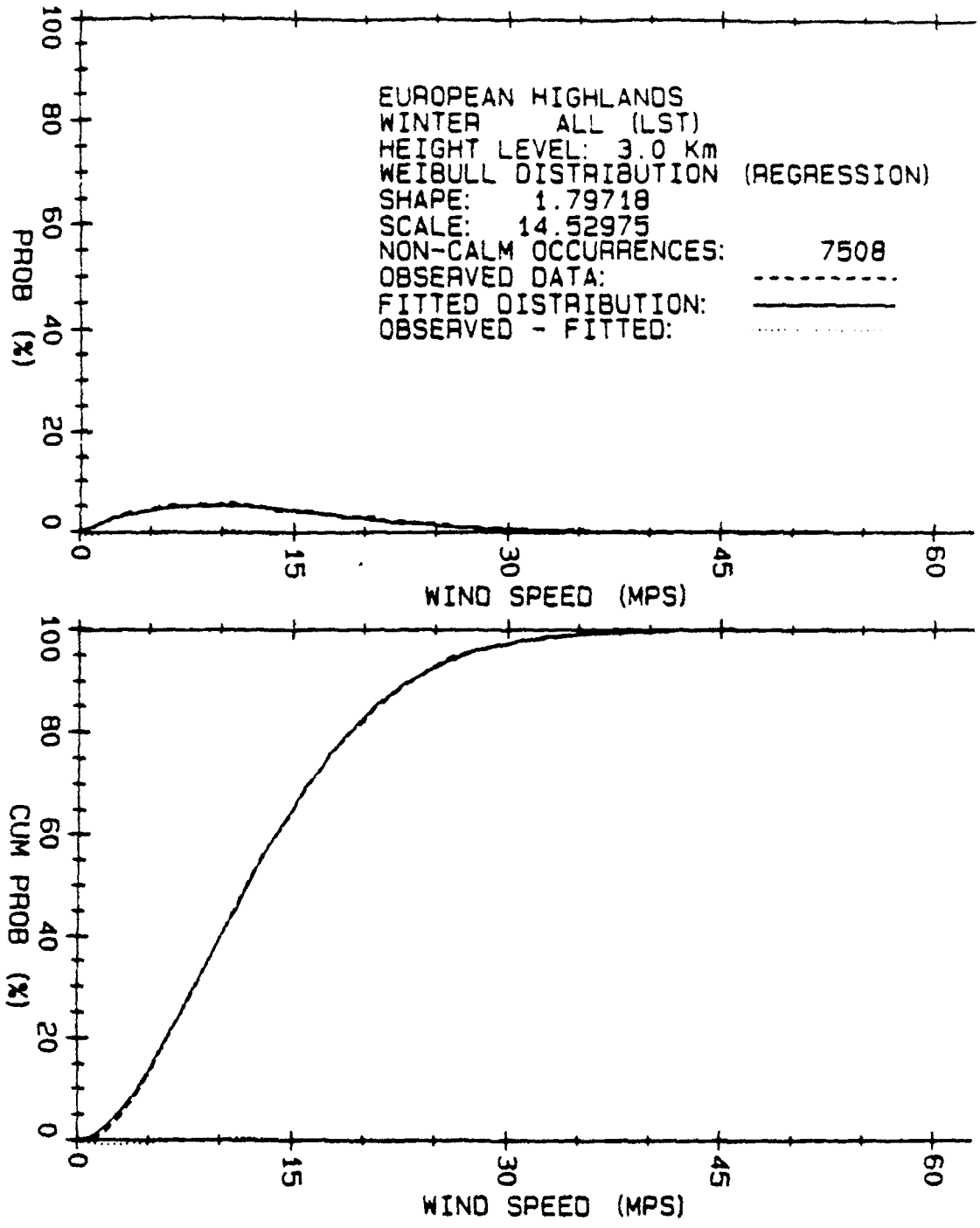

Figure 31. Regression fitted Weibull distribution for European Highlands winter wind speeds for height level 3.0 km.

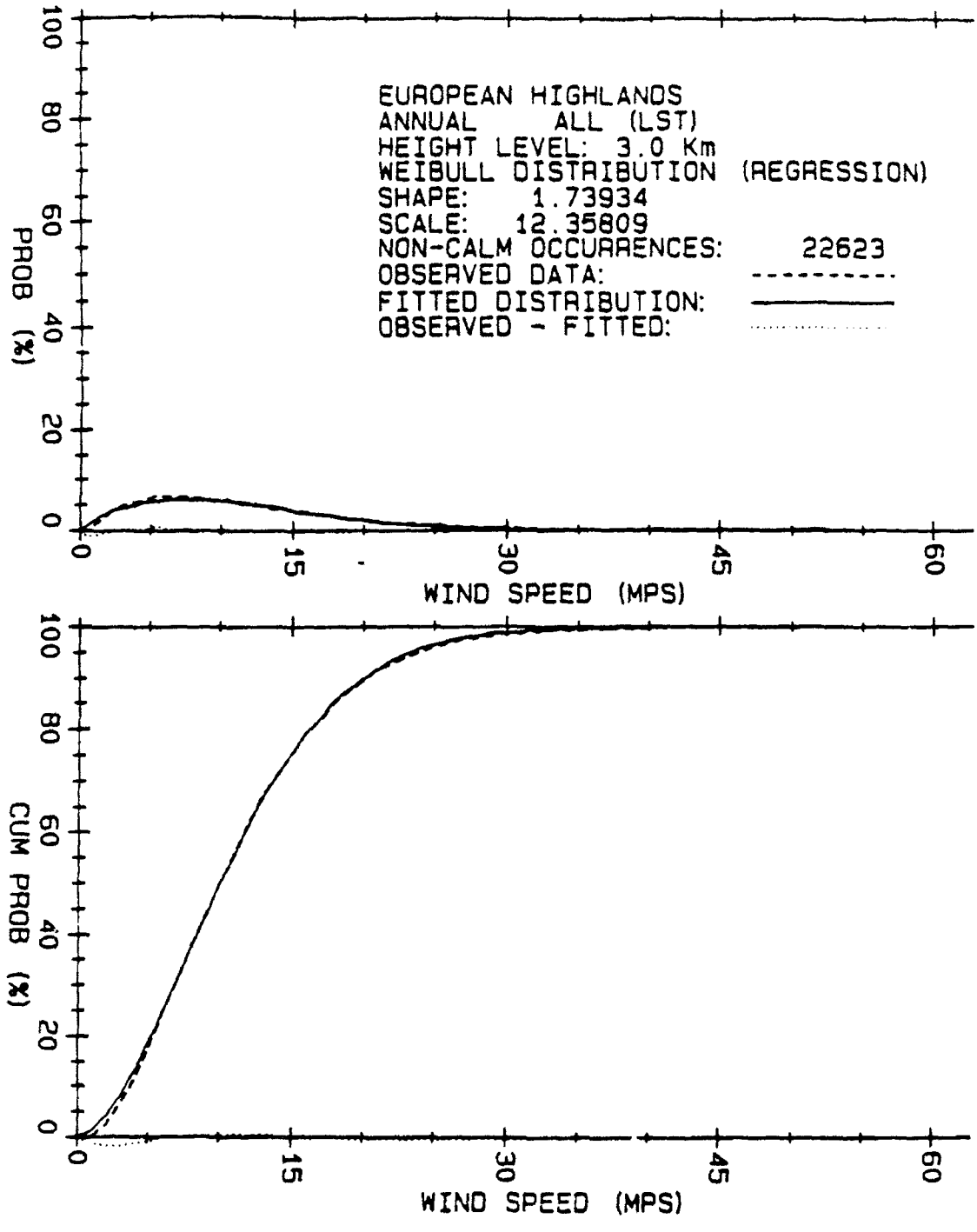

Figure 32. Regression fitted Weibull distribution for European Highlands wind speeds for height level 3.0 km.

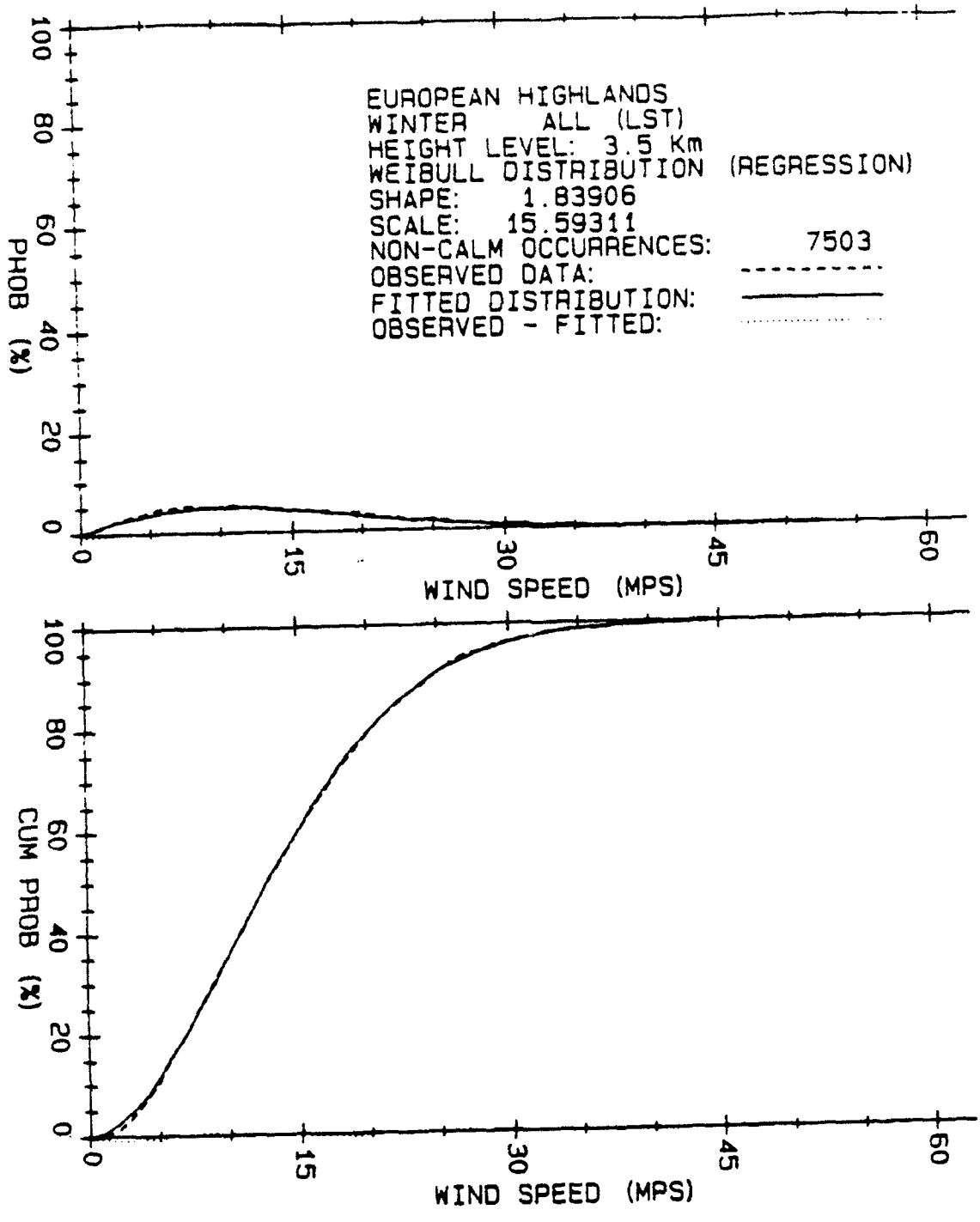

Figure 33. Regression fitted Weibull distribution for European Highlands winter wind speeds for height level 3.5 km.

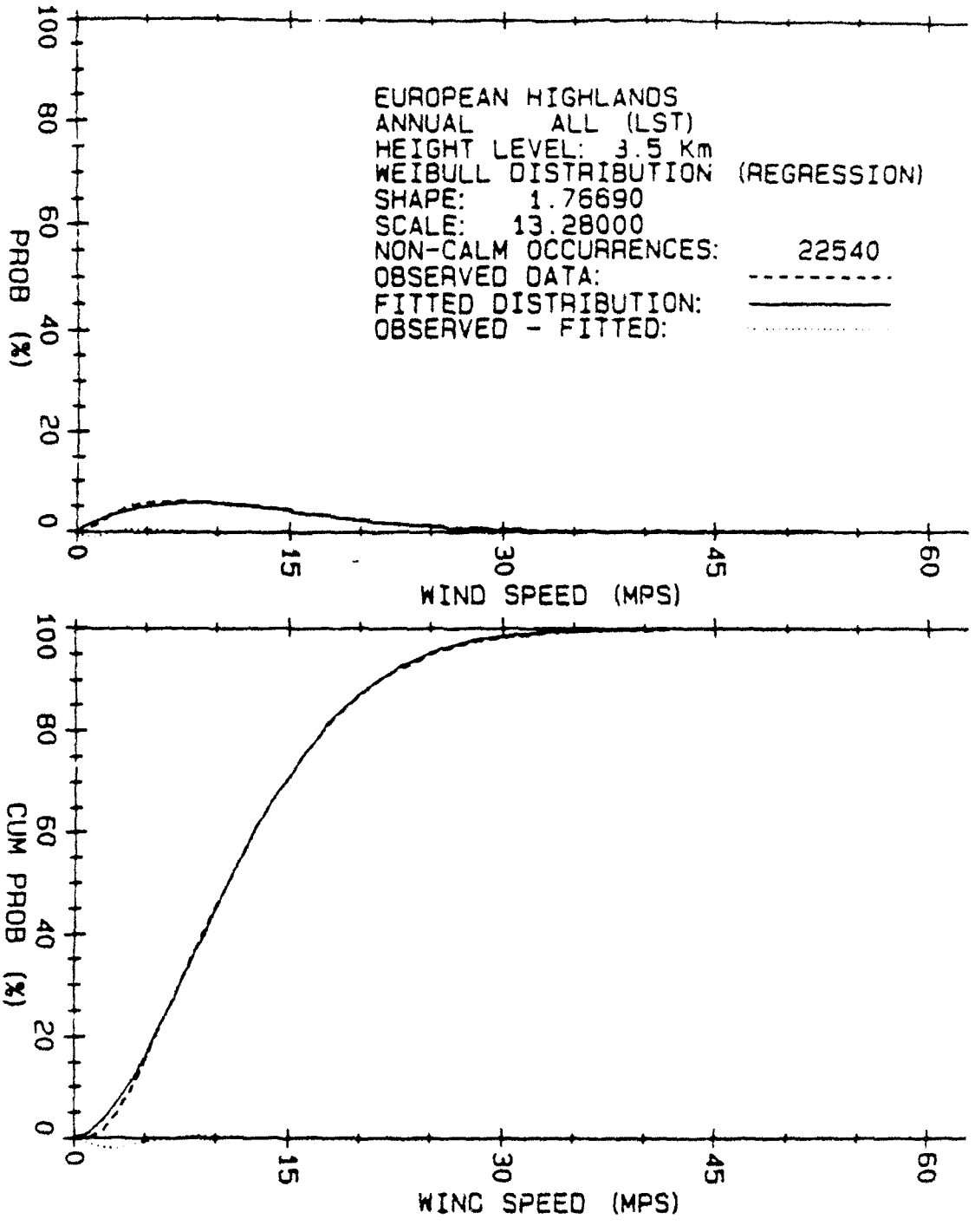

Figure 34. Regression fitted Weibull distribution for European Highlands wind speeds for height level 3.5 km.

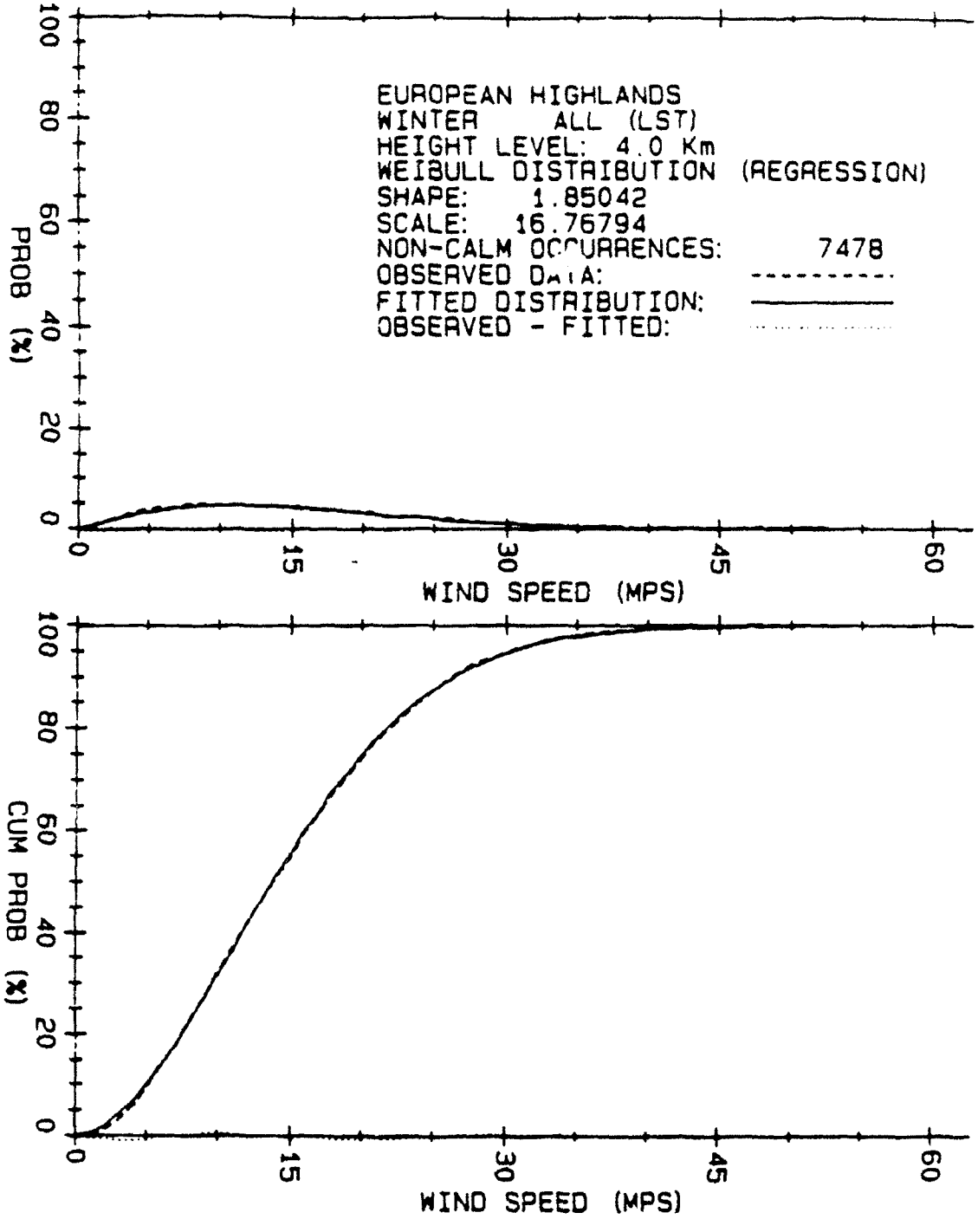

Figure 35. Regression fitted Weibull distribution for European Highlands winter wind speeds for height level 4.0 km.

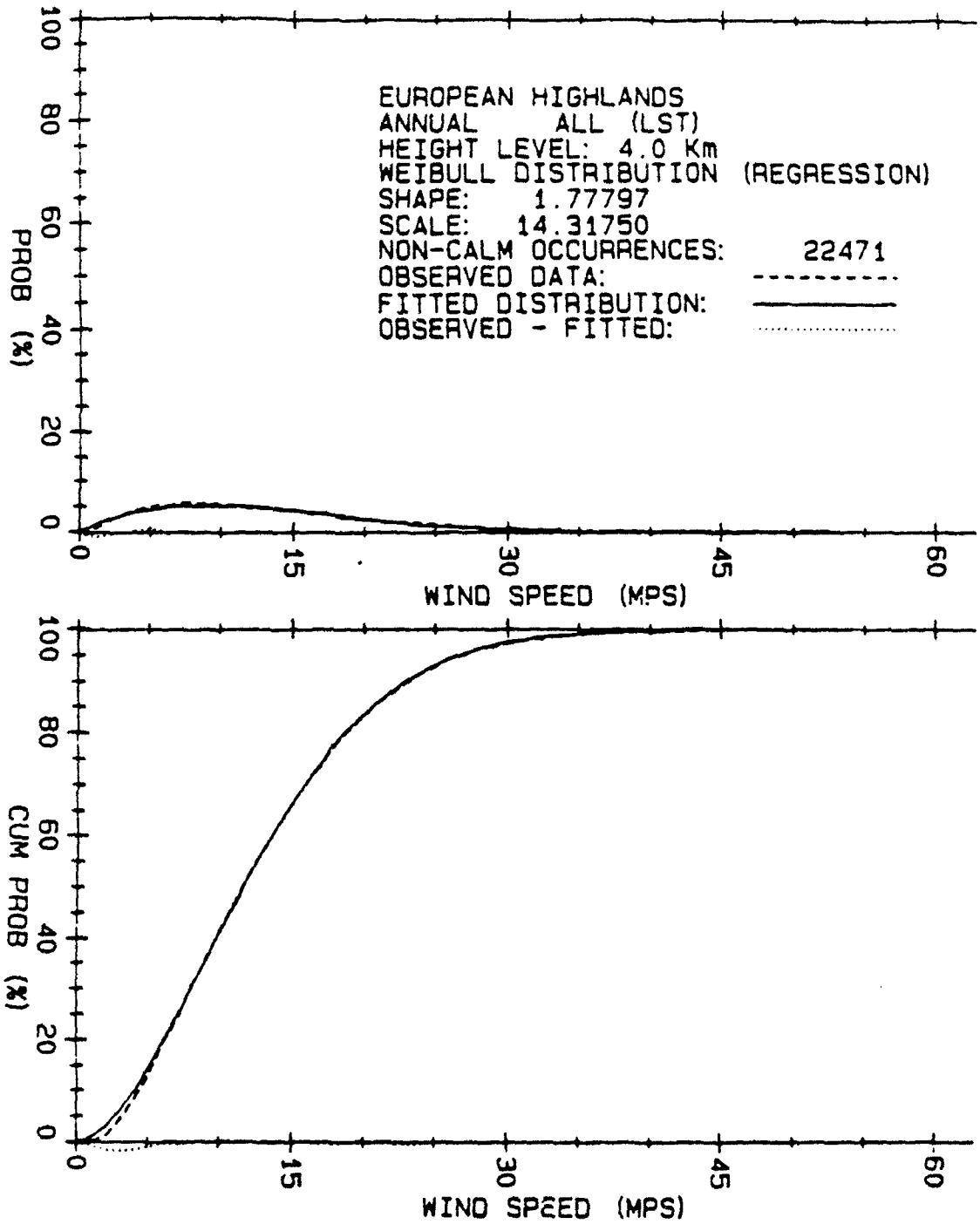

Figure 36. Regression fitted Weibull distribution for European Highlands wind speeds for height level 4.0 km.

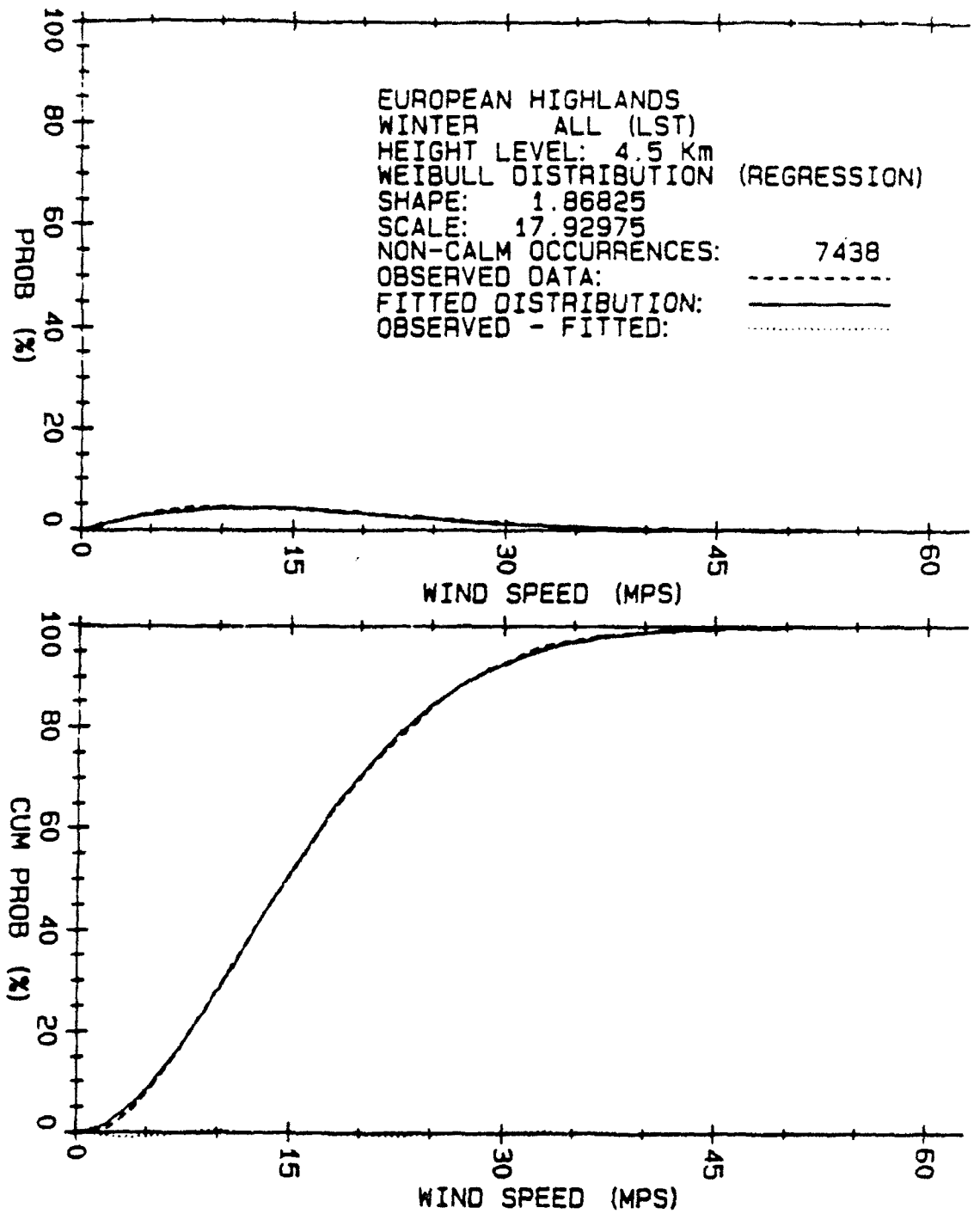

Figure 37. Regression fitted Weibull distribution for European Highlands winter wind speeds for height level 4.5 km.

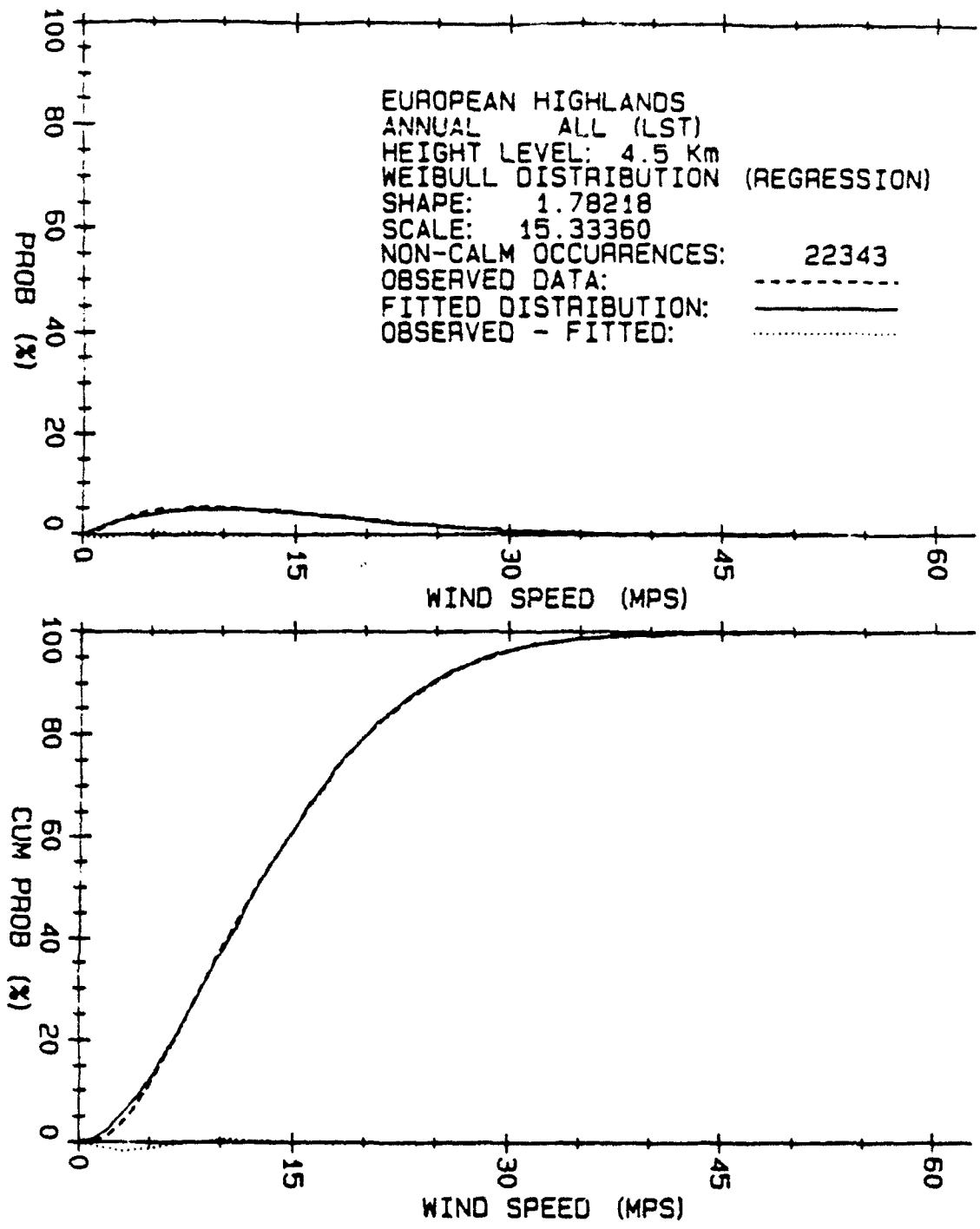

Figure 38. Regression fitted Weibull distribution for European Highlands wind speeds for height level 4.5 km.

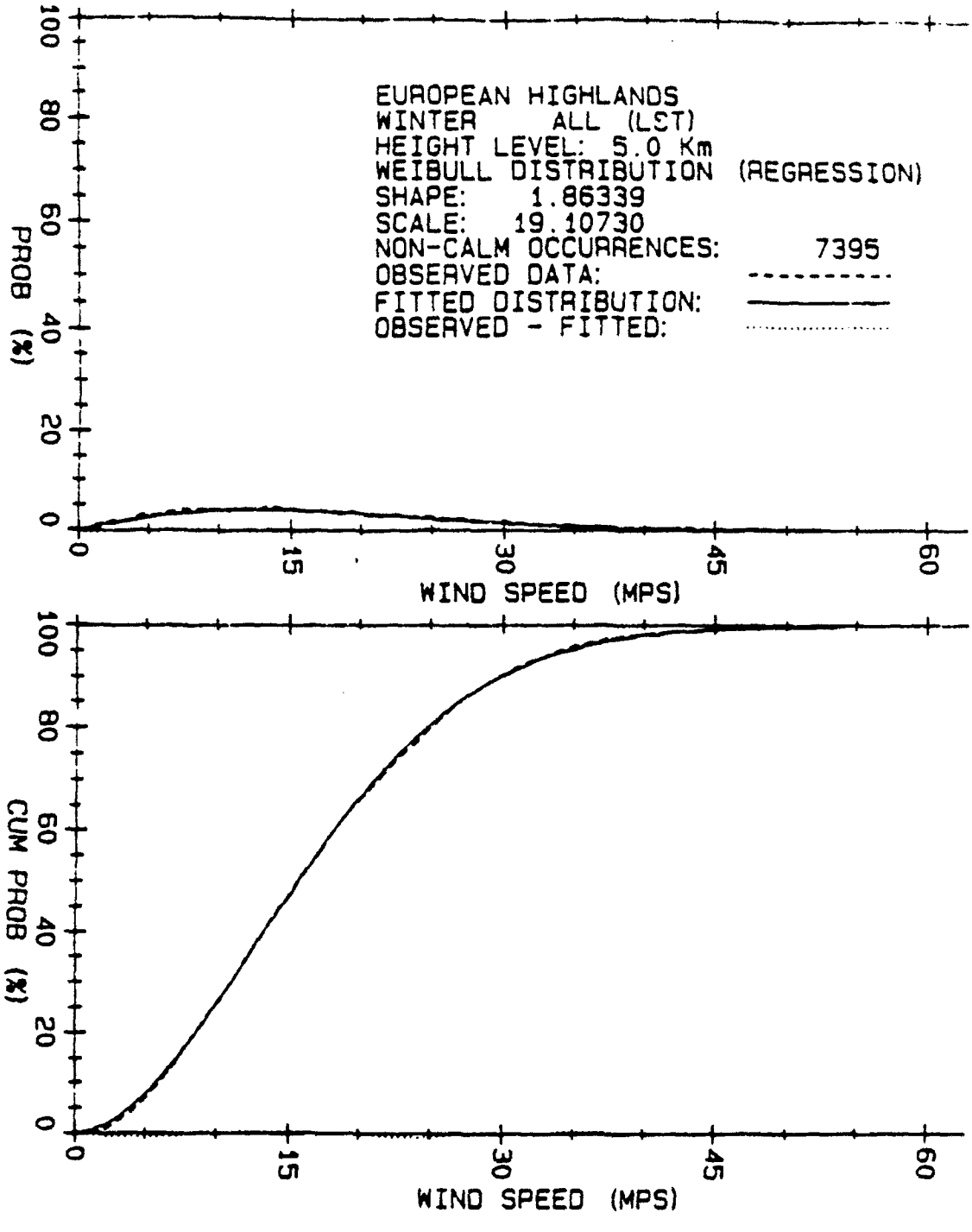

Figure 39. Regression fitted Weibull distribution for European Highlands winter wind speeds for height level 5.0 km.

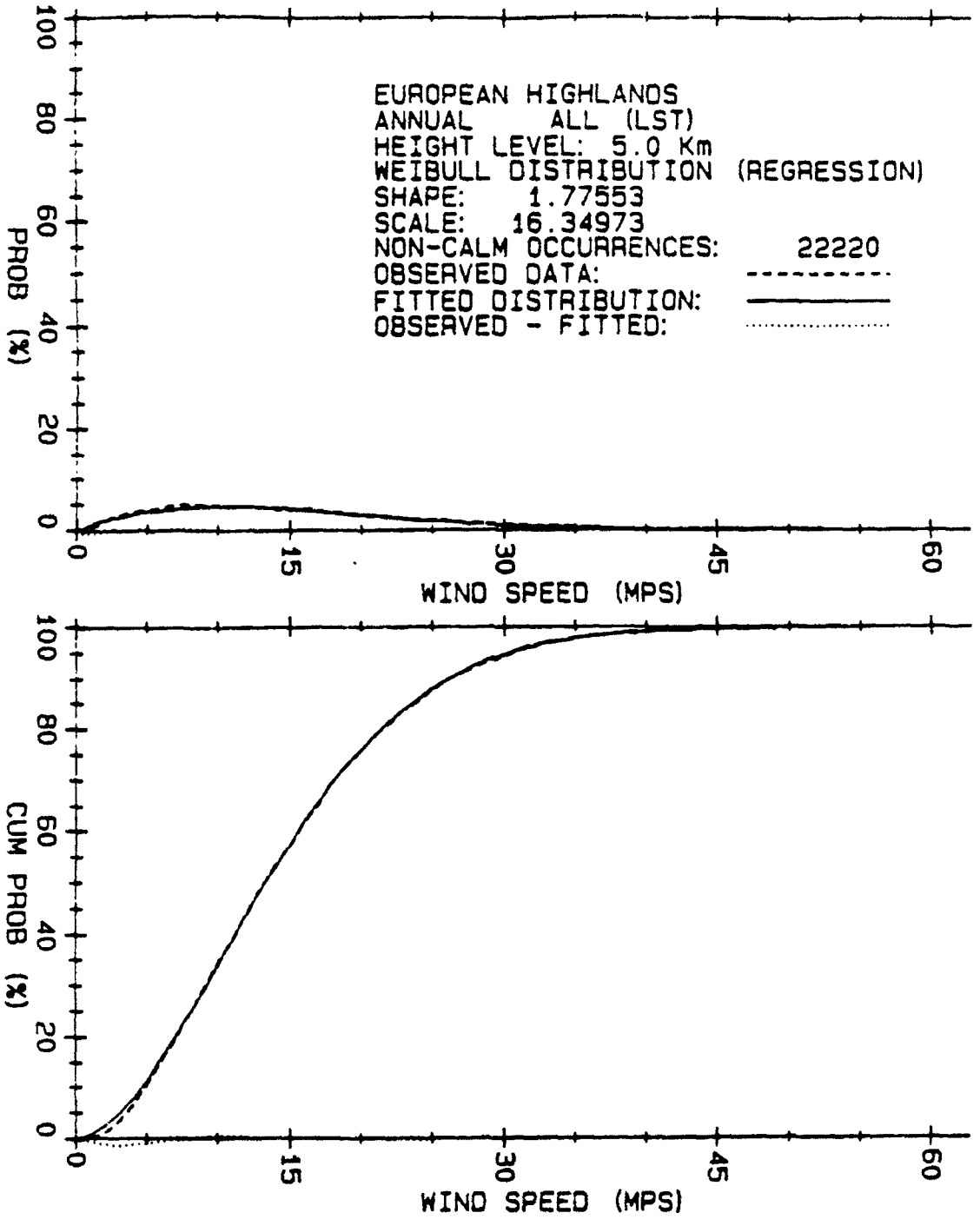

Figure 40. Regression fitted Weibull distribution for European Highlands wind speeds for height level 5.0 km.

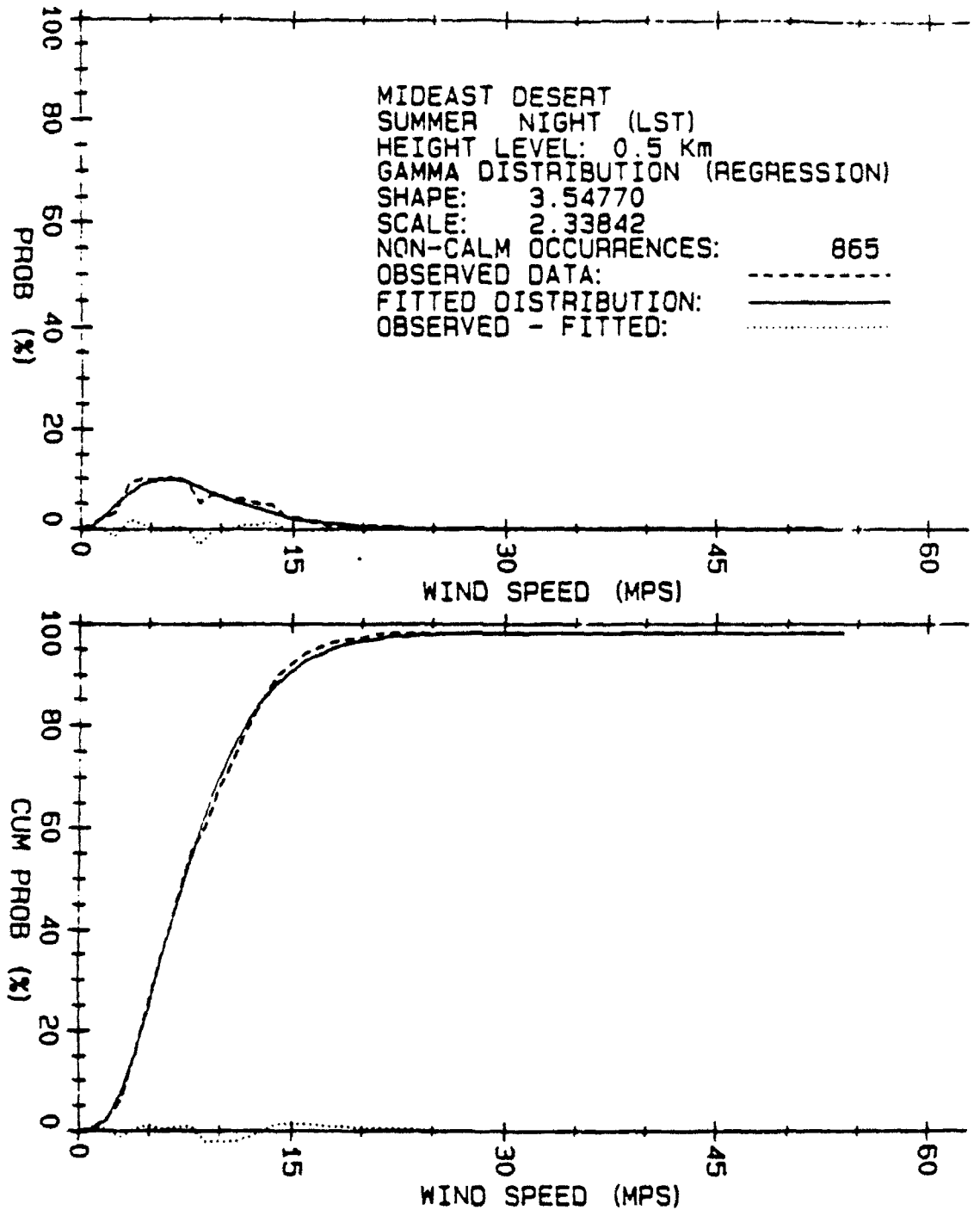

Figure 41. Regression fitted gamma distribution for Mideast Desert nighttime summer wind speeds for height level 0.5 km.

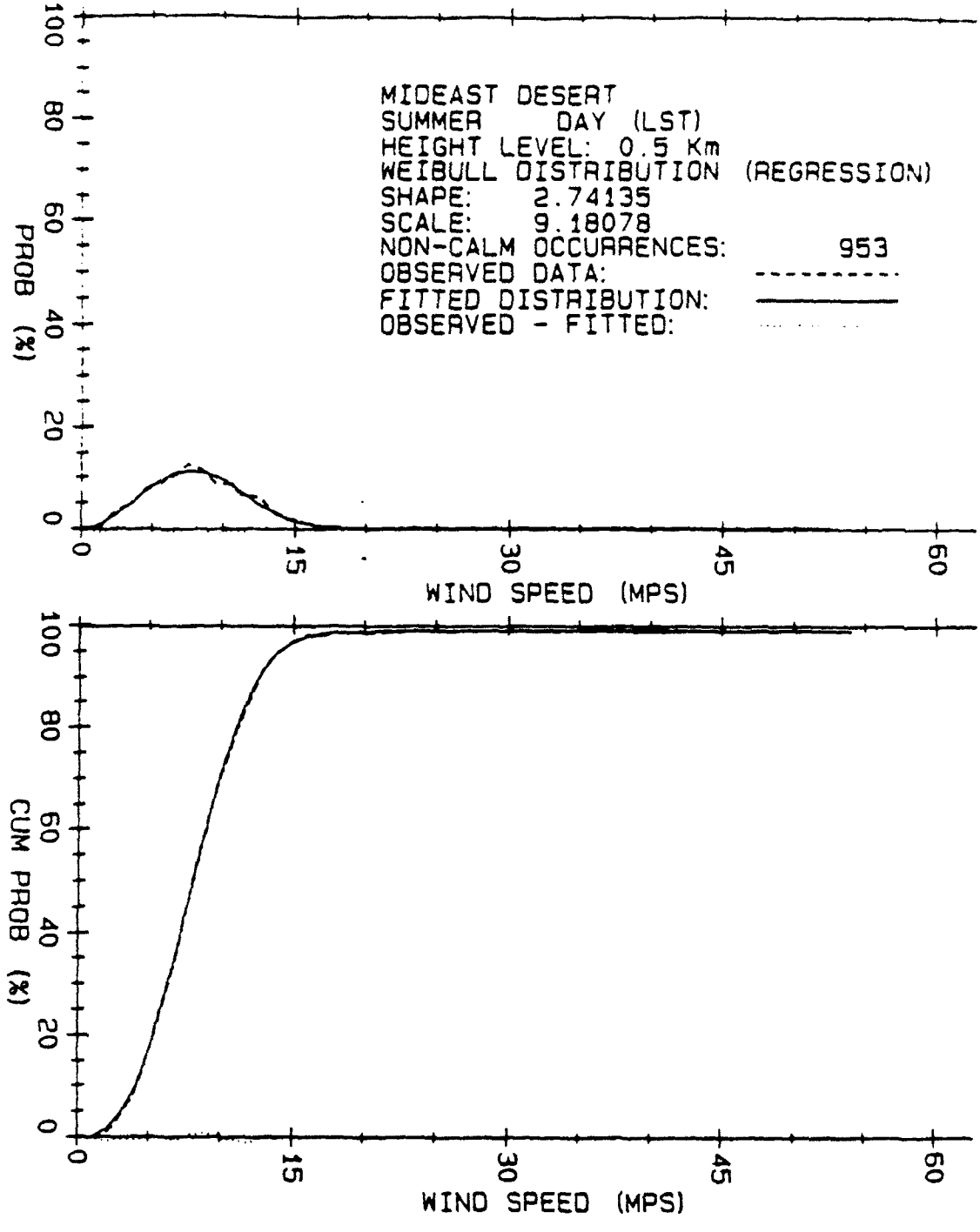

Figure 42. Regression fitted Weibull distribution for Mideast Desert daytime summer wind speeds for height level 0.5 km.

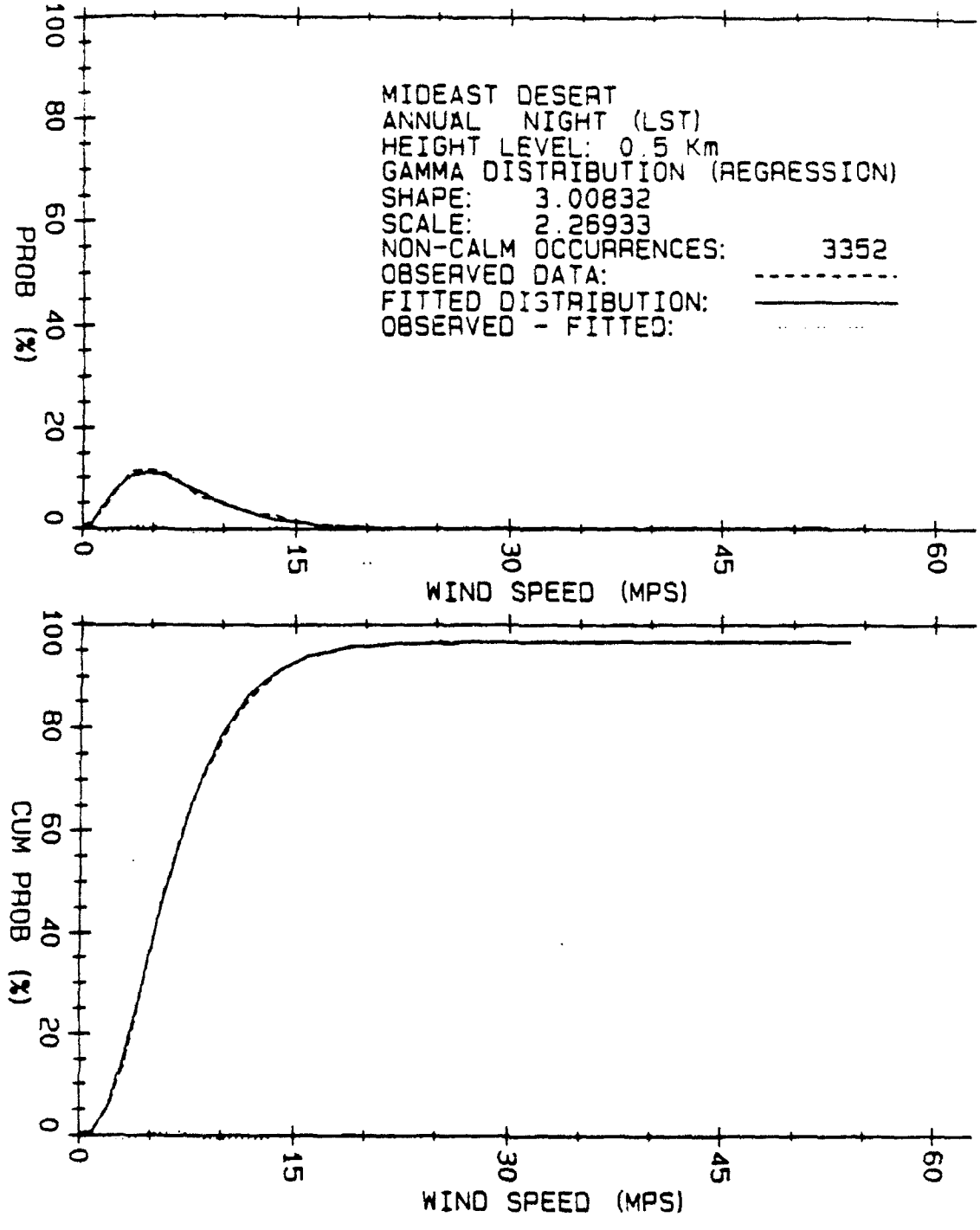

Figure 43. Regression fitted gamma distribution for Mideast Desert nighttime wind speeds for height level 0.5 km.

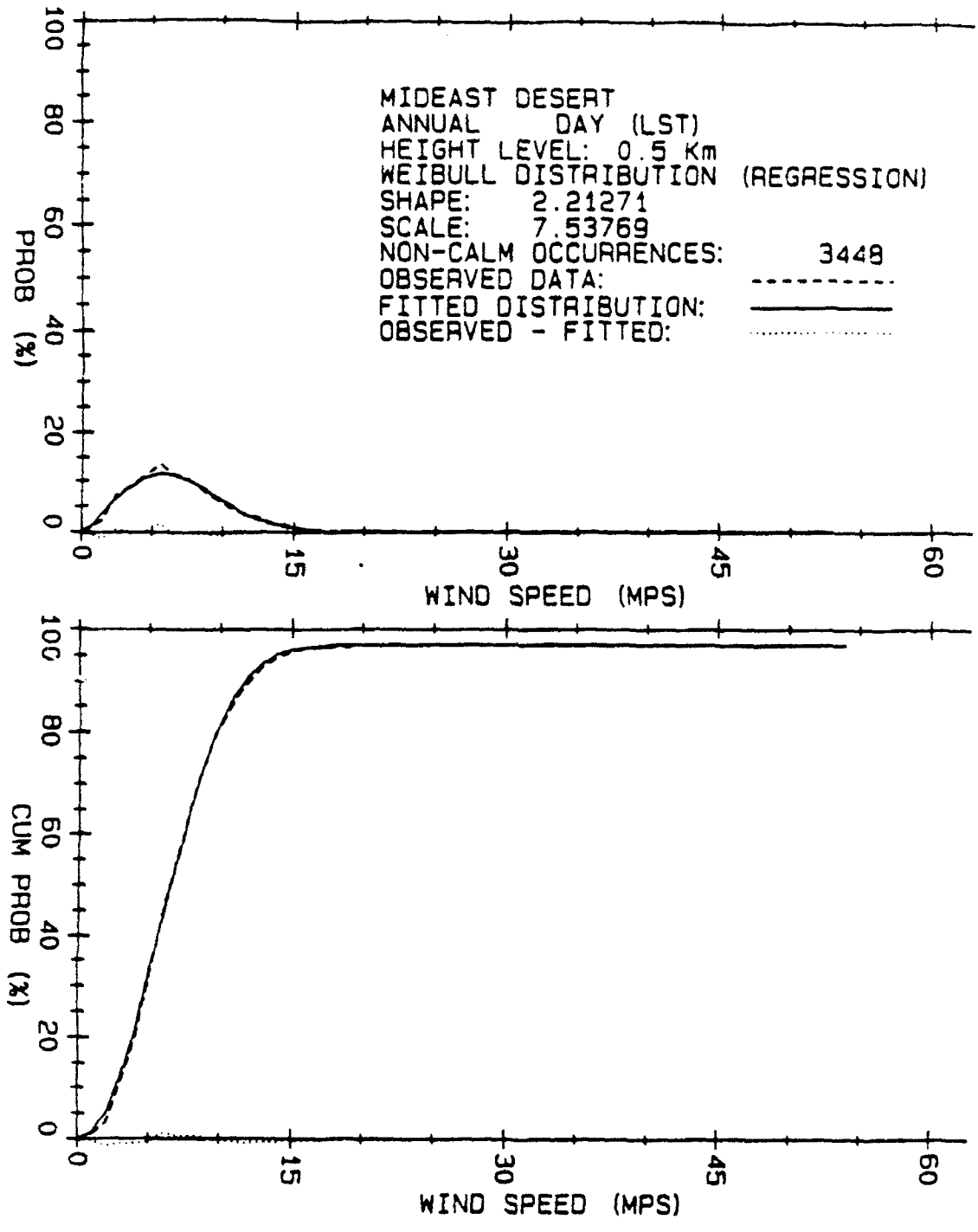

Figure 44. Regression fitted Weibull distribution for Mideast Desert daytime wind speeds for height level 0.5 km.

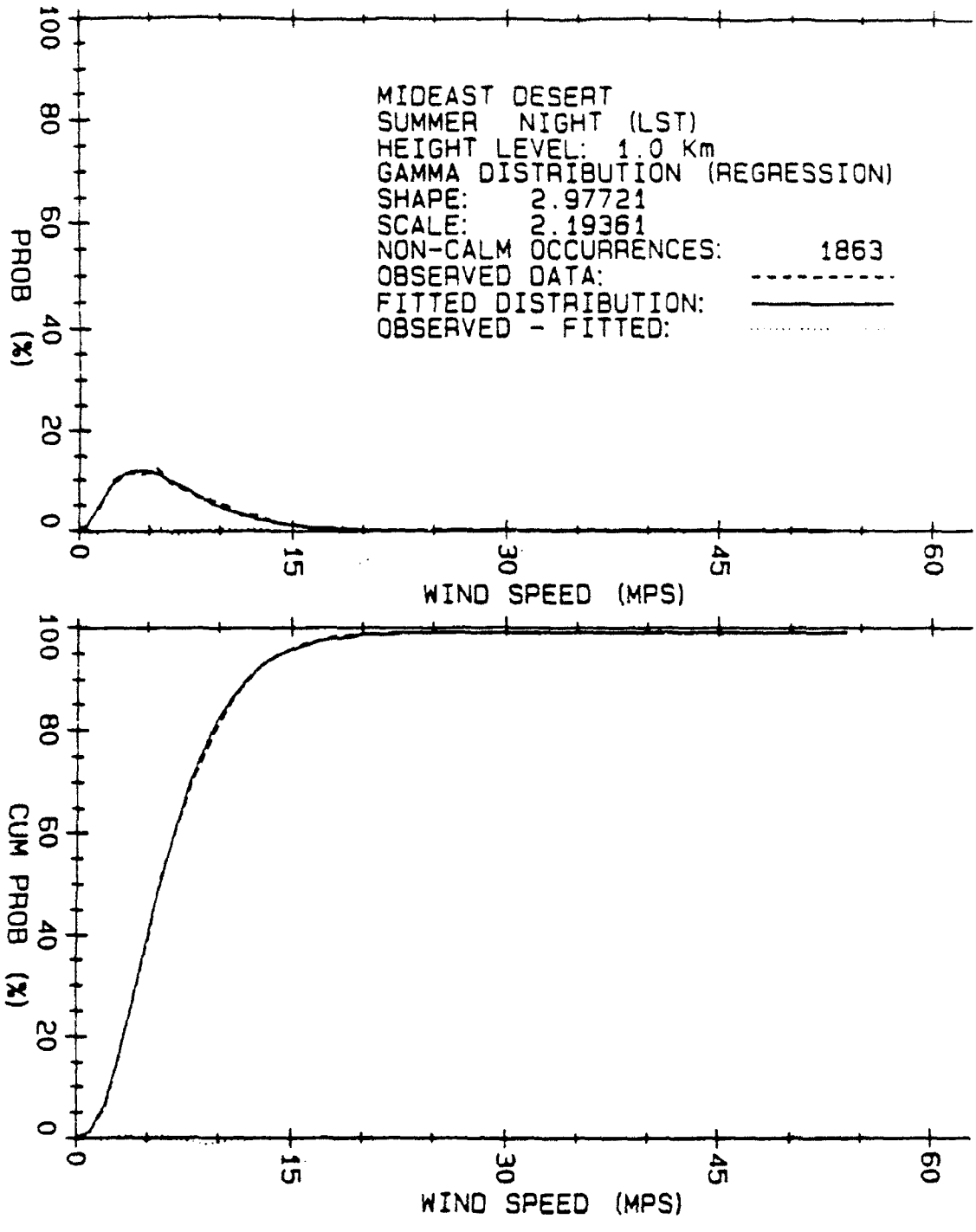

Figure 45. Regression fitted gamma distribution for Mideast Desert nighttime summer wind speeds for height level 1.0 km.

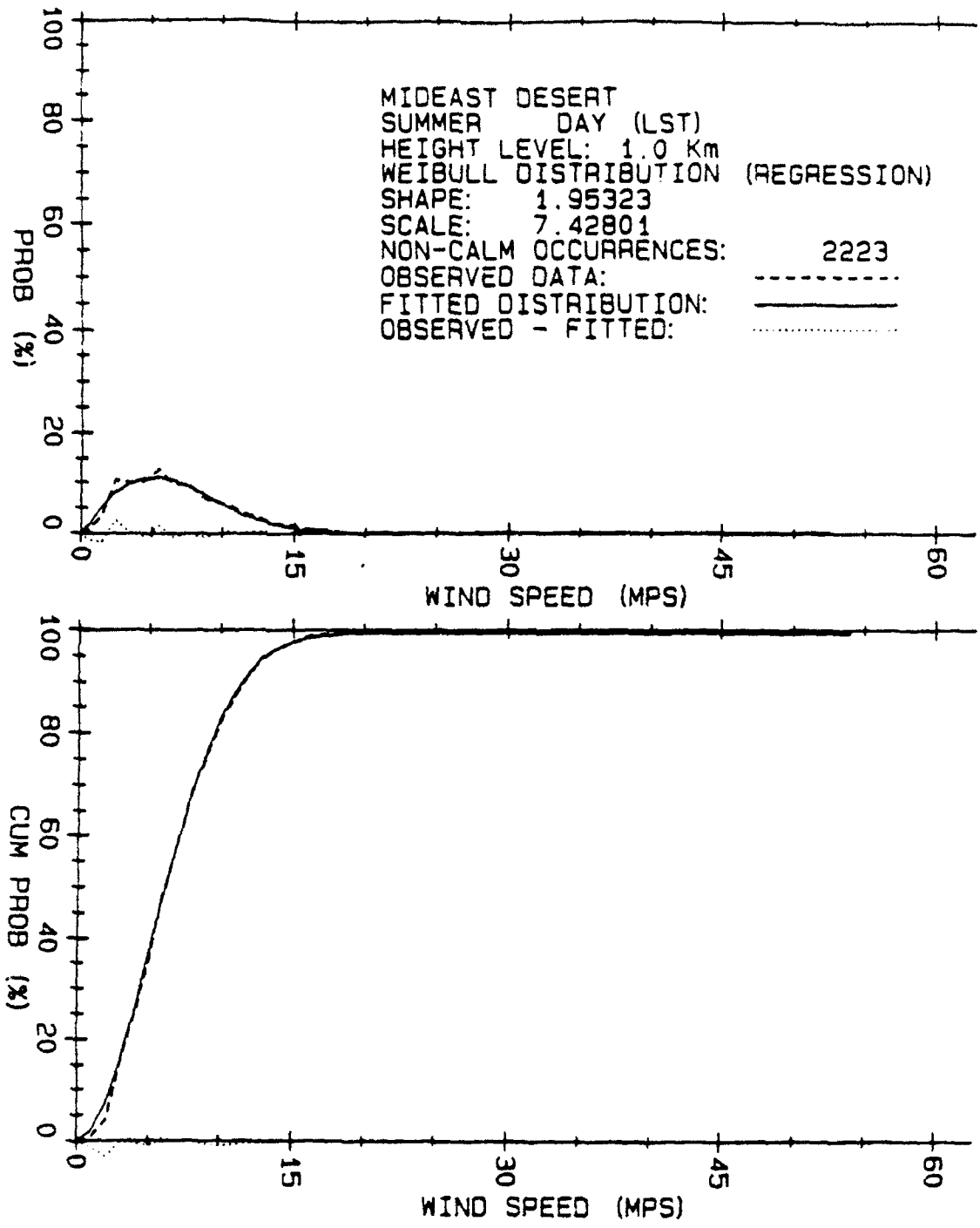

Figure 46. Regression fitted Weibull distribution for Mideast Desert daytime summer wind speeds for height level 1.0 km.

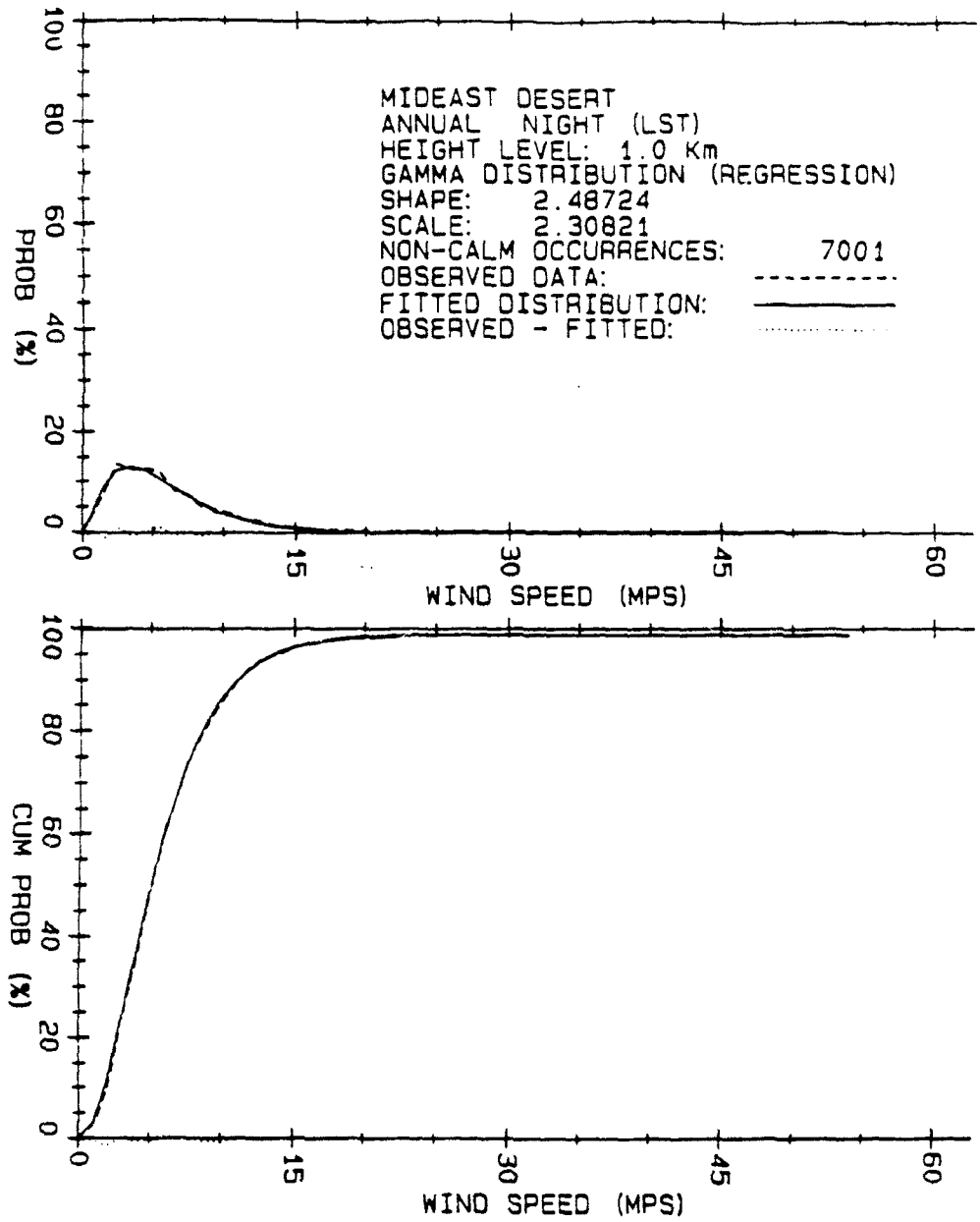

Figure 47. Regression fitted gamma distribution for Mideast Desert nighttime wind speeds for height level 1.0 km.

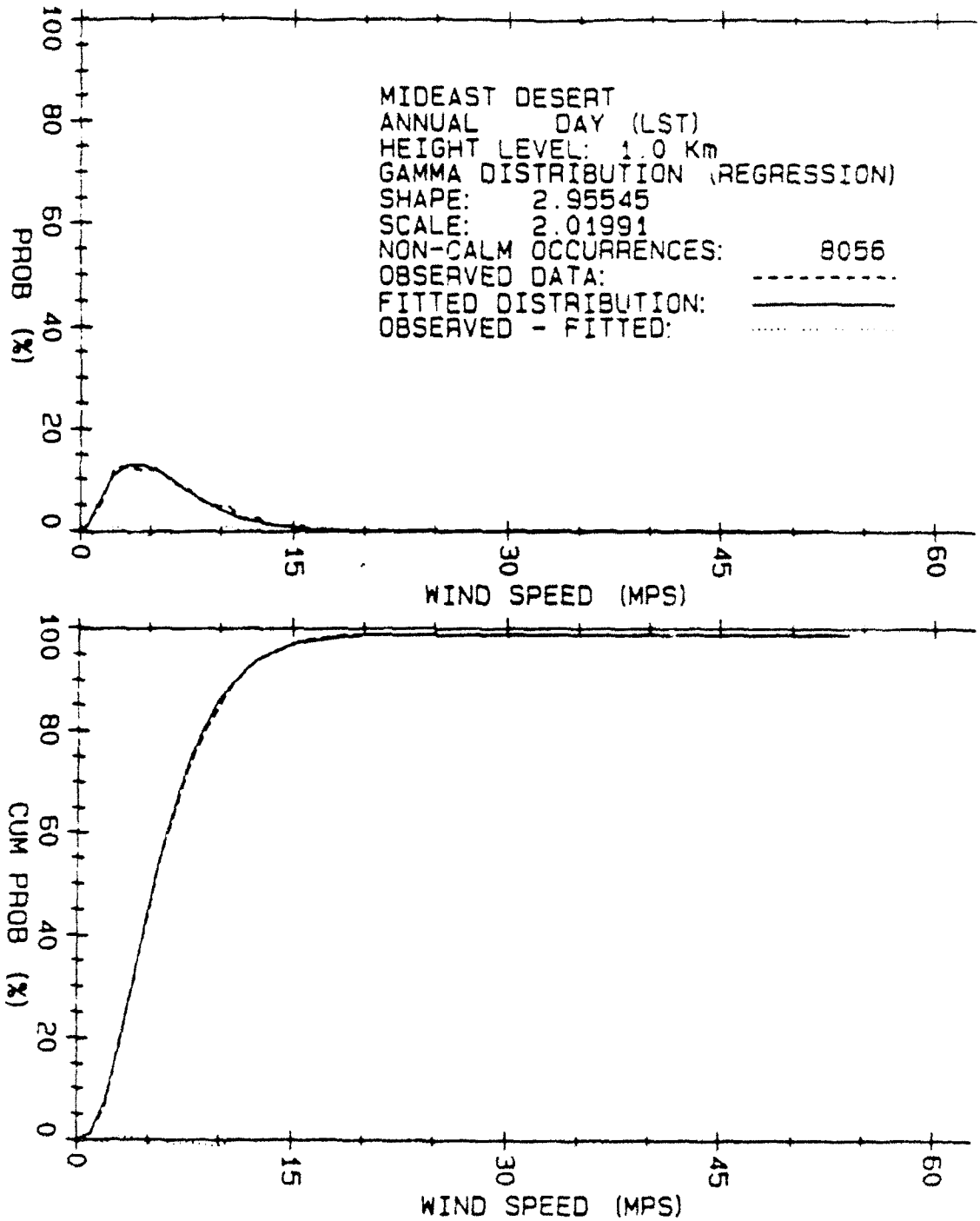

Figure 48. Regression fitted gamma distribution for Mideast Desert daytime wind speeds for height level 1.0 km.

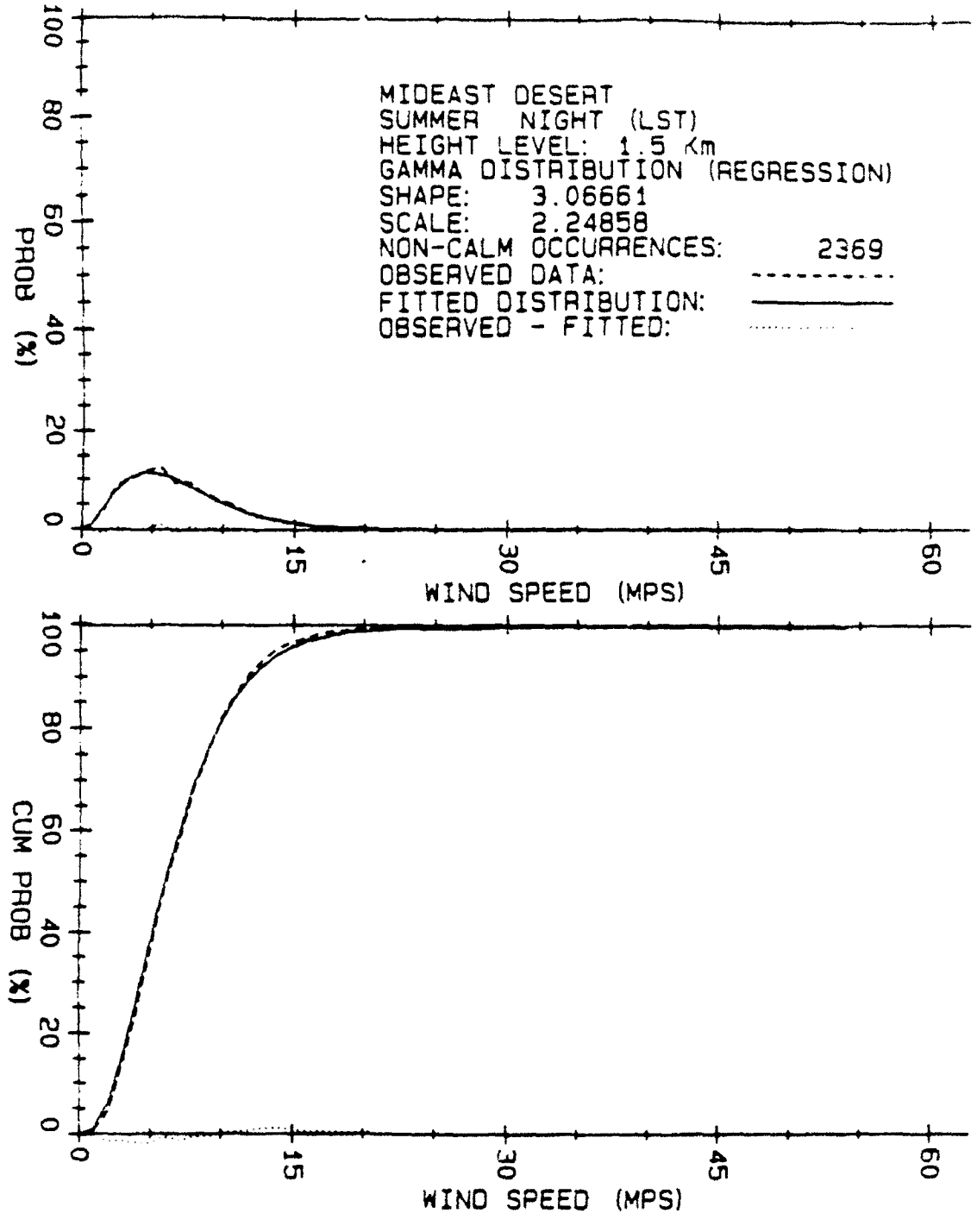

Figure 49. Regression fitted gamma distribution for Mideast Desert nighttime summer wind speeds for height level 1.5 km.

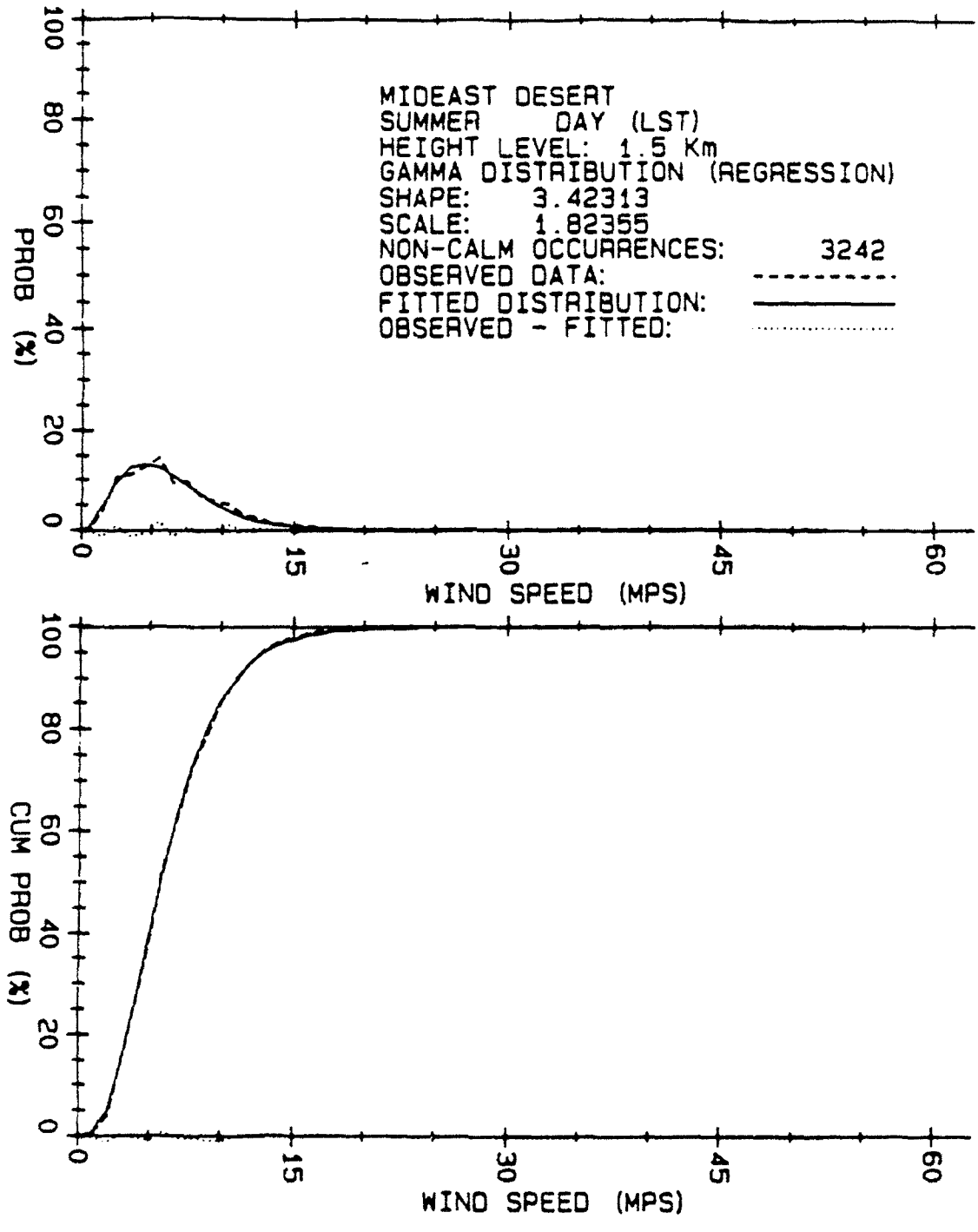

Figure 50. Regression fitted gamma distribution for Mideast Desert daytime summer wind speeds for height level 1.5 km.

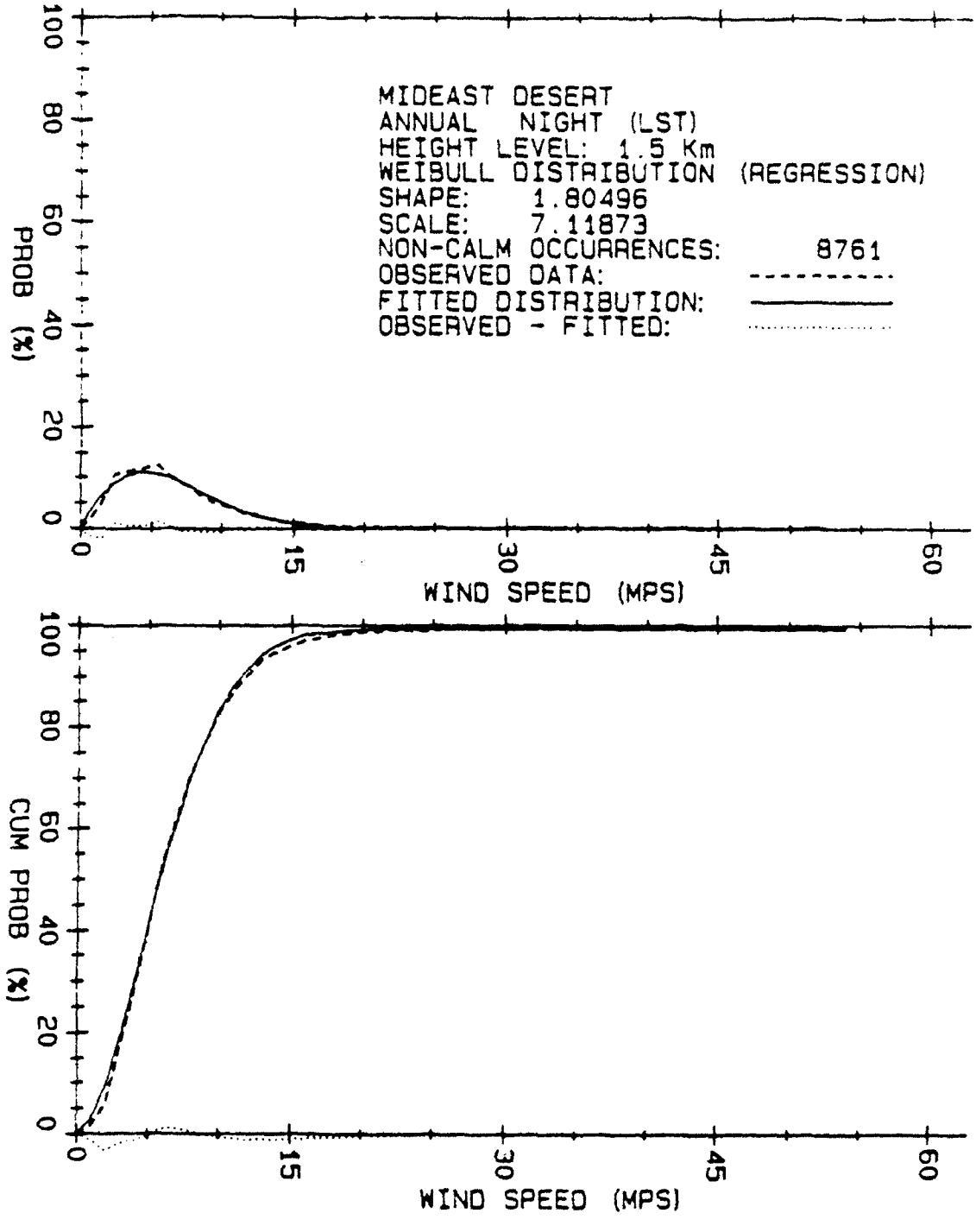

Figure 51. Regression fitted Weibull distribution for Mideast Desert nighttime wind speeds for height level 1.5 km.

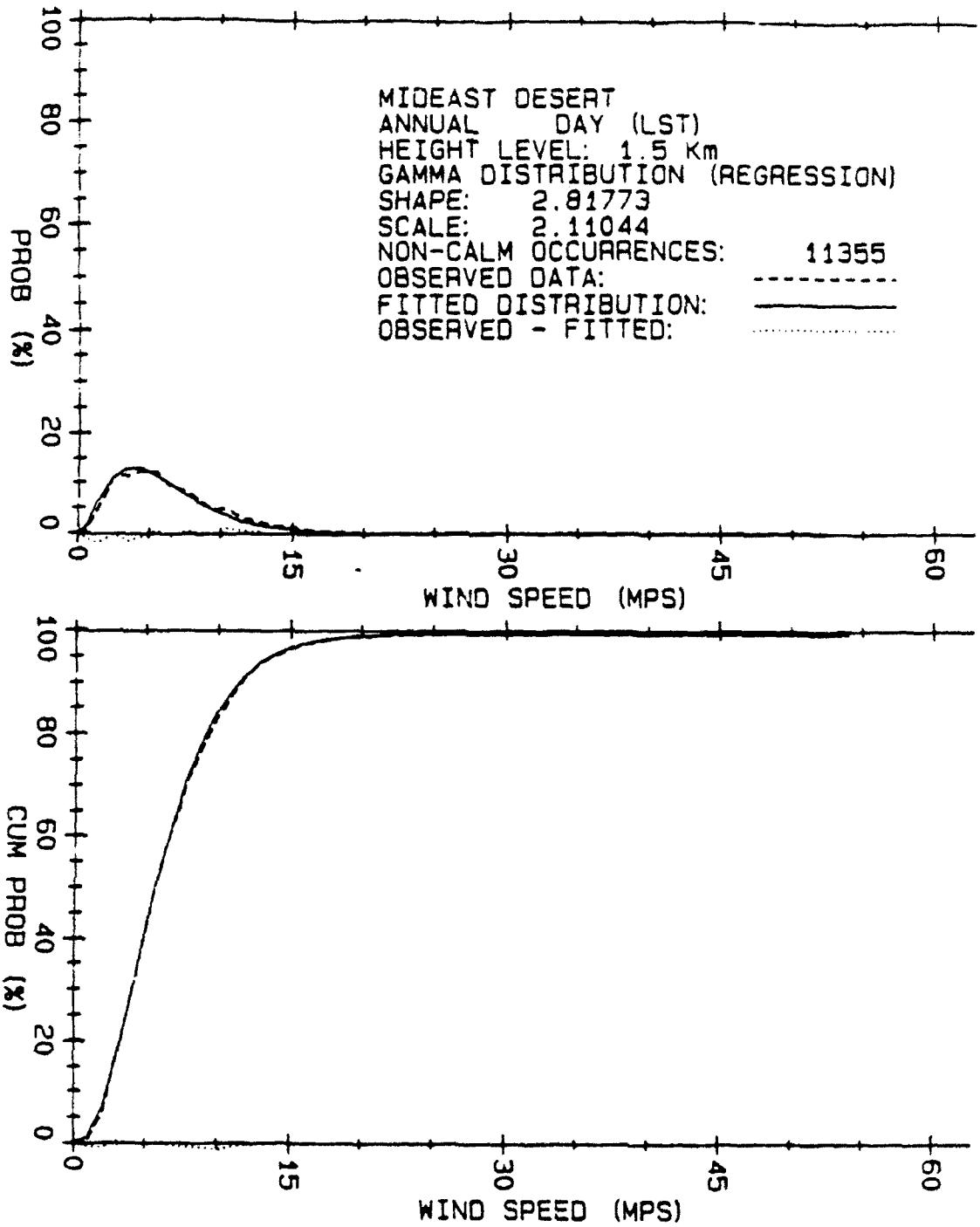

Figure 52. Regression fitted gamma distribution for Mideast Desert daytime wind speeds for height level 1.5 km.

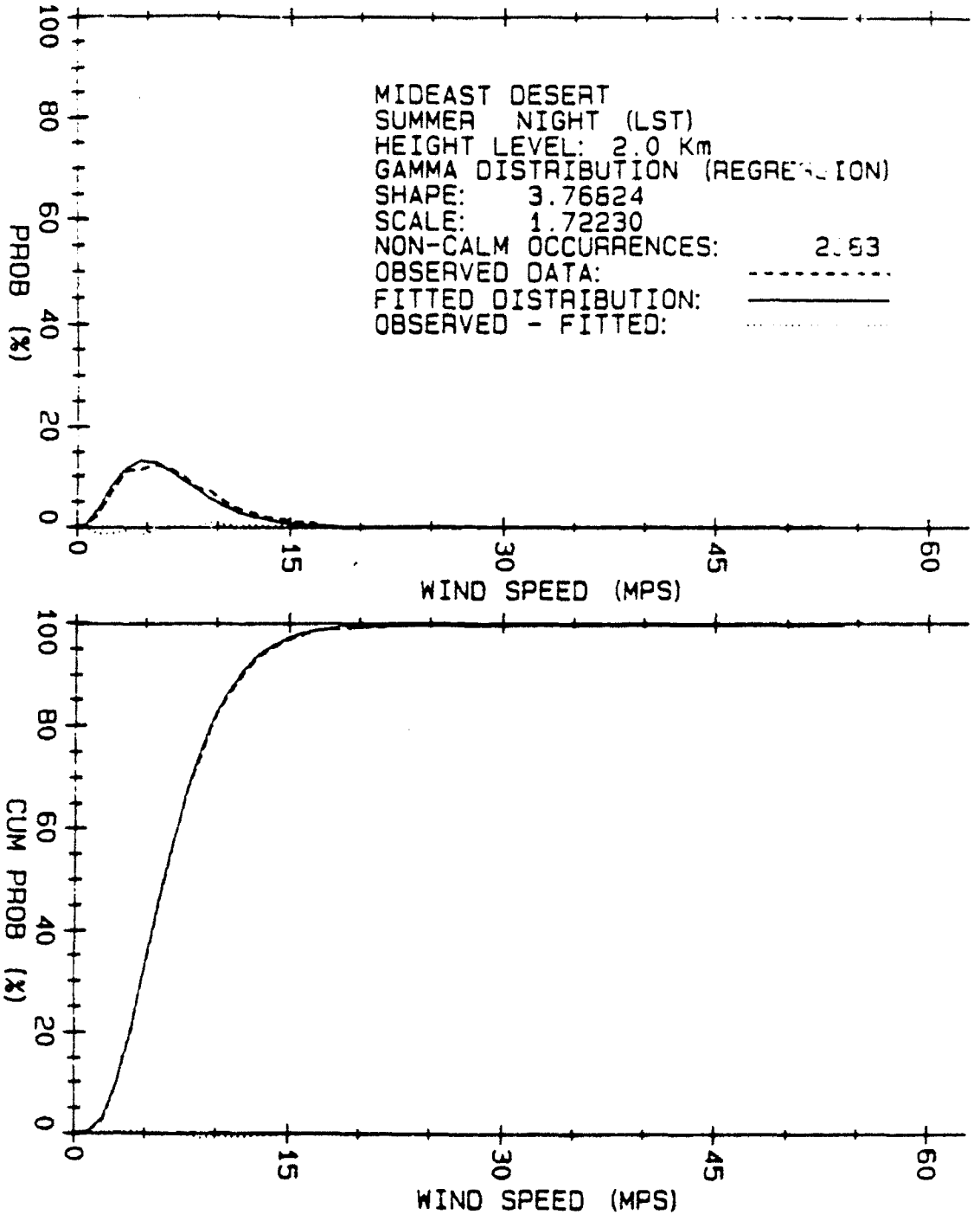

Figure 53. Regression fitted gamma distribution for Mideast Desert nighttime summer wind speeds for height level 2.0 km.

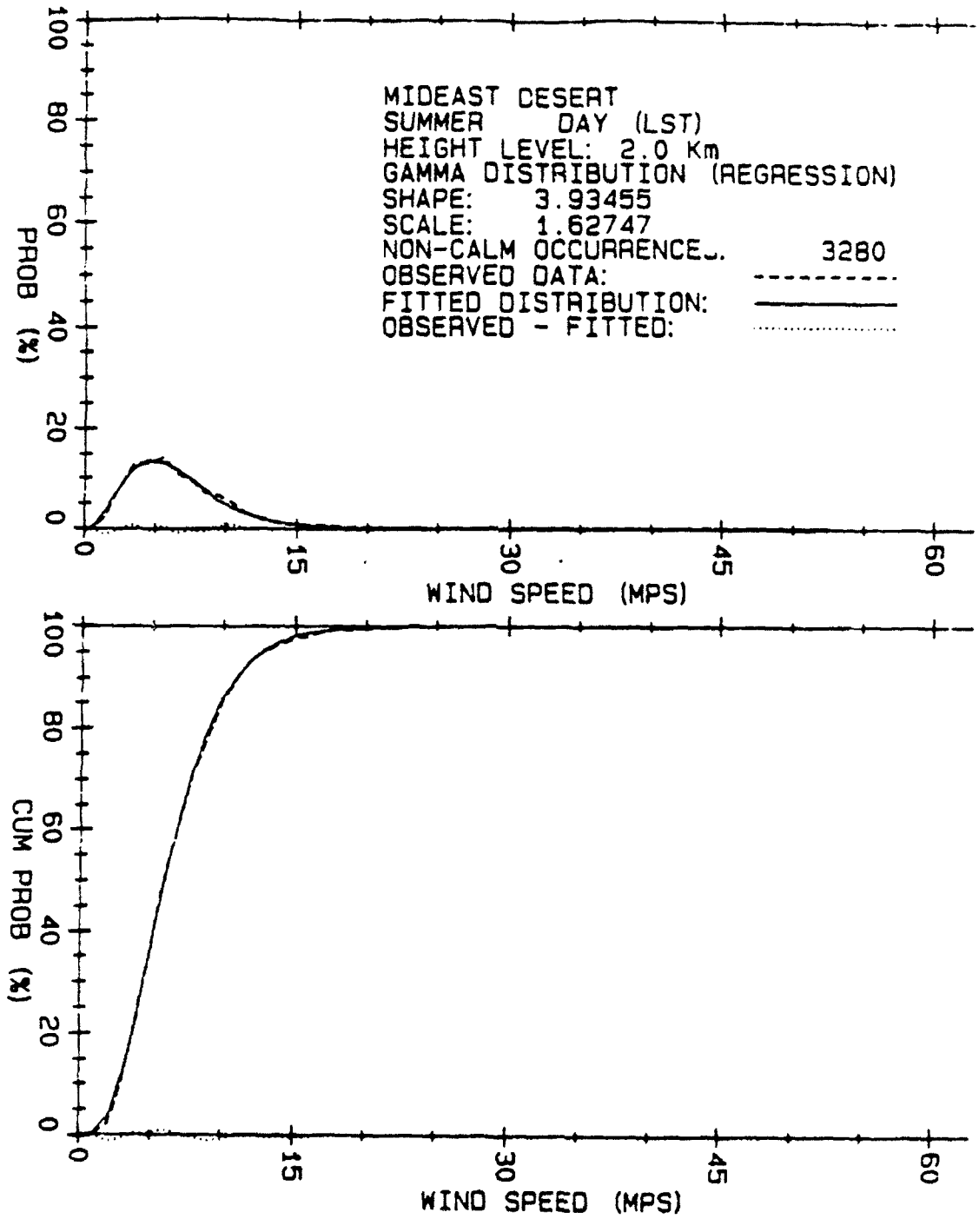

Figure 54. Regression fitted gamma distribution for Mideast Desert daytime summer wind speeds for height level 2.0 km.

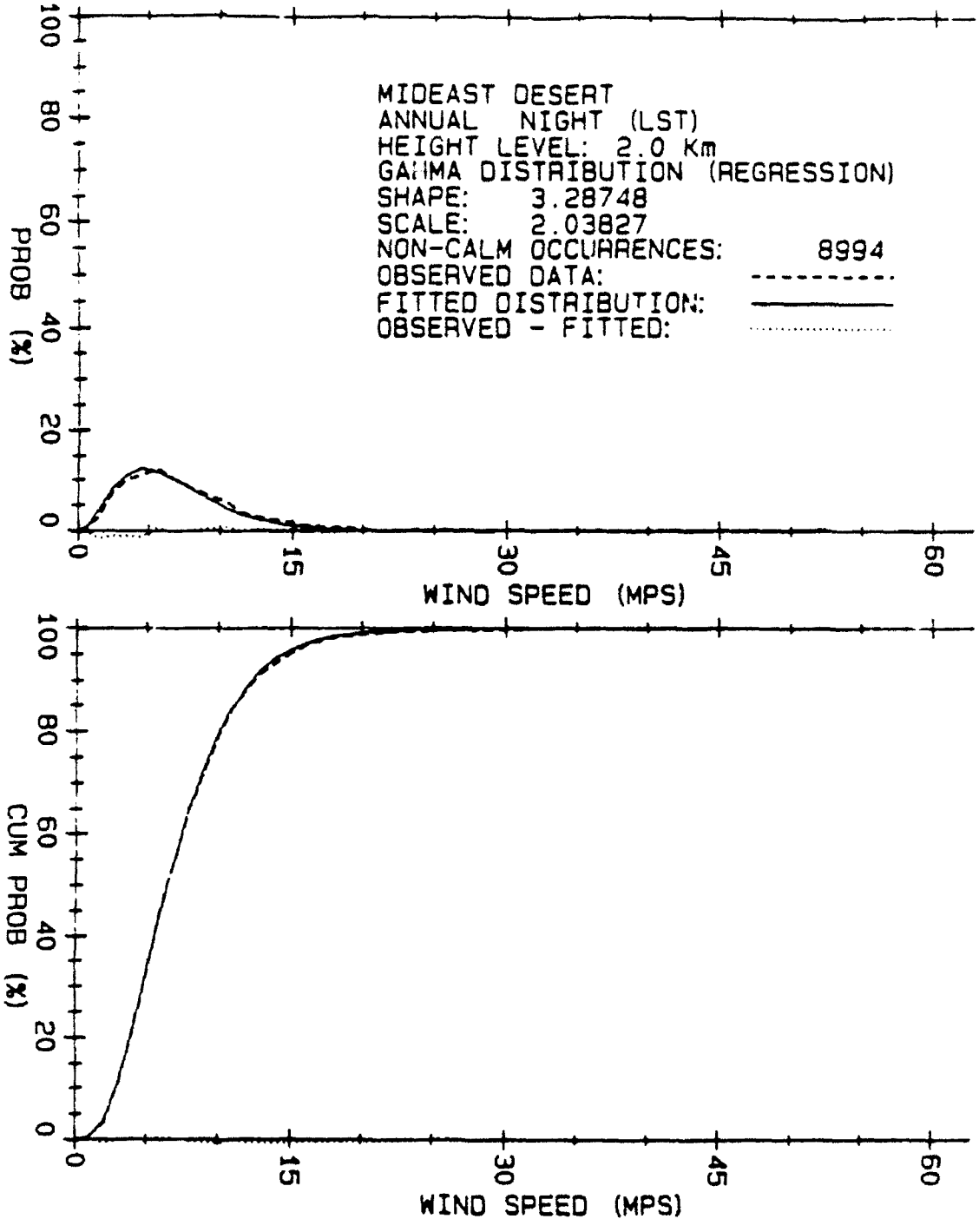

Figure 55. Regression fitted gamma distribution for Mideast Desert nighttime wind speeds for height level 2.0 km.

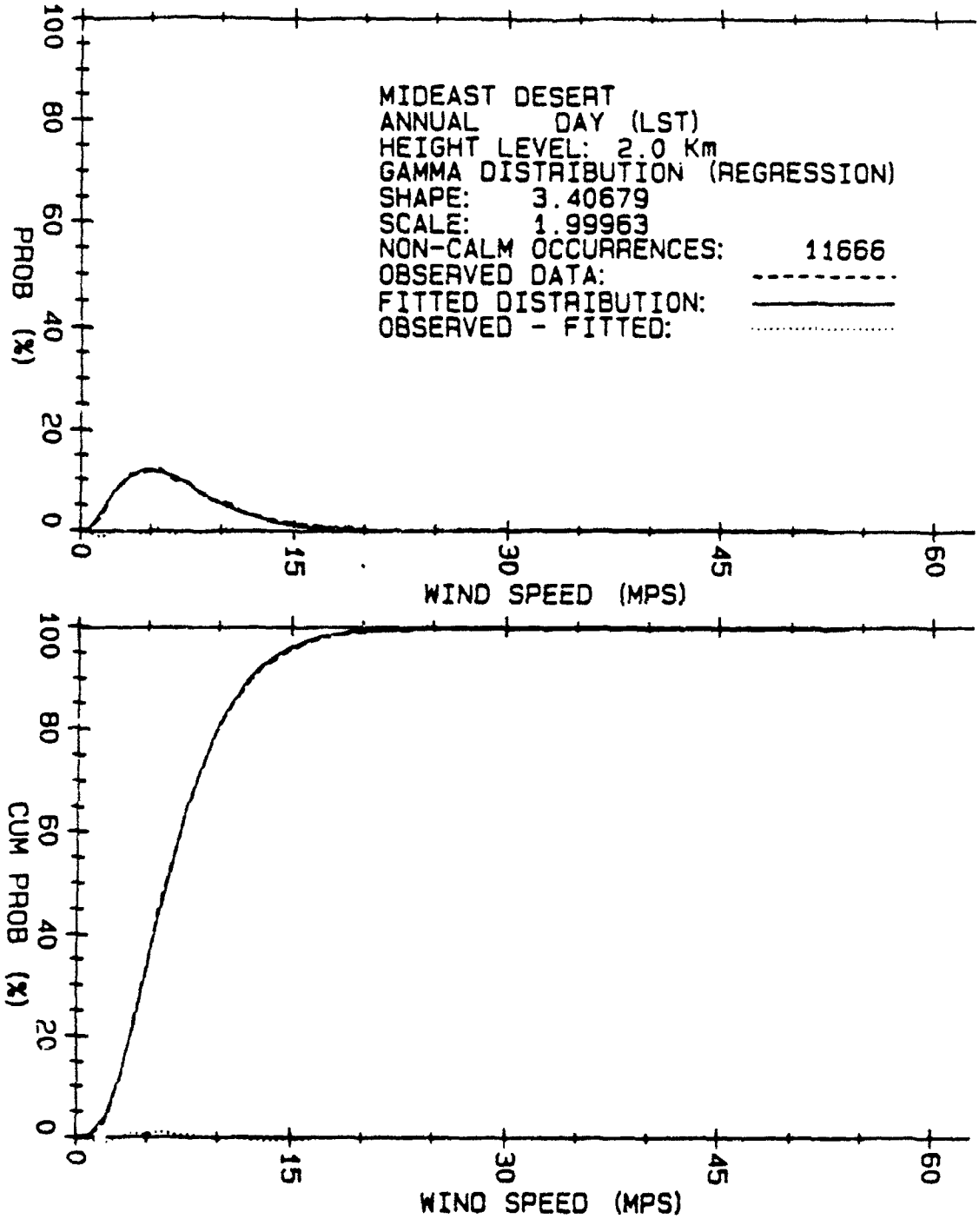

Figure 56. Regression fitted gamma distribution for Mideast Desert daytime wind speeds for height level 2.0 km.

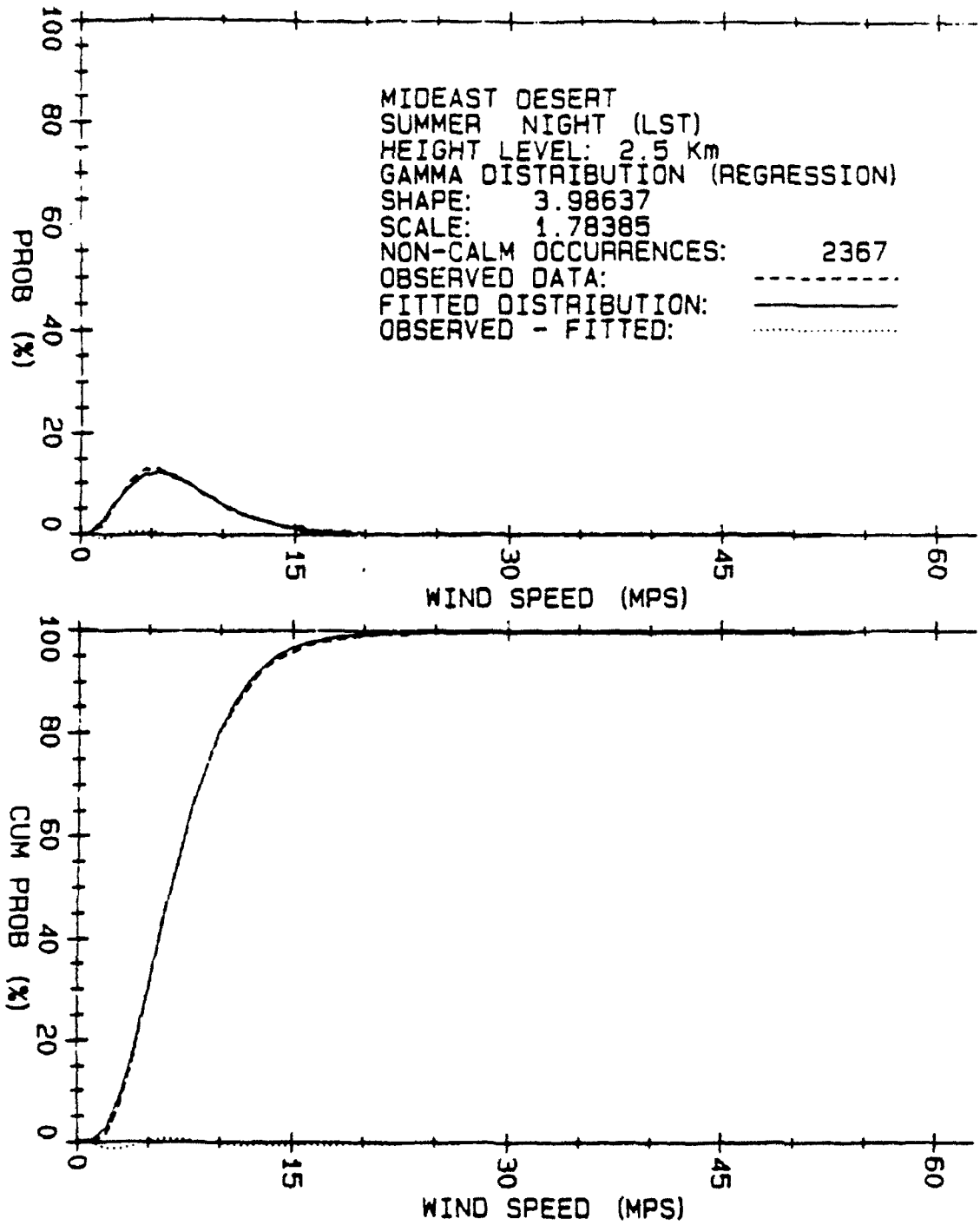

Figure 57. Regression fitted gamma distribution for Mideast Desert nighttime summer wind speeds for height level 2.5 km.

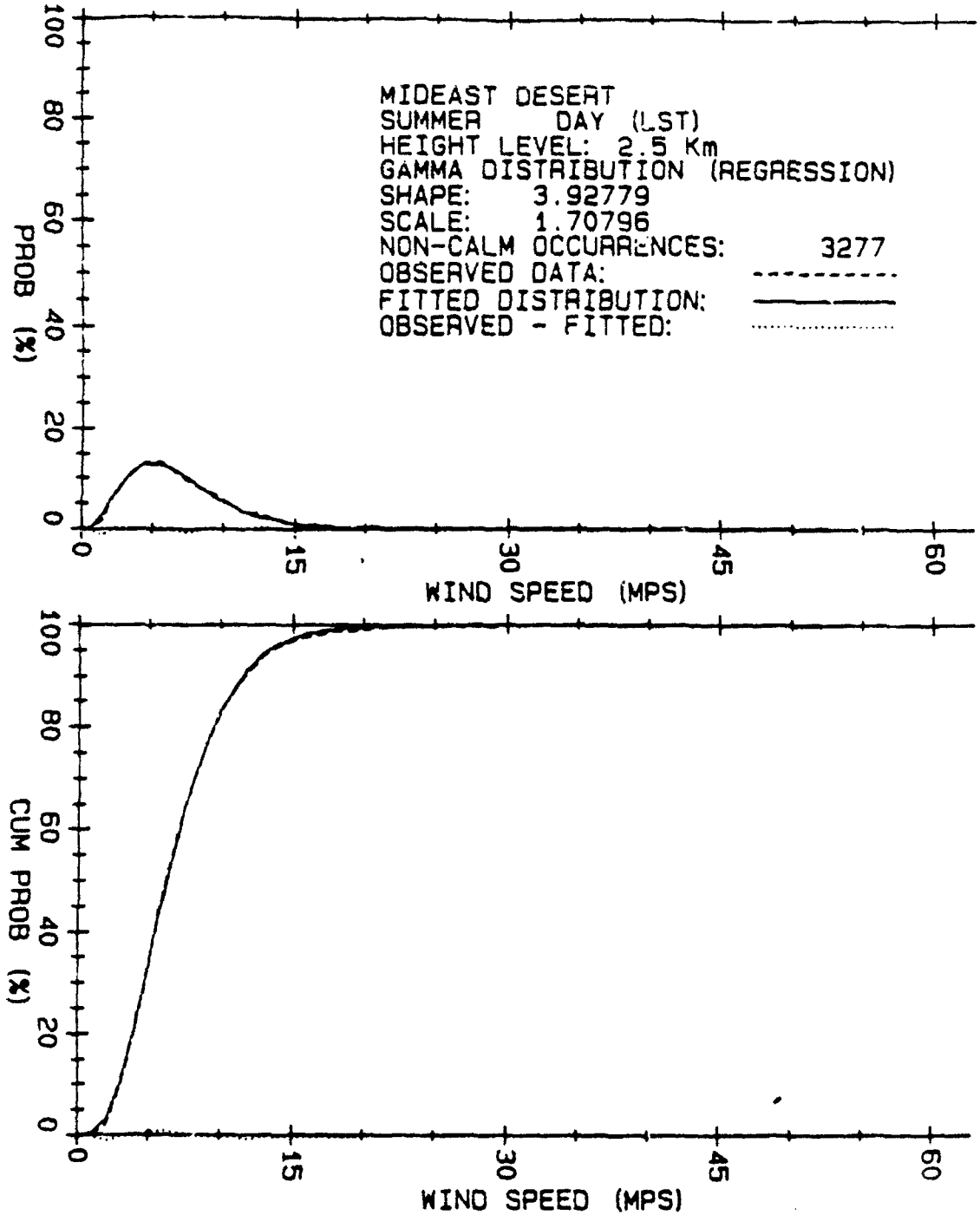

Figure 58. Regression fitted gamma distribution for Mideast Desert daytime summer wind speeds for height level 2.5 km.

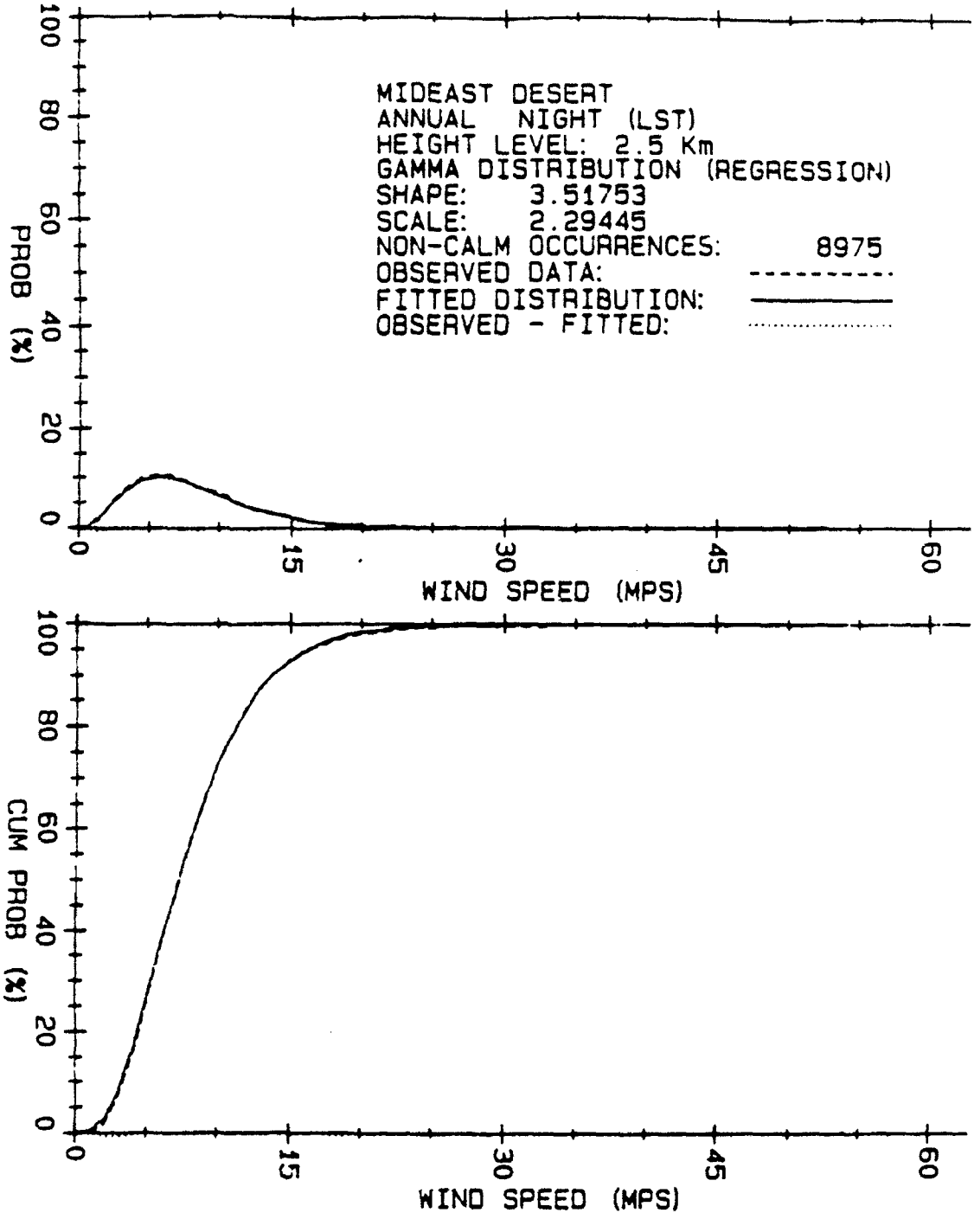

Figure 59. Regression fitted gamma distribution for Mideast Desert nighttime wind speeds for height level 2.5 km.

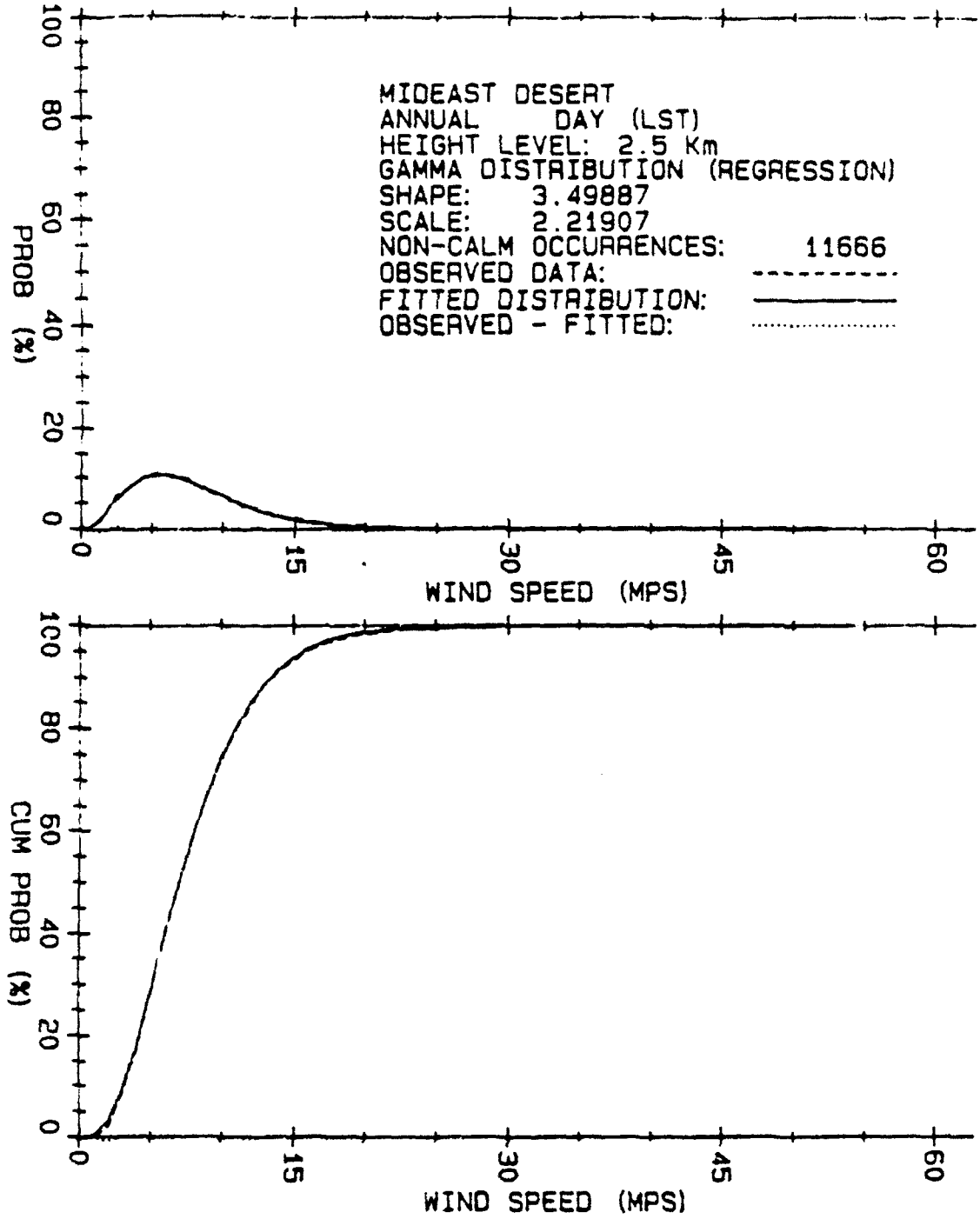

Figure 60. Regression fitted gamma distribution for Mideast Desert daytime wind speeds for height level 2.5 km.

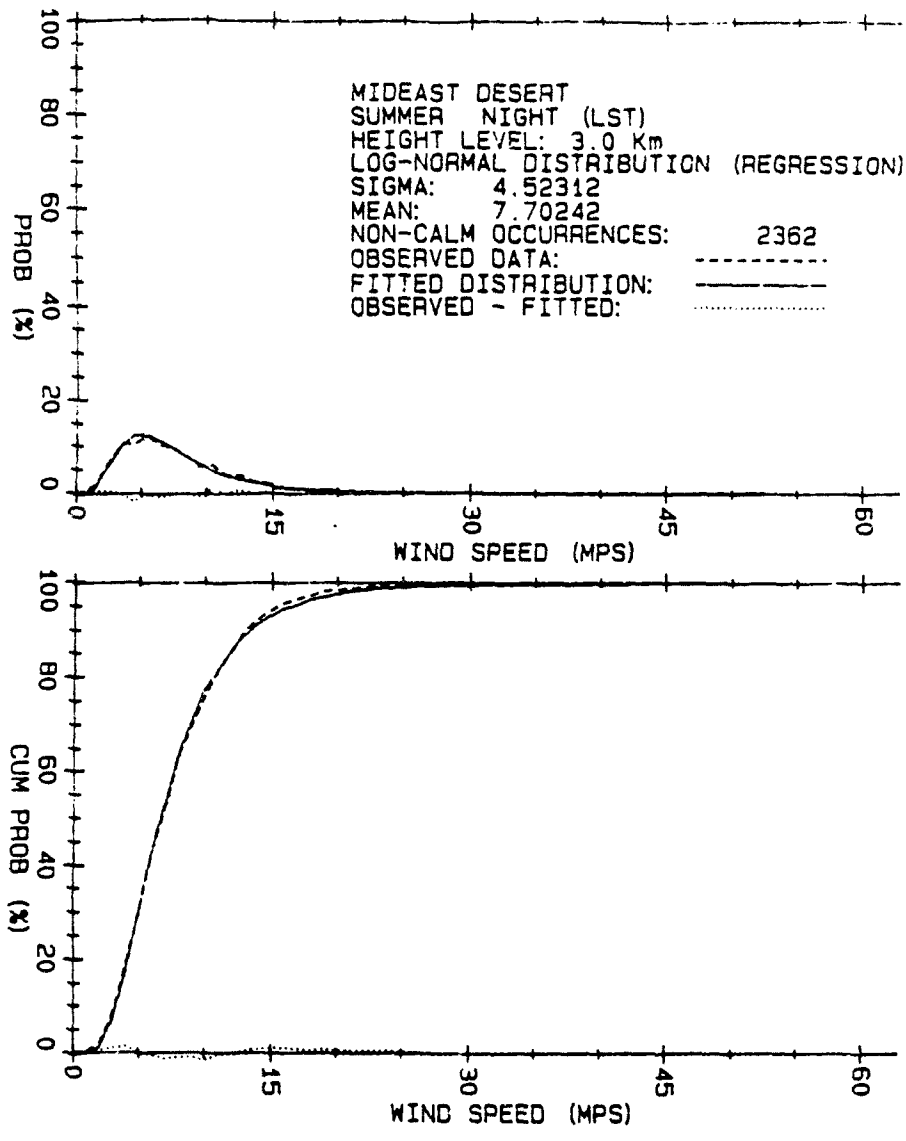

Figure 61. Regression fitted log-normal distribution for Mideast Desert nighttime summer wind speeds for height level 3.0 km.

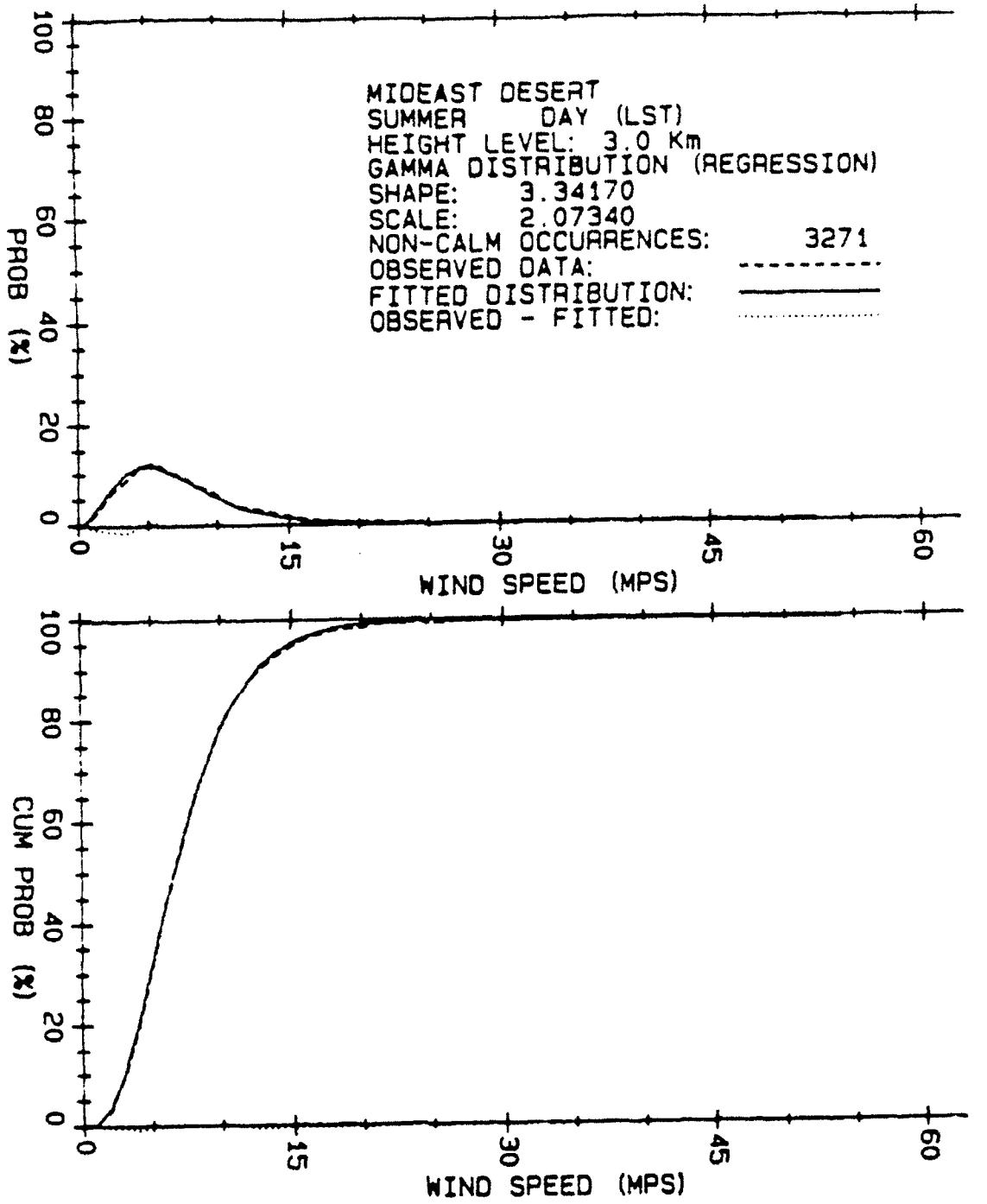

Figure 62. Regression fitted gamma distribution for Mideast Desert daytime summer wind speeds for height level 3.0 km.

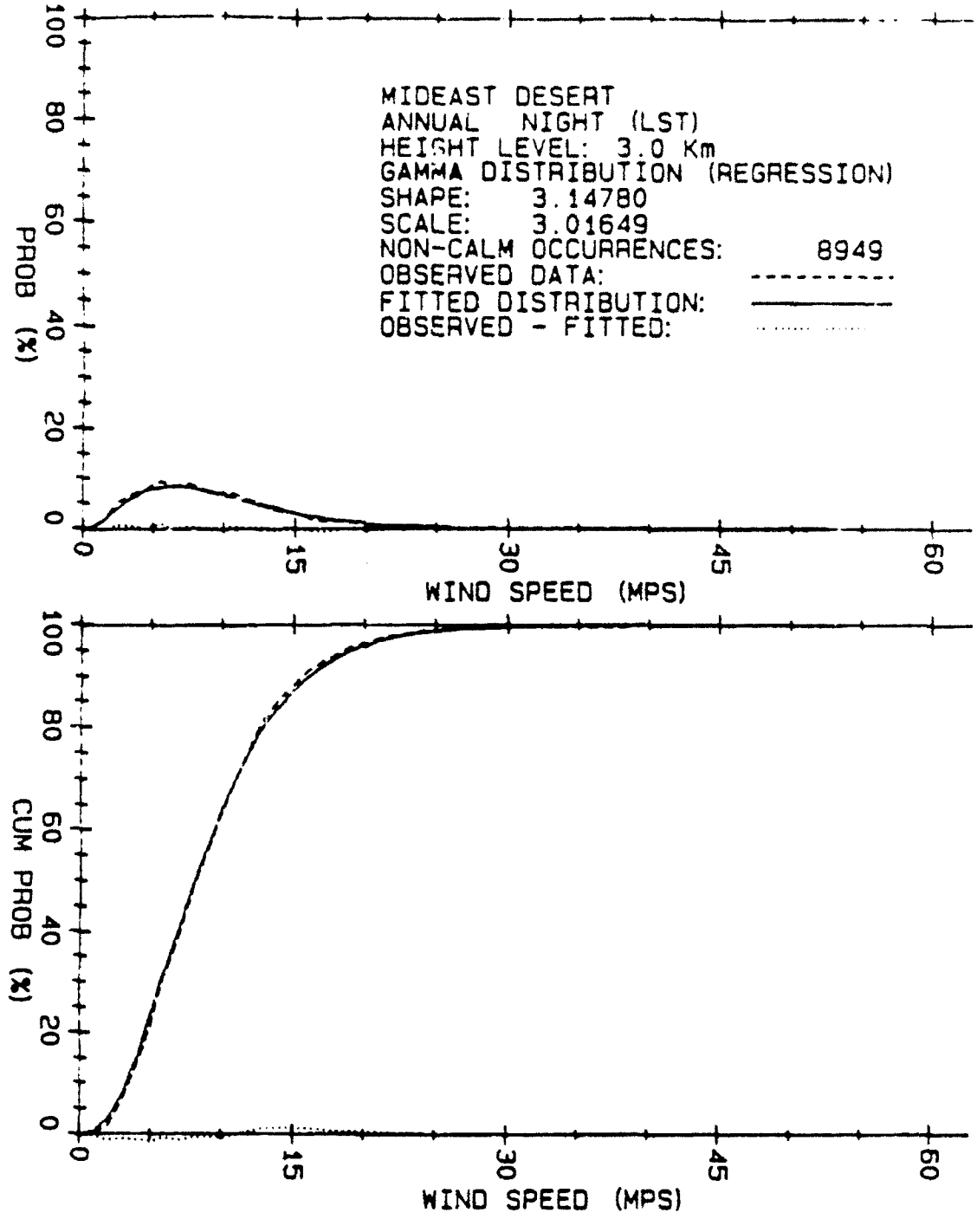

Figure 63. Regression fitted gamma distribution for Mideast Desert nighttime wind speeds for height level 3.0 km.

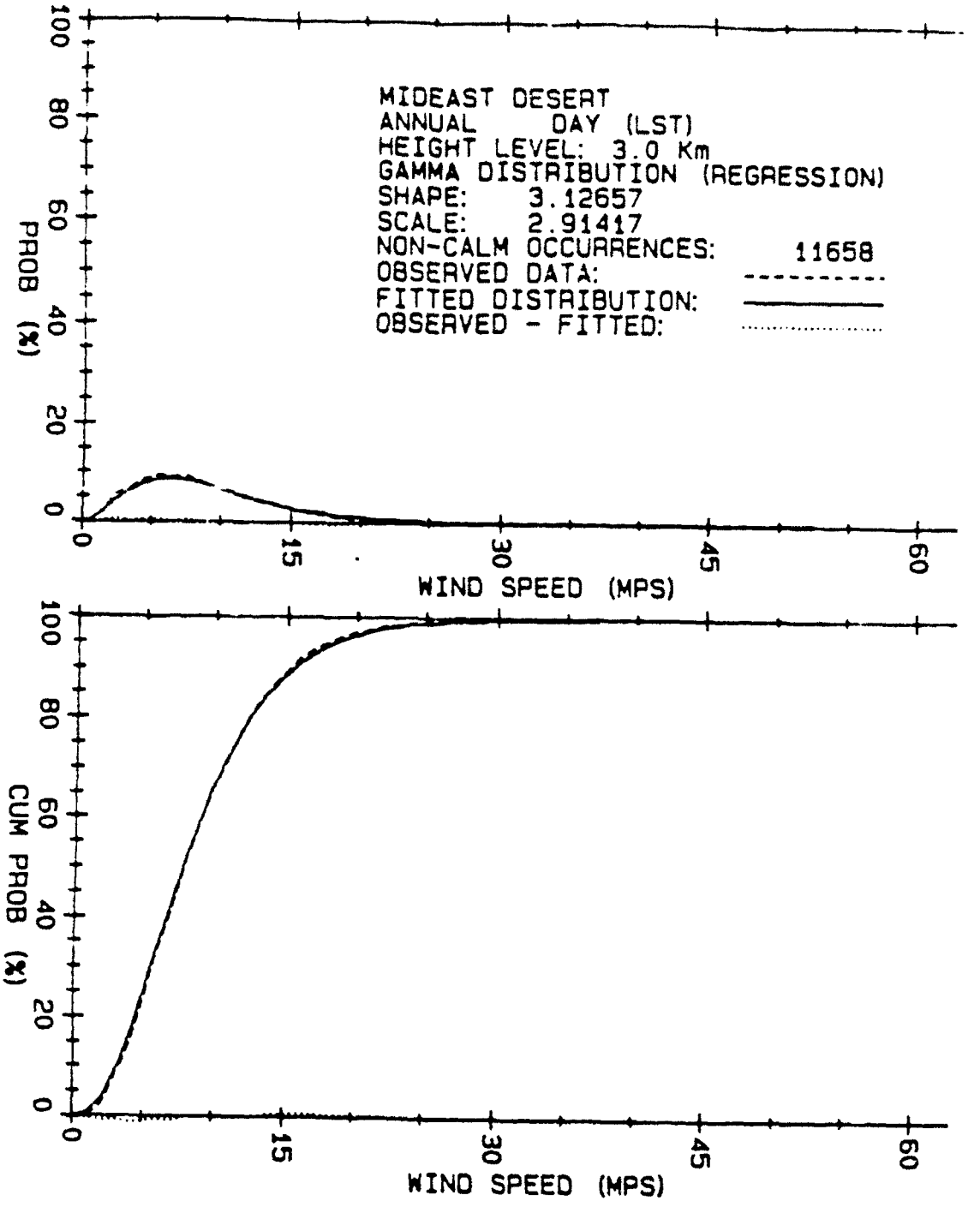

Figure 64. Regression fitted gamma distribution for Mideast Desert daytime wind speeds for height level 3.0 km.

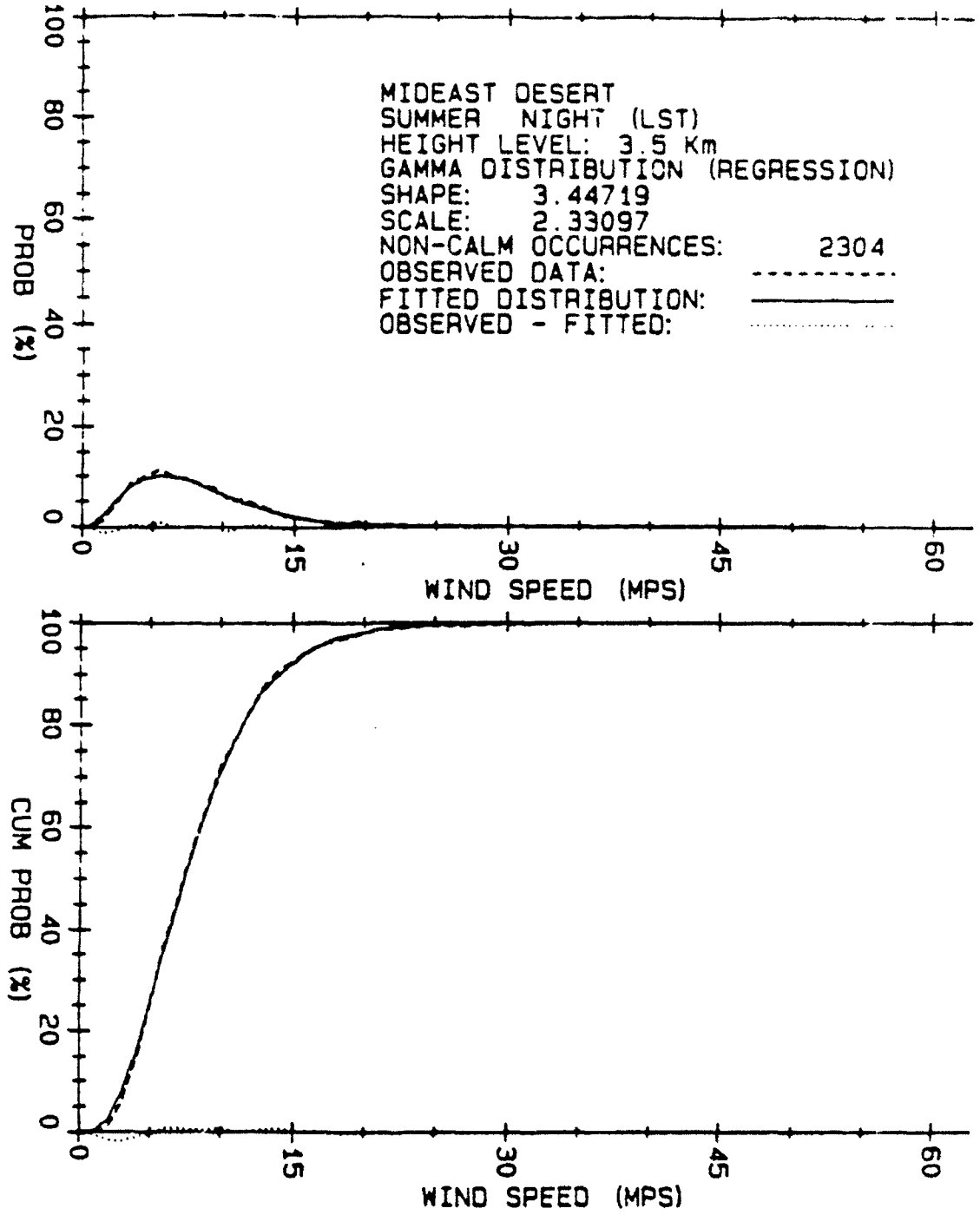

Figure 65. Regression fitted gamma distribution for Mideast Desert nighttime summer wind speeds for height level 3.5 km.

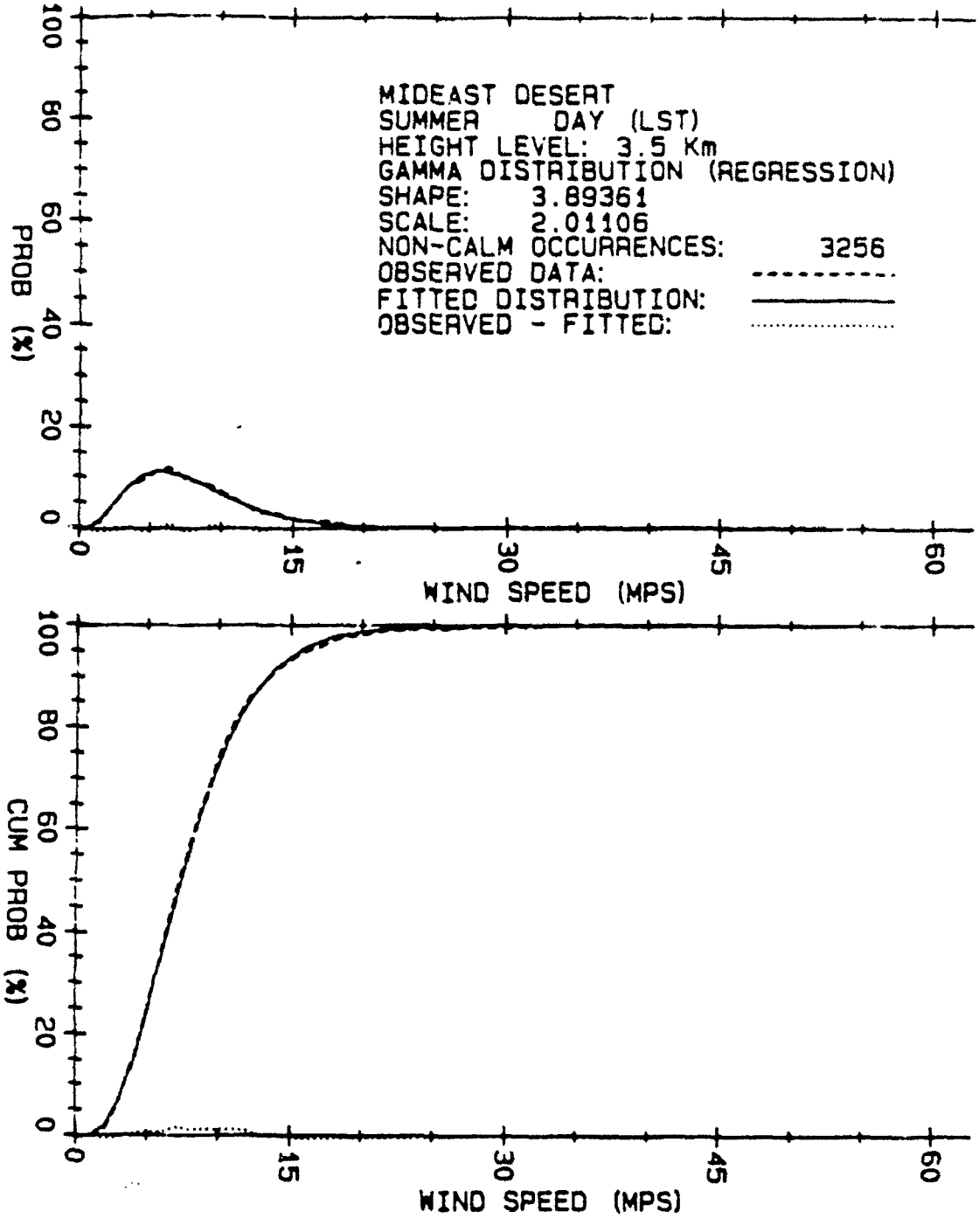

Figure 66. Regression fitted gamma distribution for Mideast Desert daytime summer wind speeds for height level 3.5 km.

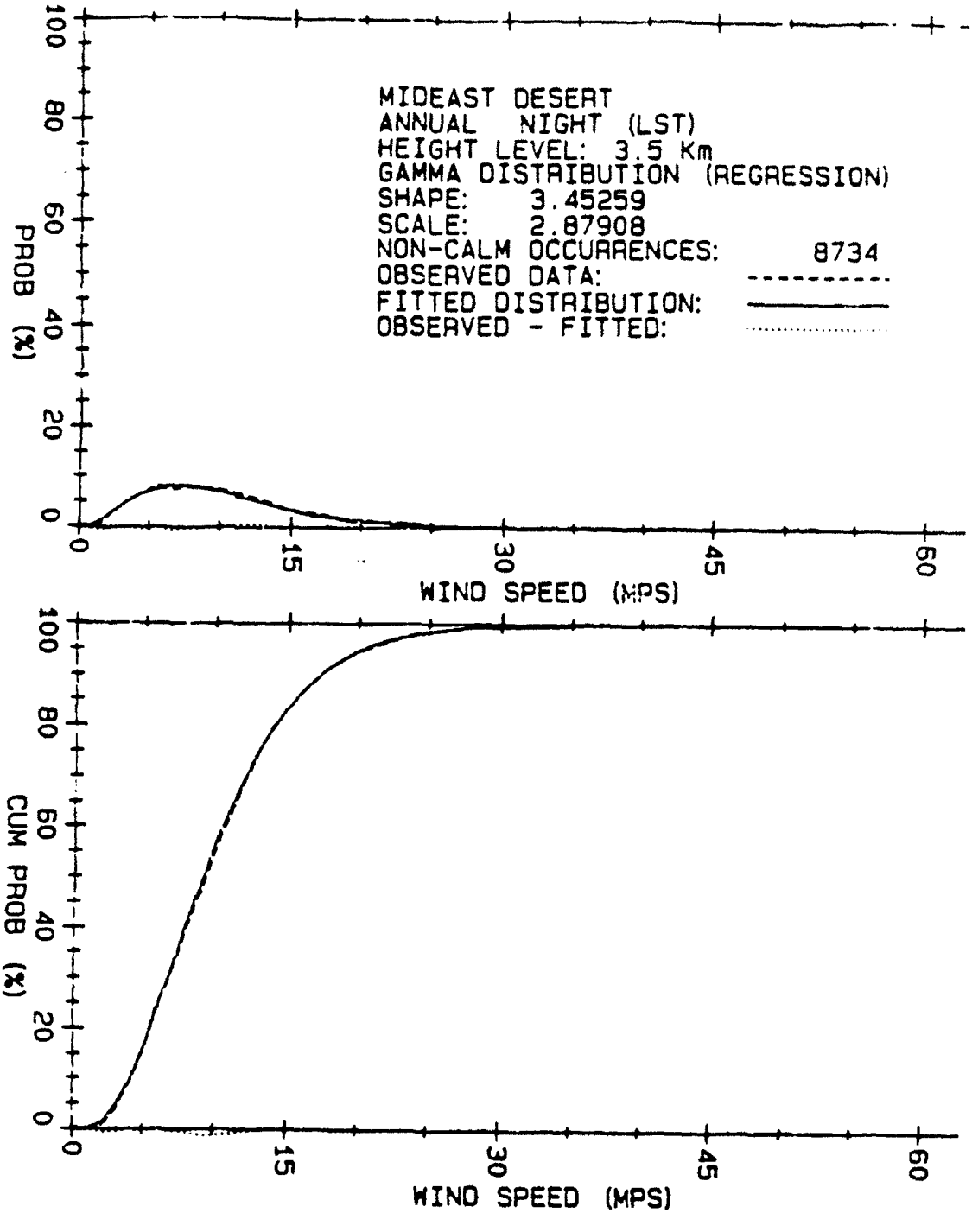

Figure 67. Regression fitted gamma distribution for Mideast Desert nighttime wind speeds for height level 3.5 km.

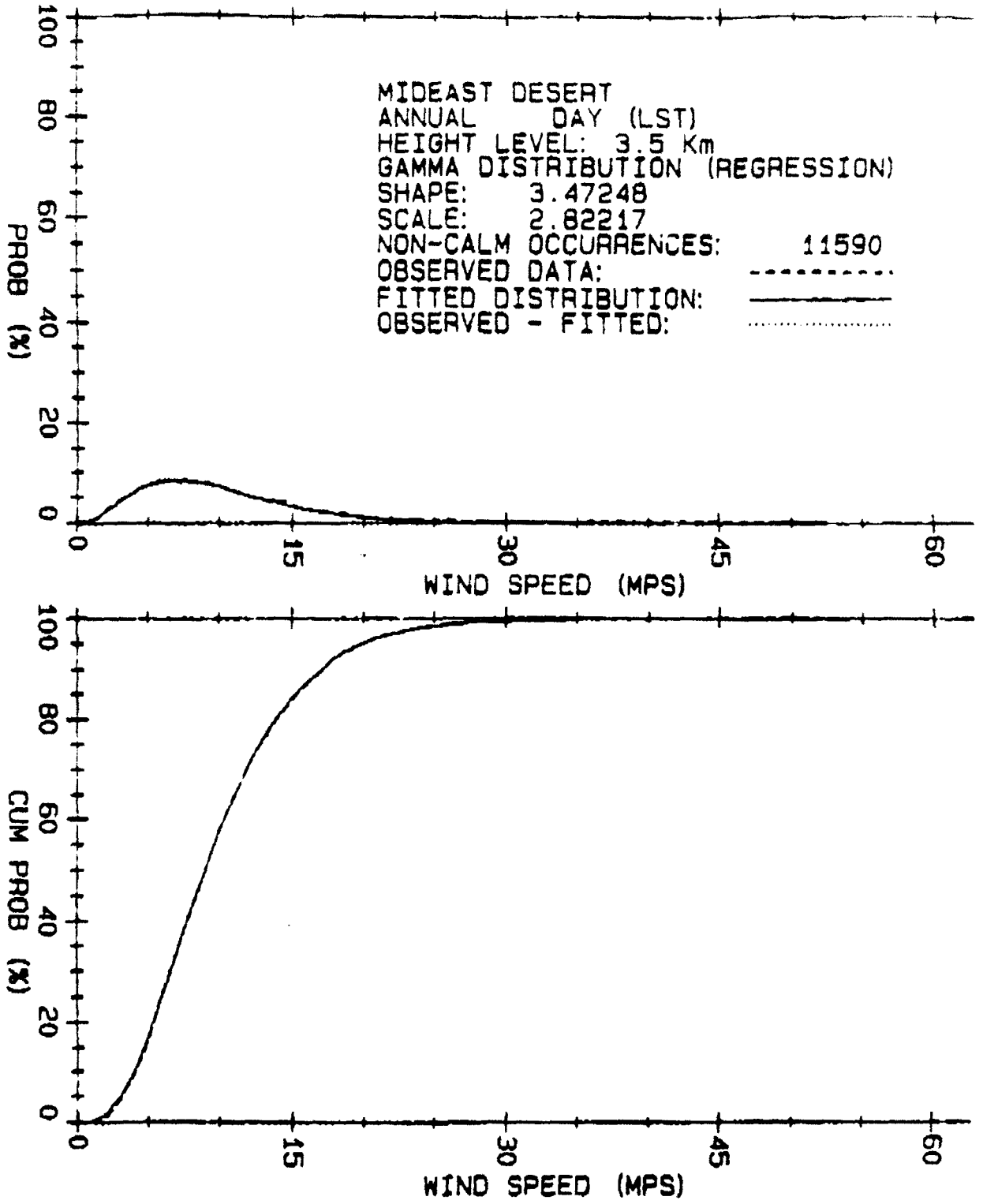

Figure 68. Regression fitted gamma distribution for Mideast Desert daytime wind speeds for height level 3.5 km.

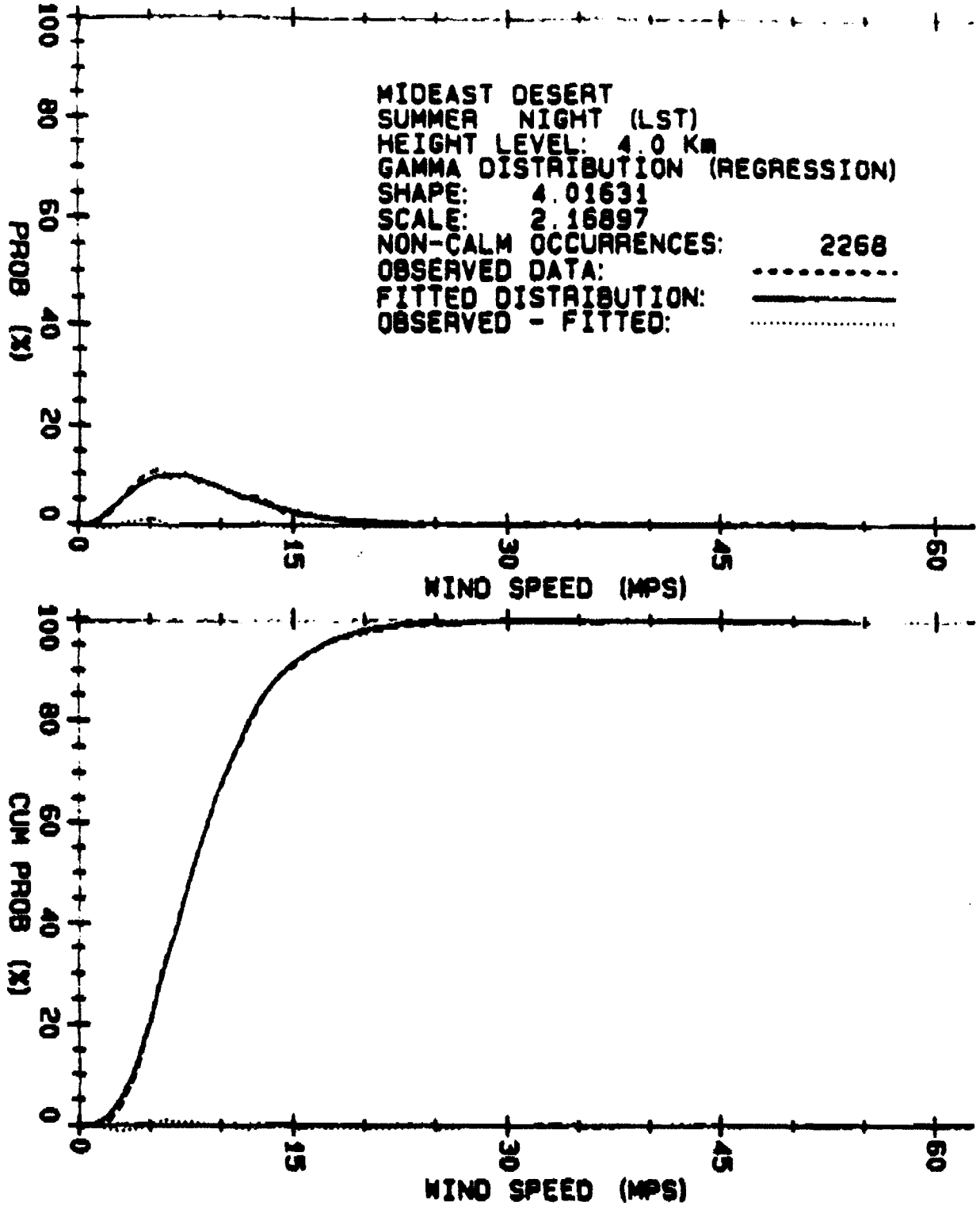

Figure 69. Regression fitted gamma distribution for Mideast Desert nighttime summer wind speeds for height level 4.0 km.

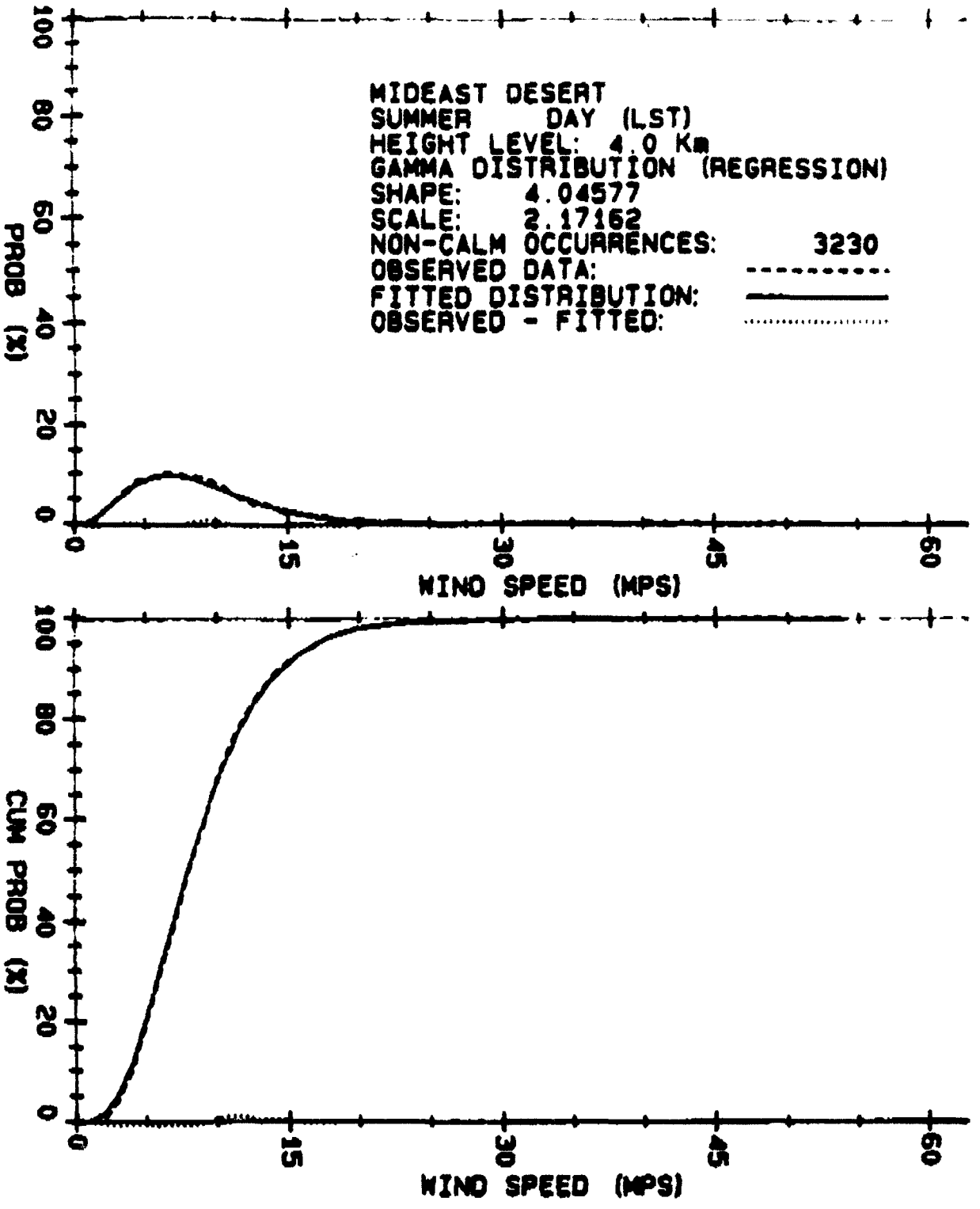

Figure 70. Regression fitted gamma distribution for Mideast Desert daytime summer wind speeds for height level 4.0 km.

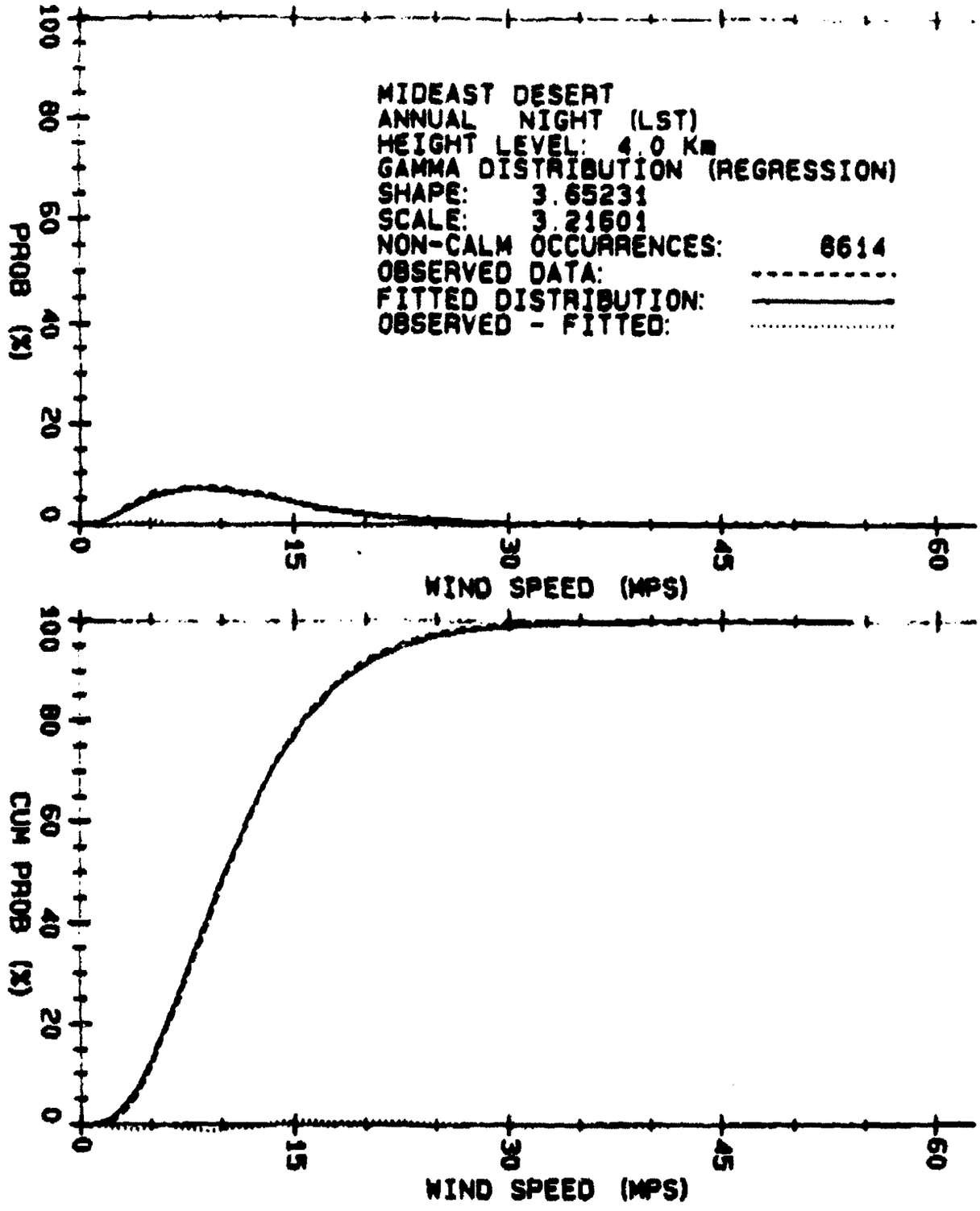

Figure 71. Regression fitted gamma distribution for Mideast Desert nighttime wind speeds for height level 4.0 km.

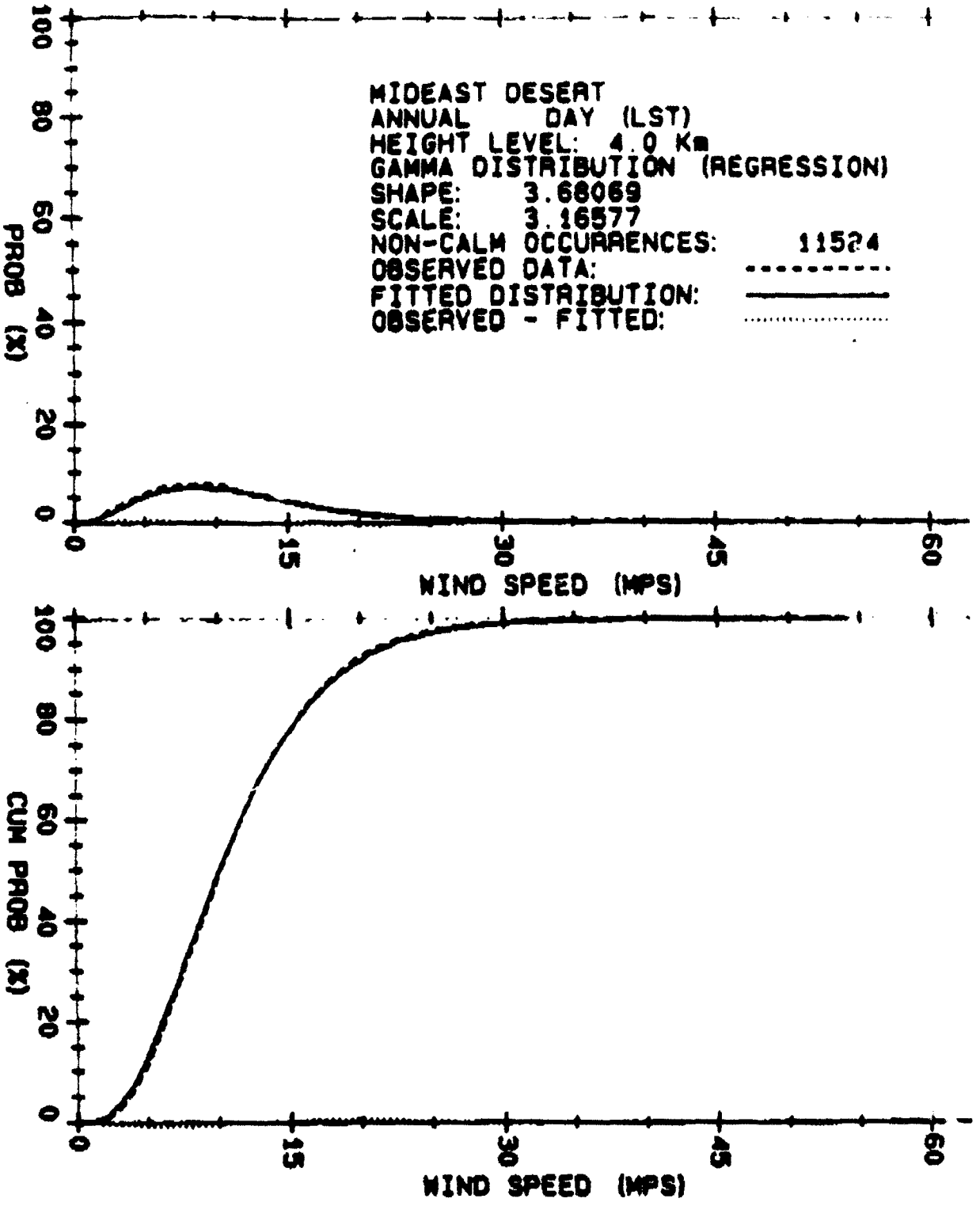

Figure 72. Regression fitted gamma distribution for Mideast Desert daytime wind speeds for height level 4.0 km.

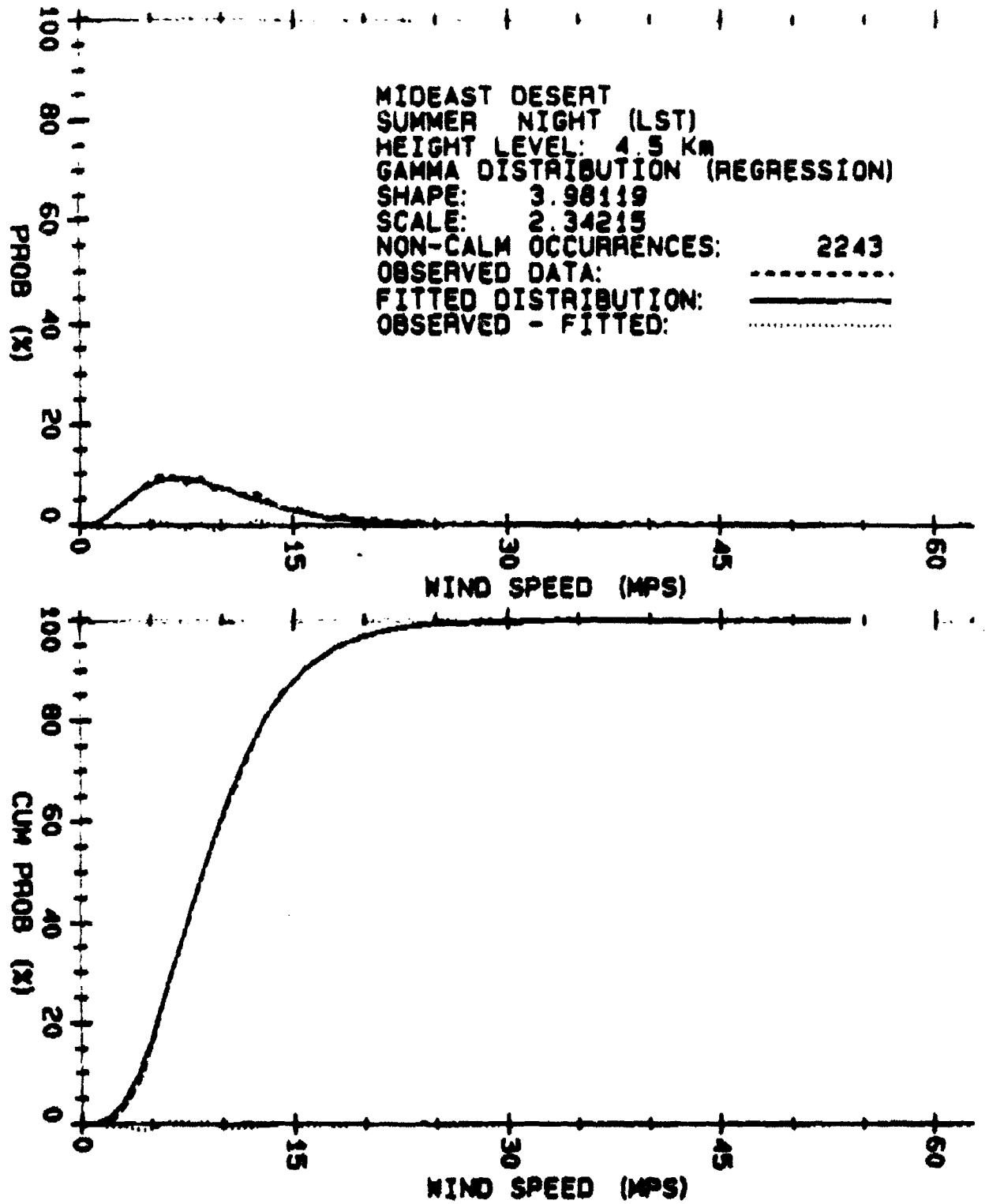

Figure 73. Regression fitted gamma distribution for Mideast Desert nighttime summer wind speeds for height level 4.5 km.

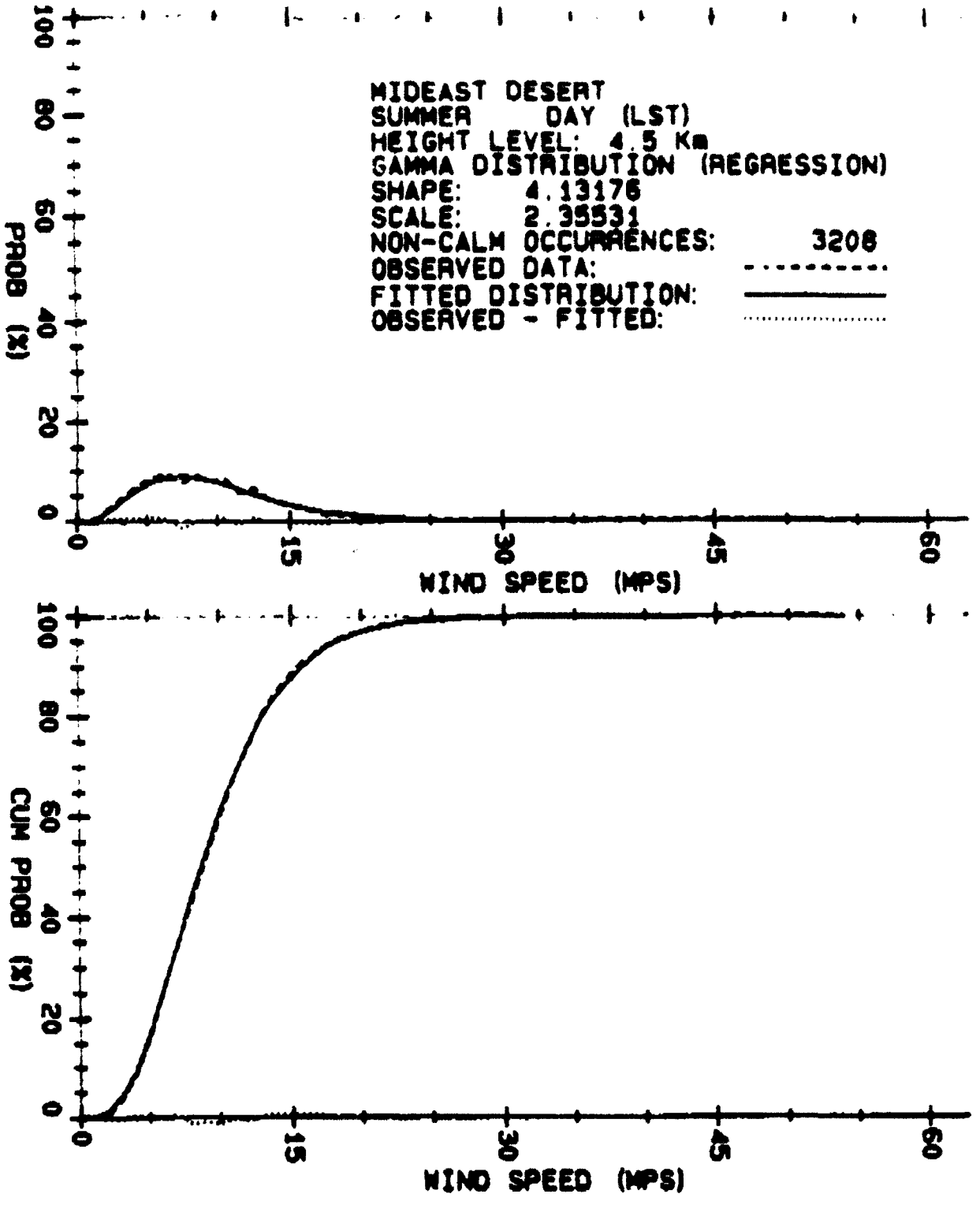

Figure 74. Regression fitted gamma distribution for Mideast Desert daytime summer wind speeds for height level 4.5 km.

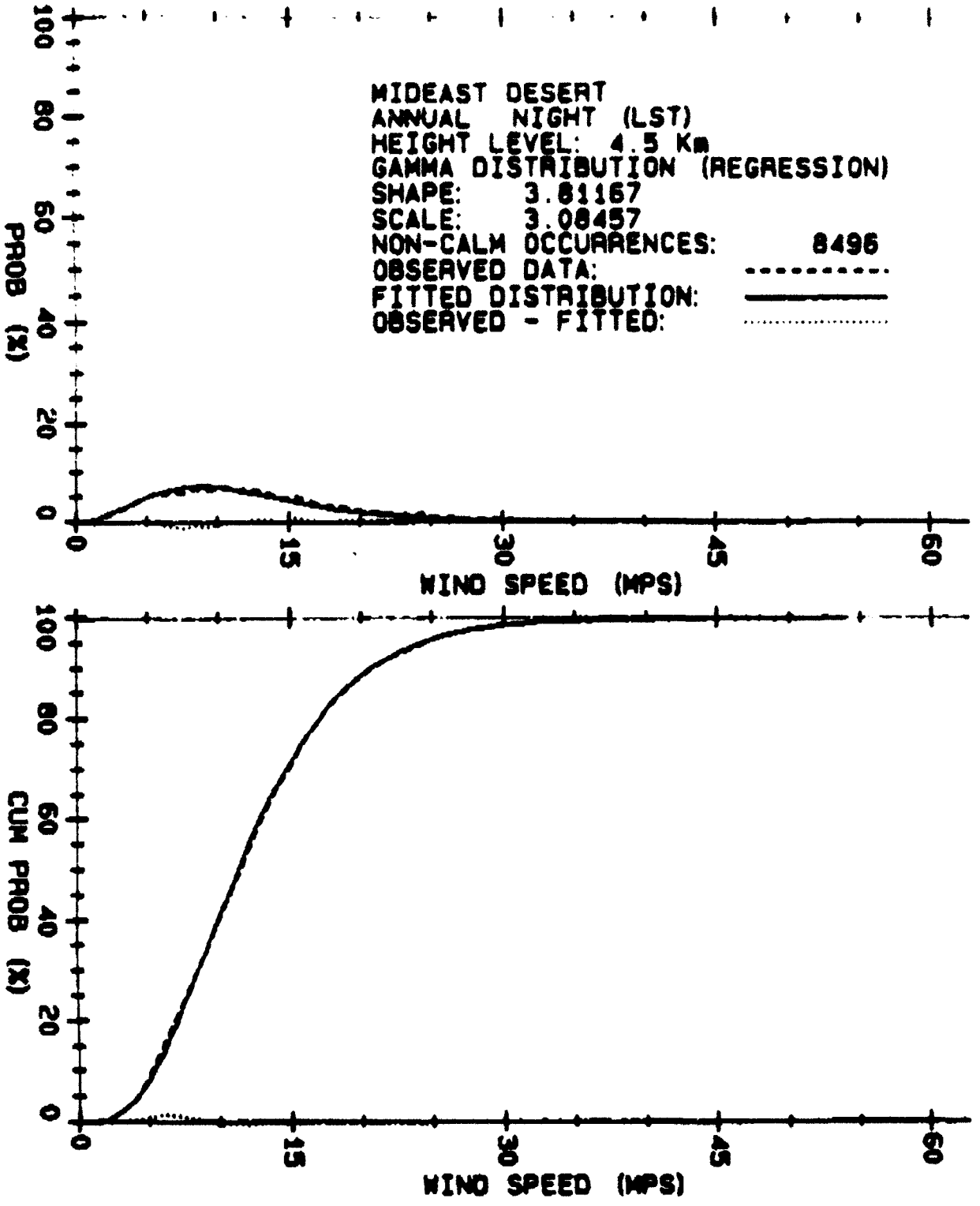

Figure 75. Regression fitted gamma distribution for Mideast Desert nighttime wind speeds for height level 4.5 km.

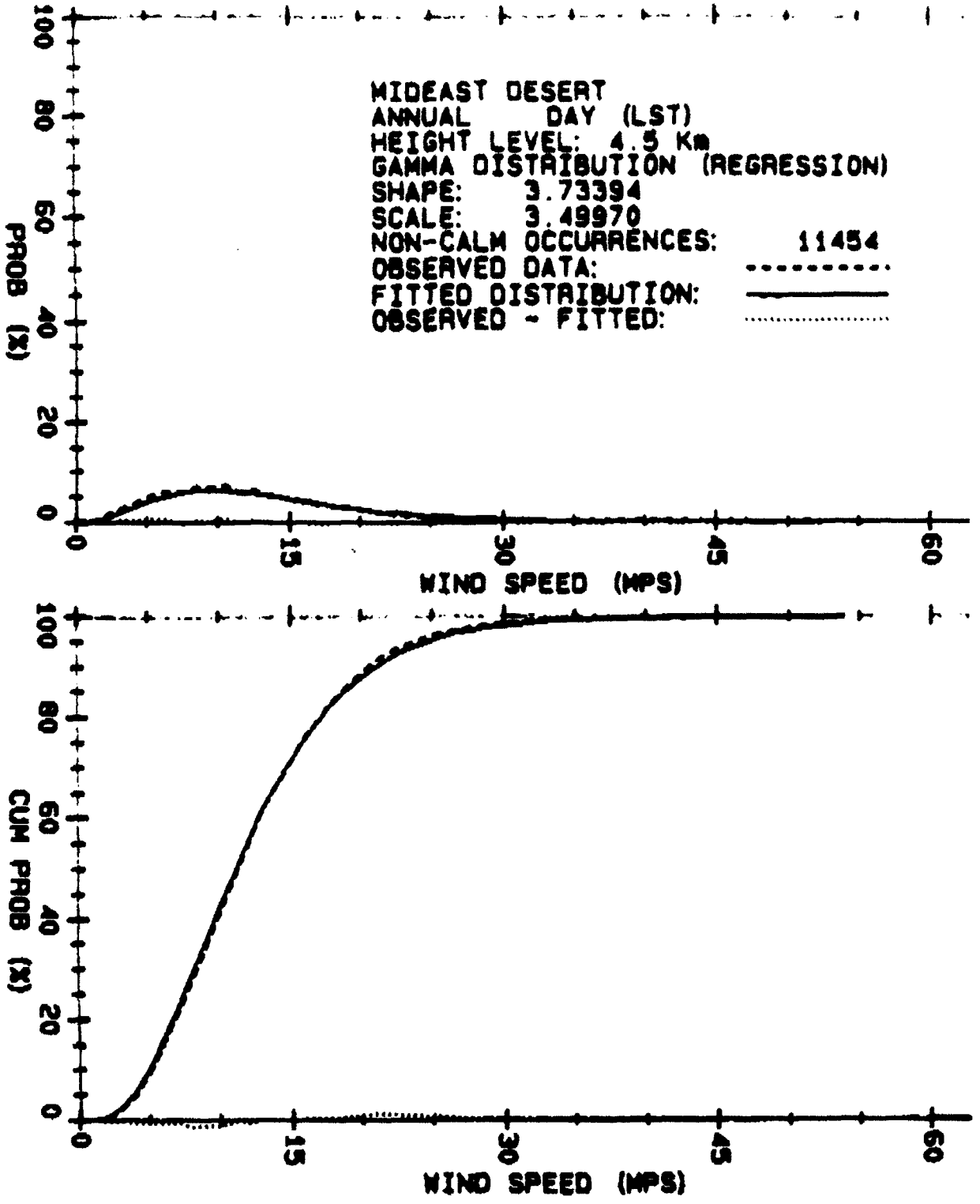

Figure 76. Regression fitted gamma distribution for Mideast Desert daytime wind speeds for height level 4.5 km.

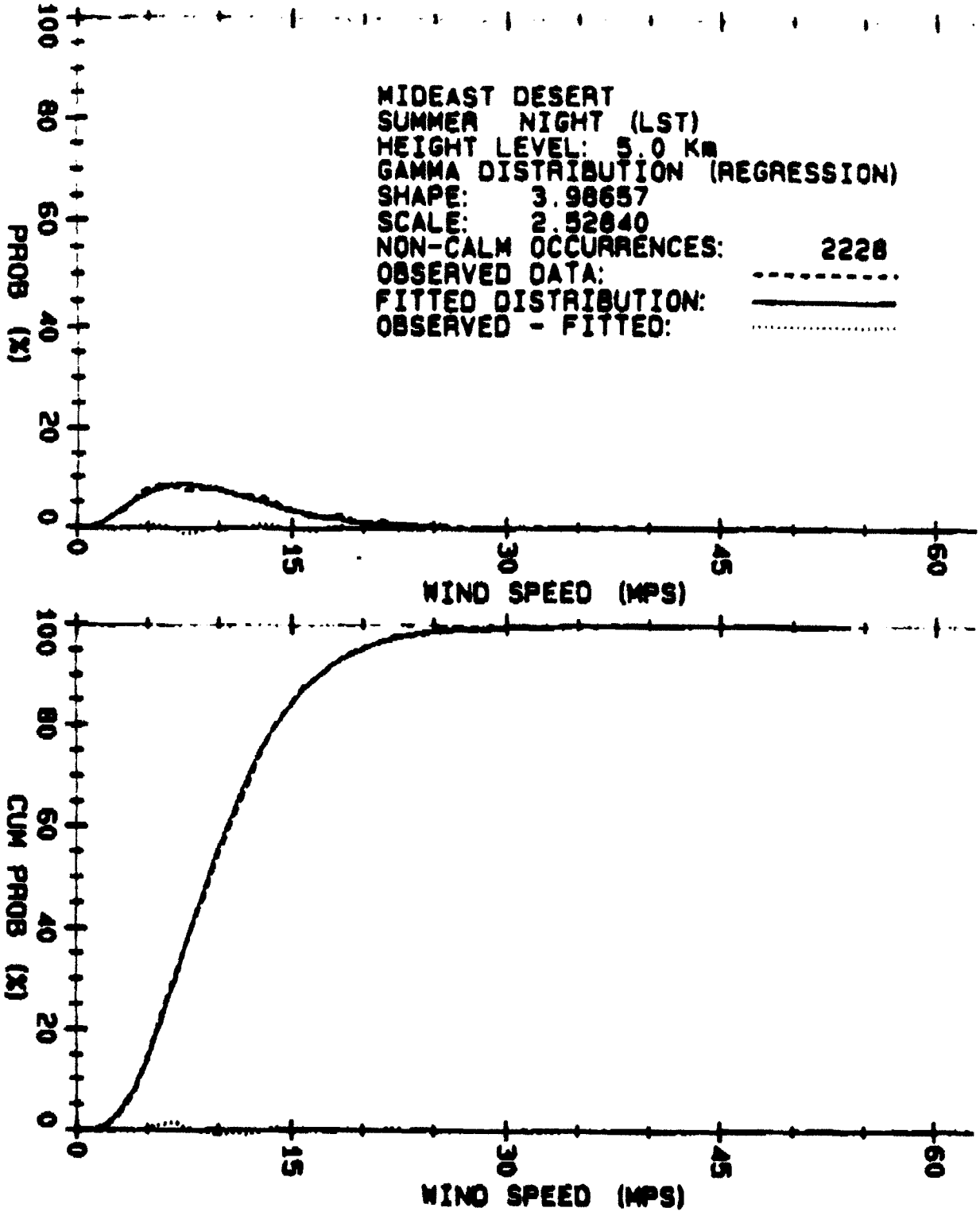

Figure 77. Regression fitted gamma distribution for Mideast Desert nighttime summer wind speeds for height level 5.0 km.

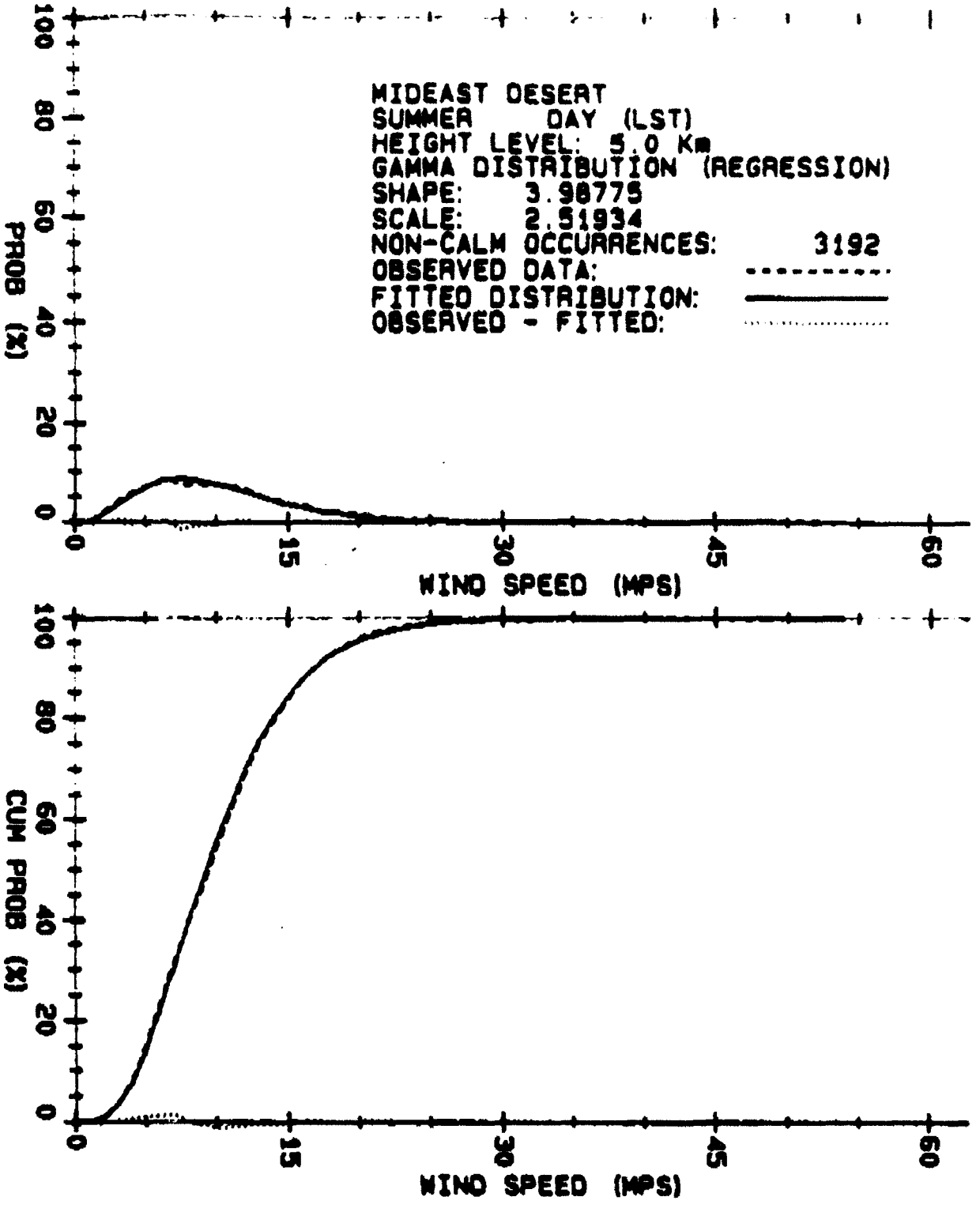

Figure 78. Regression fitted gamma distribution for Mideast Desert daytime summer wind speeds for height level 5.0 km.

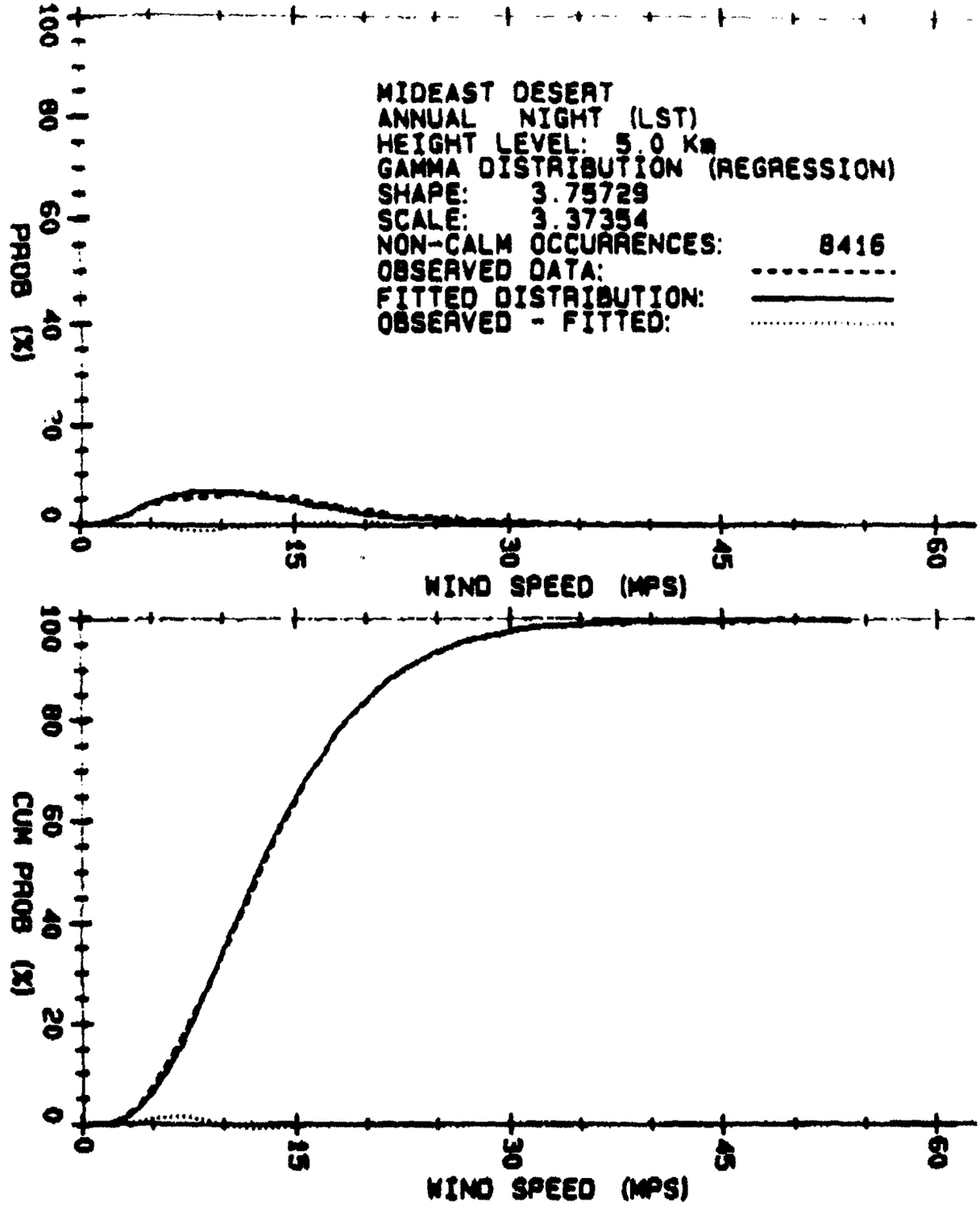

Figure 79. Regression fitted gamma distribution for Mideast Desert nighttime wind speeds for height level 5.0 km.

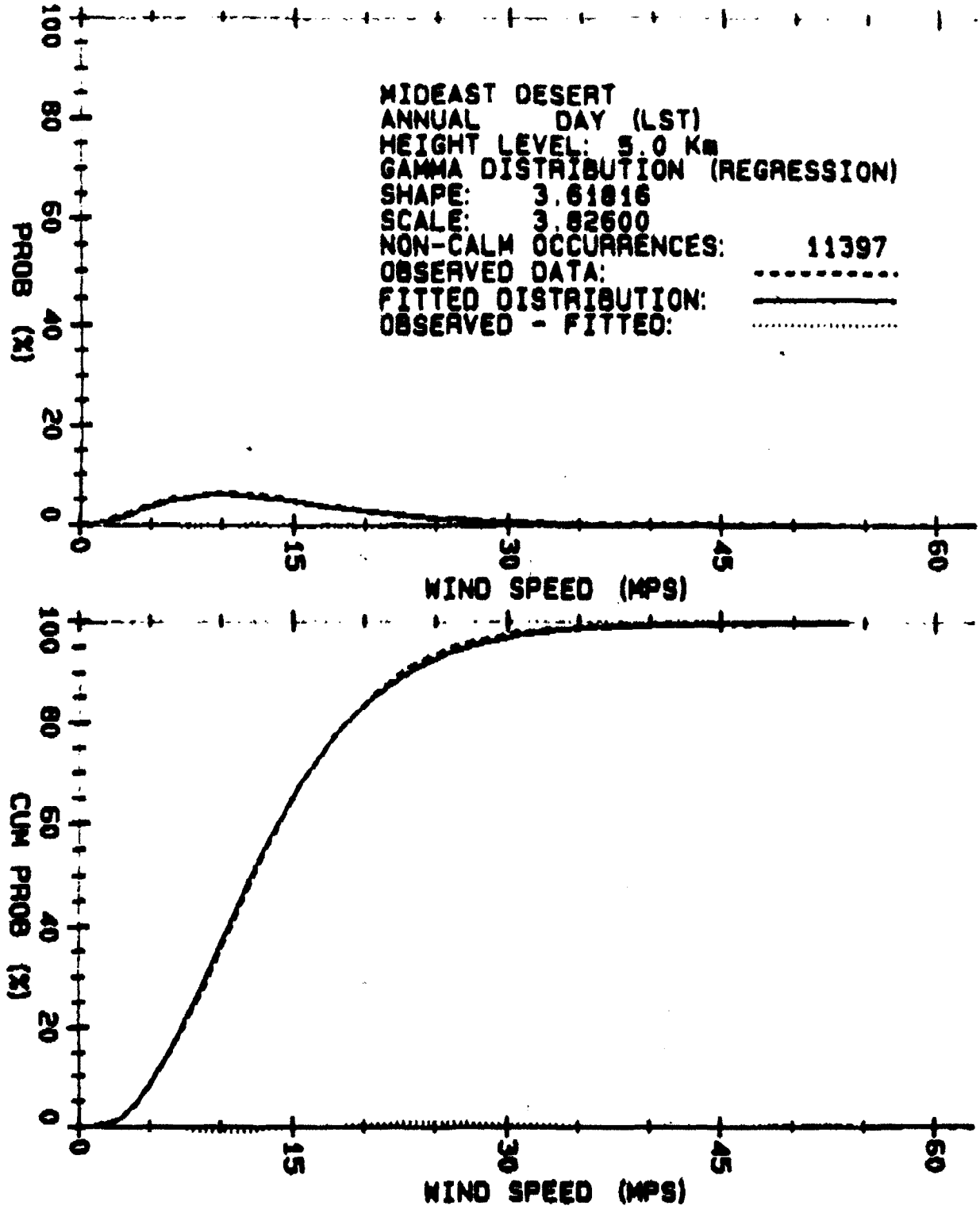

Figure 80. Regression fitted gamma distribution for Mideast Desert daytime wind speeds for height level 5.0 km.

THIS PAGE IS MISSING IN ORIGINAL DOCUMENT

PAGE 116

REFERENCES

Abramowitz, Milton, and Irene A. Stegun, 1965, Handbook of Mathematical Functions, Dover Publications, Incorporated, 1046 pp.

Avara, Elton P., and Bruce T. Miers, 1992, Surface Wind Speed Distributions, ASL-TR-0313, U.S. Army Atmospheric Sciences Laboratory, White Sands Missile Range, NM 88002-5501.

Holton, J. R., 1967, "The diurnal boundary layer wind oscillation above sloping terrain," Tellus, 19:199-205.

Miers, Bruce T., Elton P. Avara, and Louis D. Duncan, 1985a, Global Electro-Optical Systems Environmental Matrix (GEOSEM) Climatology for Mideast and Southwest Asia, ASL-TR-0172, U.S. Army Atmospheric Sciences Laboratory, White Sands Missile Range, NM 88002-5501.

Miers, Bruce T., Elton P. Avara, and Louis D. Duncan, 1985b, Global Electro-Optical Systems Environmental Matrix (GEOSEM) Climatology for Central and Northern Europe, ASL-TR-0177, U.S. Army Atmospheric Sciences Laboratory, White Sands Missile Range, NM 88002-5501.

THIS PAGE IS MISSING IN ORIGINAL DOCUMENT

PAGE 118

DISTRIBUTION LIST FOR PUBLIC RELEASE

Commandant
U.S. Army Chemical School
ATTN: ATZN-CM-CC (S. Barnes)
Fort McClellan, AL 36205-5020

Commander
U.S. Army Aviation Center
ATTN: ATZQ-D-MA
Mr. Oliver N. Heath
Fort Rucker, AL 36362

NASA/Marshall Space Flight Center
Deputy Director
Space Science Laboratory
Atmospheric Sciences Division
ATTN: E501 (Dr. George H. Fichtl)
Huntsville, AL 35802

NASA/Marshall Space Flight Center
Atmospheric Sciences Division
ATTN: Code ED-41
Huntsville, AL 35812

Deputy Commander
U.S. Army Strategic Defense Command
ATTN: CSSD-SL-L
Dr. Julius Q. Lilly
P.O. Box 1500
Huntsville, AL 35807-3801

Commander
U.S. Army Missile Command
ATTN: AMSMI-RD-AC-AD
Donald R. Peterson
Redstone Arsenal, AL 35898-5242

Commander
U.S. Army Missile Command
ATTN: AMSMI-RD-AS-SS
Huey F. Anderson
Redstone Arsenal, AL 35898-5253

Commander
U.S. Army Missile Command
ATTN: AMSMI-RD-AS-SS
B. Williams
Redstone Arsenal, AL 35898-5253

Commander
U.S. Army Missile Command
ATTN: AMSMI-RD-DE-SE
Gordon Lill, Jr.
Redstone Arsenal, AL 35898-5245

Commander
U.S. Army Missile Command
Redstone Scientific Information
Center
ATTN: AMSMI-RD-CS-R/Documents
Redstone, Arsenal, AL 35898-5241

Commander
U.S. Army Intelligence Center
and Fort Huachuca
ATTN: ATSI-CDC-C (Mr. Colanto)
Fort Huachuca, AZ 85613-7000

Northrup Corporation
Electronics Systems Division
ATTN: Dr. Richard D. Tooley
2301 West 120th Street, Box 5032
Hawthorne, CA 90251-5032

Commander - Code 3331
Naval Weapons Center
ATTN: Dr. Alexis Shlanta
China Lake, CA 93555

Commander
Pacific Missile Test Center
Geophysics Division
ATTN: Code 3250 (Terry E. Battalino)
Point Mugu, CA 93042-5000

Lockheed Missiles & Space Co., Inc.
Kenneth R. Hardy
Org/91-01 B/255
3251 Hanover Street
Palo Alto, CA 94304-1191

Commander
Naval Ocean Systems Center
ATTN: Code 54 (Dr. Juergen Richter)
San Diego, CA 92152-5000

Meteorologist in Charge
Kwajalein Missile Range
P.O. Box 67
APO San Francisco, CA 96555

U.S. Department of Commerce
Mountain Administration Support
Center
Library, R-51 Technical Reports
325 S. Broadway
Boulder, CO 80303

Dr. Hans J. Liebe
NTIA/ITS S 3
325 S. Broadway
Boulder, CO 80303

NCAR Library Serials
National Center for Atmos Rsch
P.O. Box 3000
Boulder, CO 80307-3000

HQDA
ATTN: DAMI-POI
Washington, DC 20310-1067

Mil Asst for Env Sci Ofc of
The Undersecretary of Defense
for Rsch & Engr/R&AT/E&LS
Pentagon - Room 3D129
Washington, DC 20301-3080

Director
Naval Research Laboratory
ATTN: Code 4110
Dr. Lothar H. Ruhnke
Washington, DC 20375-5000

HQDA
DEAN-RMD/Dr. Gomez
Washington, DC 20314

Director
Division of Atmospheric Science
National Science Foundation
ATTN: Dr. Eugene W. Bierly
1800 G. Street, N.W.
Washington, DC 20550

Commander
Space & Naval Warfare System Command
ATTN: PMW-145-1G (LT Painter)
Washington, DC 20362-5100

Commandant
U.S. Army Infantry
ATTN: ATSH-CD-CS-OR
Dr. E. Dutoit
Fort Benning, GA 30905-5090

USAFETAC/DNE
Scott AFB, IL 62225

Air Weather Service
Technical Library - FL4414
Scott AFB, IL 62225-5458

HQ AWS/DOO
Scott AFB, IL 62225-5008

USAFETAC/DNE
ATTN: Mr. Charles Glauber
Scott AFB, IL 62225-5008

Commander
U.S. Army Combined Arms Combat
ATTN: ATZL-CAW (LTC A. Kyle)
Fort Leavenworth, KS 66027-5300

Commander
U.S. Army Space Institute
ATTN: ATZI-SI (Maj Koepsell)
Fort Leavenworth, KS 66027-5300

Commander
U.S. Army Space Institute
ATTN: ATZL-SI-D
Fort Leavenworth, KS 66027-7300

Commander
Phillips Lab
ATTN: PL/LYP (Mr. Chisholm)
Hanscom AFB, MA 01731-5000

Director
Atmospheric Sciences Division
Geophysics Directorate
Phillips Lab
ATTN: Dr. Robert A. McClatchey
Hanscom AFB, MA 01731-5000

Raytheon Company
Dr. Charles M. Sonnenschein
Equipment Division
528 Boston Post Road
Sudbury, MA 01776
Mail Stop 1K9

Director
U.S. Army Materiel Systems
Analysis Activity
ATTN: AMXSY-MP (H. Cohen)
APG, MD 21005-5071

Commander
U.S. Army Chemical Rsch,
Dev & Engr Center
ATTN: SMCCR-OPA (Ronald Pennsyle)
APG, MD 21010-5423

Commander
U.S. Army Chemical Rsch,
Dev & Engr Center
ATTN: SMCCR-RS (Mr. Joseph Vervier)
APG, MD 21010-5423

Commander
U.S. Army Chemical Rsch,
Dev & Engr Center
ATTN: SMCCR-MUC (Mr. A. Van De Wal)
APG, MD 21010-5423

Director
U.S. Army Materiel Systems
Analysis Activity
ATTN: AMXSY-AT (Mr. Fred Campbell)
APG, MD 21005-5071

Director
U.S. Army Materiel Systems
Analysis Activity
ATTN: AMXSY-CR (Robert N. Marchetti)
APG, MD 21005-5071

Director
U.S. Army Materiel Systems
Analysis Activity
ATTN: AMXSY-CS (Mr. Brad W. Bradley)
APG, MD 21005-5071

Commander
U.S. Army Laboratory Command
ATTN: AMSLC-CG
2800 Powder Mill Road
Adelphi, MD 20783-1145

Commander
Headquarters
U.S. Army Laboratory Command
ATTN: AMSLC-CT
2800 Powder Mill Road
Adelphi, MD 20783-1145

Commander
Harry Diamond Laboratories
ATTN: SLCIS-CO
2800 Powder Mill Road
Adelphi, MD 20783-1197

Director
Harry Diamond Laboratories
ATTN: SLCHD-ST-SP
Dr. Z.G. Sztankay
Adelphi, MD 20783-1197

National Security Agency
ATTN: W21 (Dr. Longbothum)
9800 Savage Road
Ft George G. Meade, MD 20755-6000

U. S. Army Space Technology
and Research Office
ATTN: Brenda Brathwaite
5321 Riggs Road
Gaithersburg, MD 20882

OIC-NAVSWC
Technical Library (Code E-232)
Silver Springs, MD 20903-5000

The Environmental Research
Institute of MI
ATTN: IRIA Library
P.O. Box 134001
Ann Arbor, MI 48113-4001

Commander
U.S. Army Research Office
ATTN: DRXRO-GS (Dr. W.A. Flood)
P.O. Box 12211
Research Triangle Park, NC 27709

Dr. Jerry Davis
North Carolina State University
Department of Marine, Earth, &
Atmospheric Sciences
P.O. Box 8208
Raleigh, NC 27650-8208

Commander
U. S. Army CECRL
ATTN: CECRL-RG (Dr. H. S. Boyne)
Hanover, NH 03755-1290

Commanding Officer
U.S. Army ARDEC
ATTN: SMCAR-IMI-I, Bldg 59
Dover, NJ 07806-5000

U.S. Army Communications-Electronics
Command EW/RSTA Directorate
ATTN: AMSEL-RD-EW-OP
Fort Monmouth, NJ 07703-5206

Commander
U.S. Army Satellite Comm Agency
ATTN: DRCPM-SC-3
Fort Monmouth, NJ 07703-5303

6585th TG (AFSC)
ATTN: RX (CPT Stein)
Holloman AFB, NM 88330

Department of the Air Force
OL/A 2nd Weather Squadron (MAC)
Holloman AFB, NM 88330-5000

PL/WE
Kirtland AFB, NM 87118-6008

Director
U.S. Army TRADOC Analysis Command
ATTN: ATRC-WSS-R
White Sands Missile Range, NM 88002

Rome Laboratory
ATTN: Technical Library RL/DOVL
Griffiss AFB, NY 13441-5700

Department of the Air Force
7th Squadron
APO, NY 09403

AWS
USAREUR/AEAWX
APO, NY 09403-5000

AFMC/DOW
Wright-Patterson AFB, OH 0334-5000

Commandant
U.S. Army Field Artillery School
ATTN: ATSF-TSM-TA
Mr. Charles Taylor
Fort Sill, OK 73503-5600

Commander
Naval Air Development Center
ATTN: Al Salik (Code 5012)
Warminister, PA 18974

Commander
U.S. Army Dugway Proving Ground
ATTN: STEDP-MT-DA-M
Mr. Paul Carlson
Dugway, UT 84022

Commander
U.S. Army Dugway Proving Ground
ATTN: STEDP-MT-DA-L
Dugway, UT 84022

Commander
U.S. Army Dugway Proving Ground
ATTN: STEDP-MT-M (Mr. Bowers)
Dugway, UT 84022-5000

Defense Technical Information Center
ATTN: DTIC-FDAC
Cameron Station
Alexandria, VA 22314

Commanding Officer
U.S. Army Foreign Science &
Technology Center
ATTN: CM
220 7th Street, NE
Charlottesville, VA 22901-5396

Naval Surface Weapons Center
Code G63
Dahlgren, VA 22448-5000

Commander
U.S. Army OEC
ATTN: CSTE-EFS
Park Center IV
4501 Ford Ave
Alexandria, VA 22302-1458

Commander and Director
U.S. Army Corps of Engineers
Engineer Topographics Laboratory
ATTN: ETL-GS-LB
Fort Belvoir, VA 22060

TAC/DOWr
Langley AFB, VA 23665-5524

U.S. Army Topo Engineering Center
ATTN: CETEC-ZC
Fort Belvoir, VA 22060-5546

Commander
Logistics Center
ATTN: ATCL-CE
Fort Lee, VA 23801-6000

Commander
USATRADOC
ATTN: ATCD-FA
Fort Monroe, VA 23651-5170

Science and Technology
101 Research Drive
Hampton, VA 23666-1340

Commander
U.S. Army Nuclear & Cml Agency
ATTN: MONA-ZB Bldg 2073
Springfield, VA 22150-3198